

POLITECNICO DI MILANO

Facoltà di Ingegneria Civile, Ambientale e Territoriale

Corso di Laurea Specialistica in Ingegneria per l'Ambiente e il Territorio



EXPERIMENTAL ASSESSMENT OF ALUMINIUM RECOVERY FROM MSWI BOTTOM ASH

Supervisor: **Ing. Mario GROSSO**

Co-Supervisor: **Ing. Laura BIGANZOLI**

Master's Thesis by:

Leopoldo Gorla

Matr. 751063

Academic Year 2010/2011

Table of Contents

ABSTRACT	9
SUMMARY AND CONCLUSIONS	11
1. INTRODUCTION	19
1.1. Overview and objectives of the present study	19
1.2. Aluminium recycling in Europe.....	21
1.3. Recovery of aluminium scraps from MSWI bottom ash.....	24
1.4. Aluminium corrosion in high-temperature oxidizing atmospheres.....	30
1.5. Aluminium corrosion in aqueous solutions.....	32
1.6. Aluminium scraps corrosion in WTE plants	33
2. MATERIALS AND METHODS.....	35
2.1. Overview of the experimental campaigns.....	35
2.2. Description of Valmadrera WTE plant.....	38
2.3. Waste charge preparation and feeding	45
2.4. Sampling of incineration residues.....	52
2.5. Samples treatment and laboratory analysis	58
2.5.1. Bottom ash samples treatment	58
2.5.2. Fly ash samples treatment.....	59
2.5.3. Determination of metallic Al content through the “soda attack” method.....	64
2.5.4. Determination of total Al content through X-Ray Fluorescence Spectroscopy (XRF).....	67
2.5.5. Determination of metallic Al content through Optical Emission Spectroscopy (OES).....	70
2.5.6. Measuring precision of XRF and soda attack method	71
3. EVALUATION OF THE RESULTS	73
3.1 Aluminium beverage cans.....	73
3.1.1. Bottom ashes	73
3.1.2. Fly ashes	82
3.1.3. Mass balance.....	84
3.2 Aluminium trays.....	87
3.2.1 Bottom ashes	87
3.2.2. Fly ashes	95
3.2.3. Mass balance.....	97
3.3 Aluminium spray cans	100
3.3.1 Bottom ashes.....	100
3.3.2 Fly ashes	108
3.3.3 Mass balance.....	109
3.4 Aluminium and poly laminated foils	111
3.4.1 Bottom ashes	111
3.4.2 Fly ashes	120
3.4.3 Mass balance.....	122
3.5. Conclusions.....	125
3.5.1. Partitioning of aluminium in the incineration residues	125
3.5.2. Aluminium oxidation and potential for energy recovery	128
3.5.2. Other metals in the ingots from the melting process	132
4. FUTURE PERSPECTIVES AND IMPROVEMENTS.....	133
ACKNOWLEDGEMENTS	137
BIBLIOGRAPHY	139

List of Figures

Figure I - Scheme of the general approach used in the present project.	13
Figure II A - Partitioning of total aluminium recovered in the incineration residues for each type of tested packaging.....	14
Figure II B - Partitioning of metallic aluminium recovered in the incineration residues for each type of tested packaging.....	14
Figure 1.2.1 - Aluminium potentially recoverable from MSWI bottom ash in 2007, 2015 and 2020 in Italy (Grosso et al., 2011).....	23
Figure 1.3.1 - Aluminium mass balance excerpted from a study conducted by the Department of Environmental Engineering of Politecnico di Milano in 2009 on aluminium recovery from waste incineration (CiAl, 2010).	29
Figure 1.6.1 - Results of laboratory pot furnace tests carried out by Hu et al. (2011) on aluminium packaging.	34
Figure 2.2.1 - Design of the forward-acting grate of line 3 of Valmadrera incineration plant.	40
Figure 2.2.2 - Flue gas treatment layout of Valmadrera incineration plant (line 3).	40
Figure 2.2.3 - Temperatures measured during the days of the experimental campaigns.	42
Figure 2.2.4 - Primary air, secondary air and flue gas recirculation during the days of the experimental campaigns.....	43
Figure 2.2.5 - Steam flow rate and pressure during the days of the experimental campaigns.	43
Figure 2.2.6 - Stack concentrations of HCl, NO _x and SO ₂ during the days of the experimental campaigns.....	44
Figure 2.2.7 - Stack concentrations of NH ₃ , TOC and dust during the days of the experimental campaigns.....	44
Figure 2.3.1 - Doped waste charge preparation and feeding into the furnace.	45
Figure 2.3.2 - Doped waste charge preparation: residual waste from Seruso selection plant (mainly plastic and paper).	46
Figure 2.3.3 - Doped waste charge preparation: aluminium beverage cans used for Test 1.....	46
Figure 2.3.4 - Doped waste charge preparation: after the second mixing performed through the waste grab, the doped waste is ready to be introduced into the feeding hopper of Valmadrera WTE plant.	47
Figure 2.3.5 - Cage before and after the test.	49
Figure 2.3.6 - Cages in the furnace right before the discharge in the quenching water.	49
Figure 2.3.7 - Trend of metallic aluminium (mass % on bottom ashes dry weight) recovered from bottom ash samples taken during Test 2 on aluminium trays.	50
Figure 2.4.1 - Layout of Valmadrera WTE plant.	53
Figure 2.4.2 - Sampling of bottom ashes.	54
Figure 2.4.3 - Bottom ash samples.	54
Figure 2.4.4 - Sampling of fly ashes.	55
Figure 2.4.5 - Fly ash samples.	55
Figure 2.4.6 - Time schedule of the experimental campaigns.	56
Figure 2.5.1 - Samples treatment and analysis.	60
Figure 2.5.2 - Illustration of bottom ash samples treatment and preparation for the laboratory analysis.	61
Figure 2.5.3 - Laboratory device used to measure metallic aluminium content with the “soda attack” method.	64
Figure 2.5.4 - Units forming the laboratory device used to measure the metallic aluminium content through the “soda attack” method.	65
Figure 2.5.5 - Sample tablets ready for XRF analysis.	68
Figure 2.5.6 - Press machine used for the preparation of the tablets.	68
Figure 2.5.7 - Equipment for XRF analysis.	68
Figure 2.5.8 - Quantometer used for the determination of metallic aluminium content in the ingots from the melting process.	70
Figure 2.5.9 - Metal ingots after the OES analysis.	70
Figure 2.5.10 - Evaluation of the sensitivity for the instrument used in the soda attack analysis (fly ash samples taken during Test 1 on aluminium beverage cans).	72

Figure 3.1.1 - Trend of metallic aluminium percentage content (on the dry weight) in the ingots resulting from the melting process (Test 1).	75
Figure 3.1.2 - Numerical integration of recoverable aluminium curve.	77
Figure 3.1.3 - Trends of total and metallic aluminium percentage content (on the dry weight) in the fraction below 0.8 mm resulting from the first screening (Test 1).	79
Figure 3.1.4 - Trends of total and metallic aluminium percentage content (on the dry weight) in the fraction below 0.8 mm resulting from the second screening (Test 1).	80
Figure 3.1.5 - Percentage content of total and metallic aluminium measured in fly ash samples (Test 1).	82
Figure 3.2.1 - Trend of metallic aluminium percentage content (on the dry weight) in the ingots resulting from the melting process (Test 2).	89
Figure 3.2.2 - Trends of total and metallic aluminium percentage content (on the dry weight) in the fraction below 0.8 mm resulting from the first screening (Test 2).	93
Figure 3.2.3 - Trends of total and metallic aluminium percentage content (on the dry weight) in the fraction below 0.8 mm resulting from the second screening (Test 2).	93
Figure 3.2.4 - Percentage content of total and metallic aluminium measured in fly ash samples (Test 2).	96
Figure 3.3.1 - Trend of metallic aluminium percentage content (on the dry weight) in the ingots resulting from the melting process (Test 3).	102
Figure 3.3.2 - Trends of total and metallic aluminium percentage content (on the dry weight) in the fraction below 0.8 mm resulting from the first screening (Test 3).	104
Figure 3.3.3 - Trends of total and metallic aluminium percentage content (on the dry weight) in the fraction below 0.8 mm resulting from the second screening (Test 3).	104
Figure 3.3.4 - Trend of metallic aluminium percentage content (on the dry weight) in the ingots resulting from the melting process (Test 3).	106
Figure 3.3.5 - Percentage content of total aluminium measured in fly ash samples (Test 3).	108
Figure 3.4.1 - Trend of metallic aluminium percentage content (on the dry weight) in the ingots resulting from the melting process of the 0.8 - 5 mm and > 5 mm sub-fractions (Test 4).	113
Figure 3.4.2 - Trends of total and metallic aluminium percentage content (on the dry weight) in the fraction below 0.8 mm resulting from the first screening (Test 4).	118
Figure 3.4.3 - Trends of total and metallic aluminium percentage content (on the dry weight) in the fraction below 0.8 mm resulting from the second screening (Test 4).	118
Figure 3.4.4 - Percentage content of total and metallic aluminium measured in fly ash samples (Test 4).	121
Figure 3.5.1 - Relationship between aluminium packaging thickness and the recoverable amount of aluminium from the incineration residues.	127
Figure 3.5.2 - Relationship between aluminium packaging thickness and the overall oxidation of aluminium in the incineration residues.	129

List of Tables

Table I -	Main characteristics of Valmadrera WTE plant.....	12
Table II -	Oxidation of aluminium recovered in the incineration residues for each type of tested packaging.	16
Table 1.3.1 -	Recovery rates (referred to wet mass) of aluminium from MSWI bottom ash.	27
Table 1.6.1 -	Results of laboratory tests carried out by Buekens (1993) on aluminium packaging.	34
Table 1.6.2 -	Results of full-scale tests carried out by Buekens (1993) on aluminium packaging.	34
Table 2.1.1 -	Tested materials.	36
Table 2.2.1 -	Incinerated waste and related residues produced by line 3 of Valmadrera WTE plant.	41
Table 2.2.1 -	Average stack concentration of the main pollutants during the experimental campaigns.	41
Table 2.2.3 -	Main operating parameters of the plant during the experimental campaigns.	42
Table 2.3.1 -	Doped waste fed into the furnace during the two experimental campaigns.	48
Table 2.3.2 -	Composition of the residual waste incinerated in Valmadrera WTE plant during standard operations (average value based on the analyses of November and December 2010) and of the waste produced by Seruso selection plant (analysis of January 2011).	48
Table 2.3.3 -	Residence time of the waste from the feeding hopper to the bottom ash extraction system.	51
Table 2.5.1 -	Test to evaluate the reproducibility of measures for the XRF spectrometer used in the laboratory analysis.	71
Table 3.1.1 -	Dry weight, humidity and sub-fractions (expressed as weight percentage on dry samples) obtained from the pre-treatment bottom ash samples taken during Test 1 on aluminium beverage cans.	73
Table 3.1.2 -	Yields (%) obtained from non-ferrous metals melting process and contribution (%) of manually sorted lumps (Test 1).	74
Table 3.1.3 -	Calculation of fed packaging average contribution in the ingots (Test 1).	77
Table 3.1.4 -	Aluminium percentage content (on the dry weight) in the salt dross samples resulting from the melting process (Test 1).	78
Table 3.1.5 -	Loss of metallic aluminium during the melting process in the crucible (Test 1).	78
Table 3.1.6 -	Aluminium content in an oxidized form in the bottom ash fine fractions resulting from the first and second screening (Test 1).	81
Table 3.1.7 -	Calculation of fed packaging average contribution in the bottom ash fine fractions resulting from the first and second screening (Test 1).	82
Table 3.1.8 -	Calculation of fed packaging average contribution in fly ashes (Test 1).	83
Table 3.1.9 -	Waste and residues flow rates used in the calculation of the final mass balance for aluminium beverage cans (Test 1).	84
Table 3.1.10 -	Mass balance related to Test 1 on aluminium beverage cans.	85
Table 3.2.1 -	Dry weight, humidity and sub-fractions (expressed as weight percentage on dry samples) obtained from the pre-treatment of bottom ash samples taken during Test 2 on aluminium trays.	87
Table 3.2.2 -	Yields (%) obtained from non-ferrous metals casting process and contribution (%) of manually sorted lumps (Test 2).	88
Table 3.2.3 -	Calculation of fed packaging average contribution in the ingots (Test 2).	90
Table 3.2.4 -	Aluminium percentage content (on the dry weight) in some salt dross samples from the melting process (Test 2).	90
Table 3.2.5 -	Loss of metallic aluminium during the melting process in the crucible (Test 2).	91
Table 3.2.6 -	Calculation of fed packaging average contribution in the bottom ash fine fractions resulting from the first and second screening (Test 2).	94
Table 3.2.7 -	Aluminium content in an oxidized form in the bottom ash fine fractions resulting from the first and second screening (Test 2).	95
Table 3.2.8 -	Calculation of fed packaging average contribution in fly ashes (Test 2).	97
Table 3.2.9 -	Waste and residues flow rates used in the calculation of the final mass balance for aluminium trays (Test 2).	97
Table 3.2.10 -	Mass balance related to Test 2 on aluminium trays.	98

Table 3.3.1 - Dry weight, humidity and sub-fractions (expressed as weight percentage on dry samples) obtained from the pre-treatment of bottom ash samples taken during Test 3 on aluminium spray cans.	100
Table 3.3.2 - Yields (%) obtained from non-ferrous metals melting process and contribution (%) of manually sorted lumps (Test 3).	101
Table 3.3.3 - Aluminium percentage content (on the dry weight) in some salt dross samples resulting from the melting process (Test 3).	103
Table 3.3.4 - Loss of metallic aluminium during the melting process in the crucible (Test 3).	103
Table 3.3.5 - Calculation of fed packaging average contribution in the bottom ash fine fractions resulting from the first and second screening (Test 3).	105
Table 3.3.6 - Calculation of fed packaging average contribution in the ingots (Test 3).	107
Table 3.3.7 - Aluminium content in an oxidized form in the bottom ash fine fractions resulting from the first and second screening (Test 3).	107
Table 3.3.8 - Waste and residues flow rates used in the calculation of the final mass balance for aluminium spray cans (Test 3).	109
Table 3.3.9 - Mass balance related to Test 3 on aluminium spray cans.	109
Table 3.4.1 - Dry weight, humidity and sub-fractions (expressed as weight percentage on dry samples) obtained from the pre-treatment of bottom ash samples taken during Test 4 on aluminium and poly laminated foils.	111
Table 3.4.2 - Yields (%) obtained from non-ferrous metals melting process and contribution (%) of manually sorted lumps (Test 4).	112
Table 3.4.3 - Total recovery of metallic aluminium from the two coarse sub-fractions and contribution of the 0.8 - 5 mm sub-fraction to this value (Test 4).	114
Table 3.4.4 - Calculation of fed packaging average contribution in the ingots (Test 4).	115
Table 3.4.5 - Aluminium percentage content (on the dry weight) in the salt dross resulting from the melting process of the 0.8 - 5 mm sub-fraction (Test 4).	116
Table 3.4.6 - Loss of metallic aluminium during the melting process in the crucible (Test 4).	117
Table 3.4.7 - Calculation of fed packaging average contribution in the bottom ash fine fractions resulting from the first and second screening (Test 4).	119
Table 3.4.8 - Aluminium content in an oxidized form in the fine fractions (below 0.8 mm) resulting from the first and second screening (Test 4).	120
Table 3.4.9 - Calculation of fed packaging average contribution in fly ashes (Test 4).	122
Table 3.4.10 - Waste and residues flow rates used in the calculation of the final mass balance for aluminium and poly laminated foils (Test 4).	122
Table 3.4.11 - Mass balance related to Test 4 on aluminium and poly laminated foils.	123
Table 3.5.1 A - Partitioning of total aluminium recovered in the incineration residues for each type of tested packaging.	125
Table 3.5.1 B - Partitioning of metallic aluminium recovered in the incineration residues for each type of tested packaging.	125
Table 3.5.2 - Oxidation levels of aluminium recovered in the incineration residues for each type of tested packaging.	128
Table 3.5.3 - Metallic aluminium content in the incineration residues in standard operation conditions (i.e. non-doped waste).	130
Table 3.5.4 A - Potential for energy recovery from the oxidation of aluminium scraps during Test 1 on aluminium beverage cans.	131
Table 3.5.4 B - Potential for energy recovery from the oxidation of aluminium scraps during Test 2 on aluminium trays.	131
Table 3.5.4 C - Potential for energy recovery from the oxidation of aluminium scraps during Test 4 on aluminium and poly laminated foils.	131
Table 3.5.5 - Average contents of other non-ferrous metals and iron in the ingots from the melting process for each type of tested packaging.	132

ABSTRACT

Despite the separate and multi-material collection of aluminium is well established in Italy and in the EU Countries due to the implementation of nationwide aluminium packaging recycling schemes, a significant amount still ends up in the residual waste generally routed to incineration for energy recovery. The direct extraction of aluminium from municipal solid waste incineration (MSWI) bottom ash represents an important breakthrough in the aluminium recycling industry. However, during the combustion process, aluminium scraps contained in the waste undergo volatilization and oxidation mechanisms that are little known but certainly determine a loss of recoverable mass. The research project described in this thesis has the purpose of assessing the potential recovery of aluminium from the bottom ashes produced in a full-scale waste-to-energy (WTE) plant, in an attempt to provide useful indications for a better understanding of those parameters that affect the overall yield of the process. Two experimental campaigns were conducted on the same WTE plant in order to investigate the behaviour of four different aluminium packaging items inside the incineration furnace: during the first campaign, three types of aluminium rigid packaging (beverage cans, trays and spray cans) were tested, whereas the second campaign was devoted to aluminium flexible packaging (mix of aluminium and poly laminated thin foils). Each predetermined amount of packaging items was mixed with the residual waste ready for incineration in order to increase by four times its standard aluminium concentration. The doped waste was fed into the furnace and the solid incineration residues (i.e. bottom ashes and fly ashes) were sampled at regular intervals, before and after the effect of doping. After the simulation of an advanced treatment aimed at recovering aluminium from bottom ashes (which included the melting process in a crucible simulating the conditions of secondary aluminium production), all the samples were analyzed in laboratory for the measurement of their aluminium content. The results indicate that the structure of the packaging has a significant impact both on the recovery yield and on the average oxidation of aluminium. Aluminium recovery yield is directly related to packaging thickness and ranges between 27% for aluminium and poly laminated foils and 80% for beverage cans. In contrast, aluminium average oxidation is inversely related to packaging thickness and ranges between 9% for beverage cans and 59% for aluminium and poly laminated foils. The evaluation of the results also highlighted all the problems and limitations relevant to the planning of future experimental campaigns.

SUMMARY AND CONCLUSIONS

The research project described in this thesis has the purpose of evaluating the behaviour of aluminium packaging fed into the furnace of a full-scale WTE plant, in order to estimate the amount of aluminium potentially recoverable from MSWI bottom ash. The recovery of aluminium should be an essential step of a bottom ash treatment plant, both for the economic and environmental advantages of its recycling and for the reduction of negative effects due to its presence in the recovered inert material, which can result in swelling and expansion in some applications including road construction and concrete production.

However, during the incineration process, aluminium scraps contained in the waste undergo volatilization and oxidation processes that determine a loss of their recoverable mass from bottom ashes. The thinner fraction will volatilize in the furnace, then leave the waste entrained by the flue gas and subsequently concentrate on the surface of fly ashes, both as metallic aluminium and aluminium oxide (alumina - Al_2O_3). The remaining fraction of aluminium, despite remaining in the waste, will certainly undergo surface oxidation: a thin scale of a more or less protective oxide is formed on the surface of these scraps, as a consequence of the reactions with oxidizing compounds contained in the combustion flue gases, such as O_2 , SO_2 , HCl and molten salts which collect over the metal surface. In this case, even if a reduction of the scrap mass is not detectable, its recycling potential is lowered because the oxide cannot be recovered in the melting furnace for the production of secondary aluminium.

The actual volatilization and oxidation rates of metal scraps in the incineration furnaces are not yet well known. According to the CEN standard on energy recovery (EN 13431:2004), thin gauge aluminium foil (up to 50 μm thick) shall be considered recoverable in the form of energy, meaning that it is subjected to full and complete oxidation during the combustion process. However, detailed quantitative experimental estimates are not available. Therefore, the main goals of the study described in the present thesis are essentially two:

- The quantification of aluminium partitioning in the solid residues of the incineration process (i.e. bottom ashes and fly ashes) in order to assess how much of the aluminium fed with different types of packaging is found in the different bottom ash size fractions and how much is lost in fly ashes. Total and metallic aluminium

contents are measured separately, the latter representing the potential amount of aluminium that can be recovered.

- An estimate of the oxidation levels of aluminium recovered in the different incineration residues.

The research project was developed on a WTE plant located in Valmadrera (Province of Lecco, Lombardia, Northern Italy), whose main characteristics are summarized in Table I. It consisted of two experimental campaigns, during which the behaviour of four different aluminium packaging items was investigated. During the first campaign, three types of aluminium rigid packaging (beverage cans, trays and spray cans) were tested, whereas the second campaign was devoted to aluminium flexible packaging (mix of aluminium and poly laminated thin foils). All the tests were performed on line 3 of the plant.

Table I - Main characteristics of Valmadrera WTE plant.

Type	Forward-acting horizontal grate, wet discharge system of bottom ashes
Waste sources	Urban, urban-like non hazardous waste
Number of lines	2 (line 1 and line 3)
Hourly capacity	15.5 t h ⁻¹ (6 t h ⁻¹ on line 1 and 9.5 t h ⁻¹ on line 3)
Furnace temperature	850 - 1050 °C
O₂ in combustion chamber	5 - 6 %

An overview of the general approach used in the present research project is reported in the scheme of Figure I.

A doped waste charge was prepared by mixing the aluminium packaging items with residual waste ready for incineration in order to increase by four times its standard aluminium concentration. The doped waste charge was then fed into the furnace during approximately one or two hours.

The solid residues of the incineration process (i.e. bottom ashes and fly ashes) were sampled every 30 minutes on average, depending on the operating conditions of the plant. The sampling period lasted from 8 to 10 hours but it turned out to be too short for a complete

evaluation of the mass balance related to the introduced amount of aluminium, since the waste residence time in the furnace was much longer than expected.

The samples were analyzed in laboratory to assess the partitioning of aluminium introduced with the different types of packaging in the incineration residues and its corresponding oxidation level.

Bottom ash samples were previously treated in order to simulate an advanced system for aluminium recovery and prepare them to meet the requirements of laboratory analysis. They underwent a series of consecutive size classifications, sorting and grinding steps before the final melting process in a crucible simulating secondary aluminium production. Total and metallic aluminium contents in the fine fractions below 0.8 mm (resulting from the two screening steps, one before and the other after grinding) were respectively measured through X-Ray Fluorescence Spectroscopy (XRF) and the “soda attack” method. Metallic aluminium content in the ingots resulting from the melting process, representing the actual amount of recoverable aluminium, was measured through Optic Emission Spectroscopy (OES).

Fly ash samples were directly analyzed through XRF and soda attack to determine their total and metallic aluminium contents since they did not require any preparation for laboratory analysis.

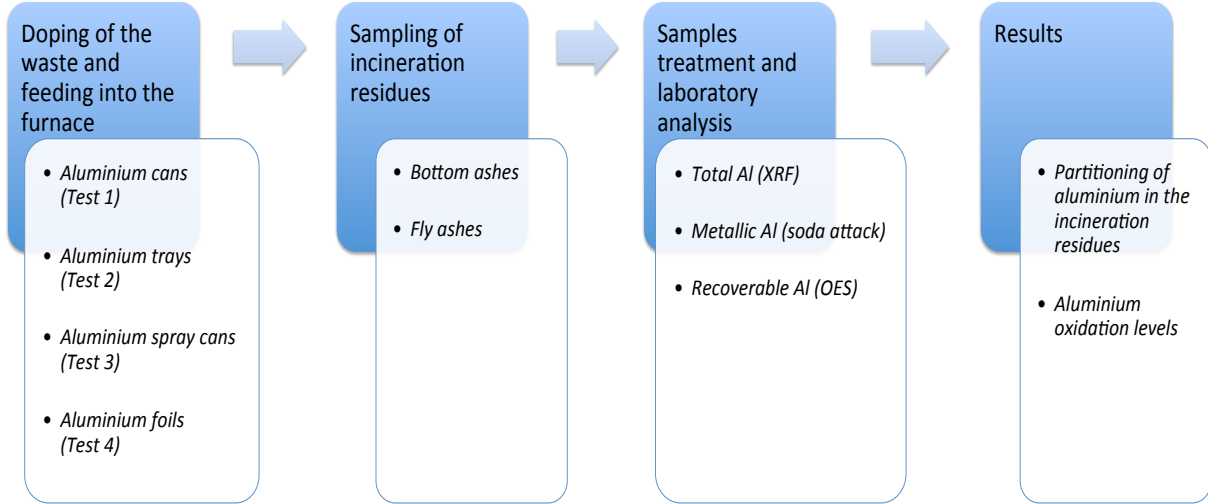


Figure I - Scheme of the general approach used in the present research project.

Figures II A-B summarize the partitioning of total (A) and metallic (B) aluminium recovered in the incineration residues for each type of tested packaging (except for spray cans, whose

results are not reliable from a scientific point of view and hereby not mentioned in the conclusions of this study, as it will be further discussed). Aluminium in the ingots from the melting process is all metallic by definition.

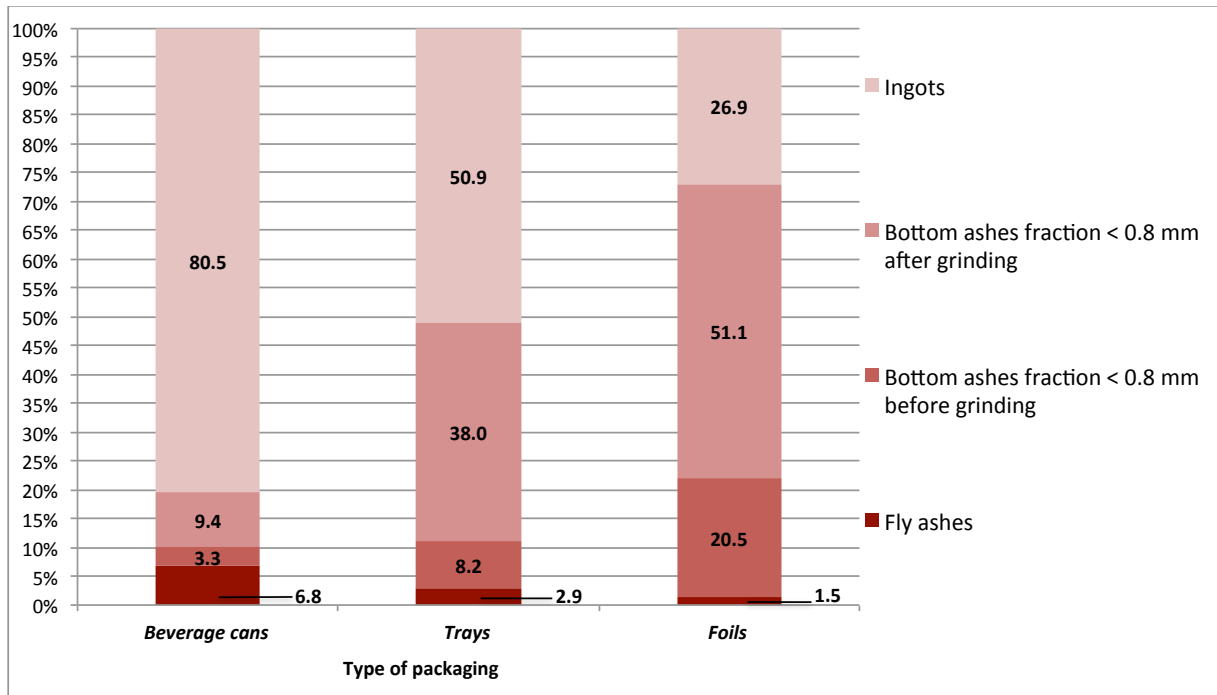


Figure II A - Partitioning of total aluminium recovered in the incineration residues for each type of tested packaging.

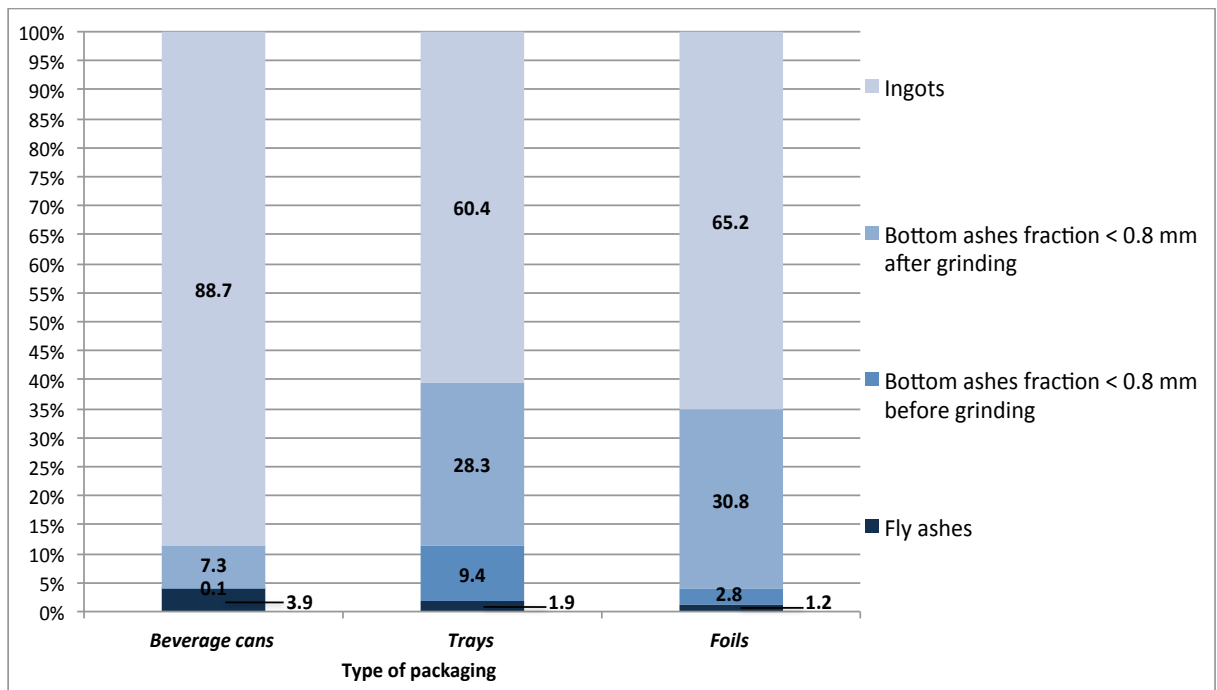


Figure II B - Partitioning of metallic aluminium recovered in the incineration residues for each type of tested packaging.

The amount of aluminium that is found in fly ashes is below 7% for all the types of packaging. In contrast, data corresponding to the bottom ash fine fractions are characterized by high variability. In any case, in both fractions aluminium metal fragments are extremely small and their recovery is virtually impossible using the current Eddy Current Separation (ECS) technology: for all the intents and purposes, their aluminium content must be considered as a loss of material.

Total aluminium partitioning in the fine fraction after the first screening step (before grinding) varies between 3.3% for beverage cans and 20.5% for foils, whereas in the fine fraction after the second screening step (after grinding) it varies between 9.4% for beverage cans and 51.1% for foils. This variability is mainly related to the packaging structure. Compared to beverage cans, the thickness and the technical strength of trays and foils are lower and, consequently, lumps that form in the furnace are very small: this facilitates their migration in the finer fractions of bottom ashes.

Concerning the ingots from the melting process, there are many differences between the three types of packaging. The partitioning of total aluminium (expressed by the ratio between the weight of aluminium recovered in the ingots and the weight of the overall amount of aluminium found in the residues) is about 80% for beverage cans, 51% for trays and 27%¹ for foils. As previously stated, data related to ingots are representative of the actual amount of aluminium that can be recovered through an advanced bottom ash treatment combined with the melting process in a saline furnace for the production of secondary aluminium. In particular, data referring to aluminium and poly laminated foils are very interesting because they emphasize the contribution of the 0.8 - 5 mm sub-fraction to the overall amount of metallic aluminium recovered in the ingots. Indeed, about 80% of this amount comes from the ingots resulting from the melting of the 0.8 - 5 mm sub-fraction, meaning that the recovery yield of aluminium from this specific packaging would increase by 390% by adding to the traditional ECS system an advanced ECS specifically calibrated on grains smaller than 5 mm. Table II shows the oxidation of aluminium recovered in the incineration residues for each type of tested packaging.

¹ Considering the ingots resulting from both the 0.8 - 5 mm and > 5 mm sub-fractions, about 21% and 6%, respectively.

Table II - Oxidation of aluminium recovered in the incineration residues for each type of tested packaging.

Residue	Aluminium oxidation (%)		
	<i>Beverage cans</i>	<i>Trays</i>	<i>Foils</i>
<i>Fly ashes</i>	47	45	66
<i>Bottom ash fraction < 0.8 mm before grinding</i>	96	4	94
<i>Bottom ash fraction < 0.8 mm after grinding</i>	30	37	75
<i>Ingots*</i>	0	0	0
AVERAGE	9.2	17.4	58.8

*Aluminium contained in the ingots is all metallic by definition.

Values reported in Table II are representative of the real oxidation level of aluminium added through the doping of the waste, as they do not include the background concentration deriving from aluminium already present in the residual non-doped waste fed into the furnace. The average oxidation levels highlight the influence of packaging thickness: the thicker the packaging, the less it is oxidized during the combustion process. This is a consequence of the smaller surface area exposed to the oxidizing gases in the furnace, due to the formation of bigger aluminium lumps.

Concerning this aspect, the packaging technical strength plays an important role too, avoiding or reducing the fragmentation of the material and the consequent increase in the exposed surface.

1. INTRODUCTION

1.1. Overview and objectives of the present study

About 4,600,000 tonnes of municipal waste have been incinerated in Italy in 2009, with the production of about 1,200,000 tonnes of bottom ashes (ISPRA, 2011). The growing cost of landfilling and the need for reducing the exploitation of natural resources have promoted in the last few years in Europe a fervent research activity on bottom ash treatments aimed at recovering metals and reusing the inert fraction, essentially in the cement and concrete industry, as well as in road construction.

These treatments include physical, chemical or thermal processes such as:

- Physical separation of the fine (more polluted) fraction with screens or drums;
- Extraction of metals through magnetic and eddy current separators;
- Washing with water or chemical solvents to remove soluble heavy metals and salts;
- Ageing process to promote the transformation of bottom ash constituents into more thermodynamically stable forms;
- Addition of Al (III) or Fe (III) salts and cements or other bonding agents to reduce the metal mobility through leaching;
- Vitrification or sintering to immobilize heavy metals into an amorphous glassy phase.

Whatever treatment is used, the recovery of ferrous and non-ferrous metals is an essential step, for both the environmental advantage of metal scraps recycling and the reduction of negative effects of metals, especially aluminium, which can result in swelling and expansion in some applications including road construction and concrete production (Pecqueur et al., 2001; Muller et al., 2006). Furthermore, the sale of metal scraps represents a significant source of income for bottom ash treatment plants.

Focusing on aluminium, despite its separate collection is well established in Italy and in the EU Countries due to its widespread utilization as a packaging material, a significant amount still ends up in the residual waste, which is generally routed to incineration for energy recovery. During this process, the scraps contained in the waste undergo volatilization and oxidation processes that determine a loss of their recoverable mass from bottom ashes. The thinner fraction will volatilize in the furnace, then leave the waste entrained by the flue gas

and subsequently concentrate on the surface of fly ashes, both as metallic aluminium and aluminium oxide (alumina - Al_2O_3). The remaining fraction of aluminium, despite remaining in the waste, will certainly undergo surface oxidation: a thin scale of a more or less protective oxide is formed on the surface of these scraps, as a consequence of the reactions with oxidizing compounds contained in the combustion flue gas, such as O_2 , SO_2 , HCl , and molten salts which collect over the metal surface. In this case, even if we do not measure a reduction of the scrap mass, its recycling potential is lowered because the oxide cannot be recovered in the melting furnace. Such oxidation can be further enhanced when bottom ashes are quenched in water after their discharge from the furnace grate (which is the case for the majority of waste incineration plants currently operating in Europe); indeed the strong thermal shock can break down the oxidation layer, facilitating a further degradation of the scraps. The result of all the processes previously described is a loss of the potentially recoverable aluminium mass, compared to what is fed to the process within the municipal waste.

The actual volatilization and oxidation rates of metal scraps in the incineration furnaces are not yet well known. According to the CEN standard on energy recovery (EN 13431:2004), thin gauge aluminium foil (up to 50 μm thick) shall be considered recoverable in the form of energy, meaning that it is subjected to full oxidation. However, detailed quantitative experimental estimates are not available. Some data about oxidation levels of flexible and rigid aluminium packaging are reported by Pruvost (2009), but they refer to experiments carried out in 1993 and described in a confidential report. Also Hu et al. (2011) reported the oxidation level of aluminium scraps after their incineration and the influence of combustion conditions on metallic aluminium losses during the incineration process, but they referred to laboratory tests performed in a laboratory scale pot.

The current research project has the purpose of evaluating the behaviour of aluminium packaging in a full-scale waste-to-energy plant, in order to quantify its partitioning in the residues of the incineration process and its corresponding oxidation level, and to estimate the potential amount of aluminium recoverable from bottom ashes. Total and metallic aluminium contents are measured separately, the latter representing the potential amount of aluminium that can be recovered.

1.2. Aluminium recycling in Europe

Recycling is a major consideration in continued aluminium use, representing one of the key attributes of this ubiquitous metal, with far-reaching economic, ecological and social implications. More than half of all the aluminium currently produced in the European Union (EU-25) originates from recycled raw materials and the trend is on the increase (EAA, 2004). In view of growing end-use demand and a lack of sufficient domestic primary aluminium production in this part of the world, Europe has a huge stake in maximizing the collection of all available aluminium, and developing the most resource-efficient scrap treatments and melting processes. The importance of efficient aluminium recycling will even further increase in the future because of rising energy constraints in this region.

The high intrinsic value of aluminium scrap has always been the main impetus for recycling, independent of any legislative or political initiative. But in addition to this obvious economic dimension, growing environmental concerns and heightened social responsibility, especially during this last decade, have served to boost the recycling activity, since recycling requires as little as 5% of the energy needed for primary aluminium production.

The aluminium economy is a cycle economy. Indeed, for most aluminium products, aluminium is not actually consumed during a lifetime, but simply used. Therefore, the life cycle of an aluminium product is not the traditional "cradle-to-grave" sequence, but rather a renewable "cradle-to-cradle". If scrap is processed appropriately, the recycled aluminium can be utilized for almost all aluminium applications, thereby preserving raw materials and making considerable energy savings.

From an environmental point of view, aluminium recycling is ecologically advantageous if the environmental impact of the collection, separation and melting of scrap is lower than that of primary aluminium production. In general, recycling of aluminium minimizes:

- Energy needs: energy savings of up to 95% are achieved per tonne of aluminium produced from scrap compared to primary aluminium production. Secondary aluminium produced from recycled metal requires only 2.8 kWh kg⁻¹, whereas primary aluminium production requires about 45 kWh kg⁻¹ (Das, 2006).
- Use of natural resources: in 2004, approximately 19 million tonnes of bauxite, 11 million tonnes of coal, 1 million tonne of natural gas and 6 million tonnes of crude oil were conserved globally as a result of aluminium recycling in Europe alone (EAA, 2004).

- Land use: aluminium scrap is a recyclable, non-hazardous and valuable raw material, which is not landfilled. If aluminium was a non-recyclable material, Europe would have landfilled 4.7 million tonnes more in 2004, which is equal to about 2 million m³ of landfill volume (EAA, 2004).
- Waste and pollution: industrial monitorings have shown that 1,370 kg of bauxite residues, 9,800 kg of CO₂ equivalent and 64 kg of SO₂ emissions are saved when producing 1 tonne of recycled aluminium instead of primary aluminium production (EAA, 2004).

Among the end-of-life product recycling, aluminium packaging fits every desired recycling and processing route. The amount of aluminium packaging effectively recycled greatly depends upon individual national requirements and the efficiency of the collection schemes; therefore rates vary from 25 to 80% across Europe. In 2010, the collection scheme in Italy has resulted in the recovery of 50,000 tons of used aluminium packaging (46,500 destined to material recycling and 3,500 to energy recovery), corresponding to the 77.9% of the amount circulating in the country (CiAl, 2010). In all cases, the value of the collected scrap covers most if not all of the related recycling costs. Most European countries have nationwide recycling schemes in place. These can be grouped into three main routes:

1. Separate collection of used beverage cans, either in designated deposit systems (Scandinavian countries and Germany), voluntary take back systems (Switzerland and Poland) or incentive-based projects (UK, Ireland, Hungary and Greece).
2. Multi-material packaging collection systems, where aluminium-containing packaging is part of the “light packaging flow” containing plastics, tinsplate, beverage cartons and sometimes paper packaging, newspapers and magazines. Here, aluminium is separated during the final step of sorting at the plant (e.g. Italy, Spain, Germany, Portugal, France, Belgium, Austria).
3. Direct extraction from the bottom ashes of municipal solid waste incinerators as aluminium lumps, in addition to the separate collection schemes (Netherlands, France, Belgium and Denmark, in particular).

Despite the separate collection and the multi-material collection of aluminium packaging is well established in almost all the EU Countries, a significant amount of this metal can still be found in the bottom ashes resulting from the incineration process of the unsorted residual waste in waste-to-energy plants: the Packaging Group of the European Aluminium

Association (EAA) and the Confederation of European Waste-to-Energy Plants (CEWEP) estimate that for the whole of Europe up to 200,000 tonnes of extra aluminium could be recycled each year from the bottom ashes, providing that more local waste management operators invest in the right separation equipment and that EU Member States take a more ambitious approach to prevent landfilling (EAA-CEWEP, 2011).

More specifically, for what concerns the situation in Italy, a study conducted by the Department of Environmental Engineering (DIAR) of Politecnico di Milano (Grosso et al., 2011) shows that, if conventional separation technologies are used, between 16,500 and 21,000 tonnes of aluminium can be recovered from bottom ashes in 2015 and between 19,000 and 28,500 tonnes in 2020; if advanced technologies² are used, the figures increase to 38,000-49,000 tonnes and to 43,500-66,000 tonnes in 2015 and in 2020, respectively. For both scenarios, the upper boundary of the range corresponds to a situation of ‘moderate’ growth in MSW production and of ‘high’ growth in commercialized aluminium packaging; the lower boundary corresponds to the opposite situation, i.e. ‘high’ growth of MSW production and ‘moderate’ growth in commercialized aluminium packaging. The results of the study are summarized in Figure 1.2.1.

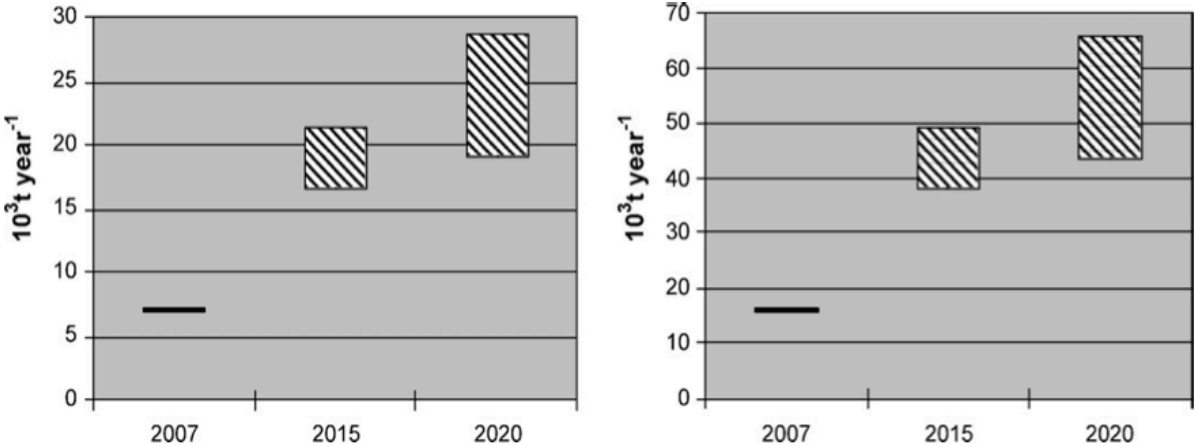


Figure 1.2.1 - Aluminium potentially recoverable from MSWI bottom ash in 2007, 2015 and 2020 in Italy (left: conventional technologies; right: advanced technologies) (Grosso et al., 2011).

² In the conventional technology scenario it is assumed that 30% of the aluminium fed to incineration plants and 40% of that fed to gasification plants can be recovered from bottom ashes. The first value is based on the literature data reported in Table 1.3.1 (Paragraph 1.3) whereas the second one assumes that metal extraction is more efficient from gasification than from incineration bottom ashes, due to a lower metal oxidation.

In the advanced technology scenario it is assumed that 70% and 80% of the aluminium fed to the furnace can be recovered from incineration and gasification bottom ashes, respectively. The first value has been defined considering the experience of Amsterdam pilot plant and other advanced technologies (Table 1.3.1). The recovery rate from gasification plants has been increased to 80% for the same reason explained before.

1.3. Recovery of aluminium scraps from MSWI bottom ash

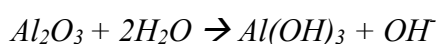
The current processes of waste incineration produce three distinct streams of solid residues: bottom ashes from the combustion, fly ashes retained during the dust collection phases and by-products resulting from acid gases neutralization. Bottom ashes represent the most relevant fraction; they are mainly composed of calcium, magnesium and iron silico-aluminates and characterized by a matrix similar to that of igneous rocks, but with much higher concentrations of metals.

Ferrous and non-ferrous metals are present in the bottom ashes in a range of 7-15% and 1-2%, respectively (Sabbas et al., 2003; Baun et al., 2007). Non-ferrous metals consist of aluminium, for more than 60%, and copper, brass and precious metals, such as gold, in minor quantity. In particular, aluminium is present in concentrations ranging from 10 mg g⁻¹ to 100 mg g⁻¹ (Bonelli, 2011), mainly in the alumino-silicates or as metal lumps resulting from the melting of aluminium items contained in the waste fed to incinerators.

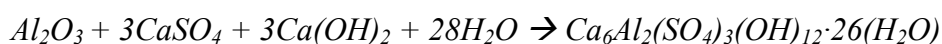
As already said, the recycling of aluminium provides major economic and ecological benefits. Furthermore, the removal of aluminium from MSWI bottom ash prevents possible negative effects such as swelling and expansion in some applications of the recovered inert material. In particular, in case of reuse of the inert material for cement and concrete production or for road beds construction, the hydration of aluminium causes the production of hydrogen that may lead to a degradation of the solid structure favouring cracks and water leaks. Indeed, in an alkaline environment, aluminium is involved in the following reactions:

- anodic process: $Al + 2H_2O \rightarrow AlO_2^- + 4H^+ + 3e^-$
- cathodic process: $2H_2O + 2e^- \rightarrow H_2 + 2OH^-$

The process is favoured by the contact between aluminium and the solution that forms from cement hydration, characterized by a pH close to 13. When the pH drops to values around 9-10, another reaction takes place:



with the production of Al(OH)₃ in a gel form. Further issues related to aluminium can occur when the material is saturated with water:



In this case, the formation of ettringite causes swelling, thus increasing the risk of cracking (CiAl, 2010).

The removal of aluminium scrap is therefore a fundamental aspect of an advanced process of bottom ash treatment, which actually consists of several steps.

Generally, the first one is the aging process, during which the material is stored for a period of time that ranges from 2-3 days up to 3-12 months. For short periods it is mostly a simple storage, whose primary purpose is to reduce the humidity in order to make the material suitable for the next stages, especially for bottom ashes extracted in a water bath. When the storage lasts more than 20 days, phenomena of carbonation and oxidation of the unburned material begin to occur and the real aging process takes place: the leaching rate of most constituents decreases, especially for heavy metals.

The second step is a size classification. In addition to a real improvement concerning the geotechnical characteristics of the inert aggregate later sent to the recovery, this step increases the percentage recovery of metals and removing the finest, most polluted fraction. Flat or rotary drum screens are used, usually with a mesh size of 20-50 mm for the coarse fraction and 2-10 mm for the fine fraction. In the most efficient configurations, the size of the coarse fraction is reduced by an additional grinding step promoting the liberation of metal particles. Generally a grid is placed as pre-treatment step to separate the material of largest size (> 15 cm), mainly consisting of unburned items and iron. The size classification can be also carried out using wet processes and, in this case, in addition to a physical separation of the material, soluble components such as copper and lead (responsible for leaching) can be extracted.

The third phase consists of the actual recovery of metals. For iron, classic magnetic separators are used. Aluminium falls into the category of non-ferrous metals such as copper and brass. These metals are removed from the flow of inert material through an "eddy current" magnetic separator, also known as Eddy Current Separator (ECS). The working principle of an ECS is quite simple: an electrical charge is induced into a conductor by changes in the magnetic flux cutting through it. Such changes in the magnetic flux can be achieved by moving permanent magnets past a conductor. The effect of these currents is to induce a secondary magnetic field around the particle; this field reacts with the magnetic field of the rotor, resulting in a combined driving and repelling force that literally ejects the conducting particle from the product stream. In most of the ECS systems, a high speed magnetic rotor is fitted within a non-metallic drum which travels much more slowly than the rotor so as to produce flux variations at the surface of the drum; the drum also acts as the head pulley of the conveyor carrying the product to be separated. As the conveyor carries the conducting particles over the drum, the magnetic field passing through the particles induces currents into them. Since these

particles are of random shapes, it is difficult for the induced current to flow within them in an orderly manner and the currents therefore tend to swirl around within the particles, hence eddy current. Non-ferrous metals, in contact with the magnetic field, are rejected with a force that is proportional to the ratio between their conductivity and their specific weight and pushed away with different trajectories from those of the inert material, whose stream is collected separately.

The machine requires a proper calibration, performed on the basis of the size of the material to be separated. The higher yields are obtained with small sized lumps, which generally should not exceed 15 cm, and for material flows below 15 t h^{-1} (Maglio, 2003). For these reasons, the first stage of granulometric classification is essential in order to create different material flows of homogeneous size and possibly place a magnetic separator and an ECS sequentially on each identified stream. Once ferrous and non-ferrous metals are recovered, bottom ashes can be subjected to washing or to neutralization processes, depending on the recovery application required for the inert fraction.

Once aluminium scraps are collected and properly treated to remove paints and other organic compounds, they are melted down in a furnace for the production of secondary aluminium. The most commonly used furnace in the secondary aluminium industry is the rotary furnace where aluminium scrap is melted under a layer of salt which consists of a mixture of approximately 30% KCl and 70% NaCl, but it may also contain small amounts of CaF_2 (Schneider et al, 1999). This salt layer fulfills a variety of tasks: it enhances the heat transfer to the metal, it prevents the oxidation of the metal and takes up contaminants, such as oxides, carbides and others contained in the scrap or produced by reactions during the melting process. The amount of salt used for the melting process depends on the scrap characteristics and varies in a range of 300 - 400 kg/t aluminium scrap. First, the salt is melted down in the rotary furnace. Then, the scrap is charged into the salt bath and finally, after the metal is molten, it is separated from the salt dross and the latter is cast into steel moulds where it cools down.

The advantage of the rotary furnace is that even highly contaminated scraps can be handled. The disadvantages are the costs for the processing of the salt dross and the high-energy demand because, in addition to the metal, the salt has to be melted down. Depending on the scrap mix, the amount of salt dross produced ranges from 400 to 700 kg/t of secondary aluminium. It contains contaminants like oxides, carbides, sulphides and traces of PCDD/F, as well as the metallic aluminium that is entrapped in the dross.

The recovery rates of aluminium from MSWI bottom ash, as reported by different authors, are depicted in Table 1.3.1.

Table 1.3.1 - Recovery rates (referred to wet mass) of aluminium from MSWI bottom ash (Grosso et al., 2011).

References		u.o.m.	Recovery rate
<i>Magnus Project NL (2003)</i>		% in mass (recovered Al/bottom ash)	1.77
<i>Aluminium and Miljo (2003)</i>	Kara > 6mm	% in mass (recovered Al/bottom ash)	0.36
	Vestforb. > 6 mm	% in mass (recovered Al/bottom ash)	0.128
	Vejen > 6 mm	% in mass (recovered Al/bottom ash)	0.288
	Odense > 6 mm	% in mass (recovered Al/bottom ash)	0.352
<i>Rem et al. (2004)</i>	Pilot plant AEB	% in mass (recovered Al/bottom ash)	1.2
<i>Association of Incinerators NL (2006)</i>		% in mass (recovered Al/bottom ash)	0.7–1.5
<i>CiAl (2006)</i>		% in mass (recovered Al/bottom ash)	0.49–1.17
<i>Alu (2006)</i>		% in mass (recovered Al/bottom ash)	0.65–0.78
<i>Muchova et al. (2007)</i>	Pilot plant AEB	% in mass (recovered Al/bottom ash)	1.62
<i>Muchova and Rem (2007)</i>		% in mass (recovered Al/bottom ash)	0.35–1.05
<i>Astrup et al. (2007)</i>		% in mass (recovered Al/bottom ash)	0.16–0.4
<i>Barcellesi (2008)</i>		% in mass (recovered Al/bottom ash)	0.8
<i>Lamers (2008)</i>		% in mass (recovered Al/bottom ash)	0.8
		% in mass (recovered Al/Al in the bottom ash)	32
<i>France Aluminium Recyclage (2006)</i>		% in mass (recovered Al/Al fed into the furnace)	35
<i>Association of Incinerators NL (2006)</i>		% in mass (recovered Al/Al fed into the furnace)	48.2
<i>Muchova and Rem (2007)</i>	State of the art	% in mass (recovered Al/Al fed into the furnace)	9–28
	Pilot plant AEB	% in mass (recovered Al/Al fed into the furnace)	80
	State of the art in NL 0-2 mm	% in mass (recovered Al/Al fed into the furnace)	0
	State of the art in NL 2-6 mm	% in mass (recovered Al/Al fed into the furnace)	7
	State of the art in NL 6-20 mm	% in mass (recovered Al/Al fed into the furnace)	45
	State of the art in NL >20 mm	% in mass (recovered Al/Al fed into the furnace)	86
	Pilot plant AEB 0-2 mm	% in mass (recovered Al/Al fed into the furnace)	0
	Pilot plant AEB 2-6 mm	% in mass (recovered Al/Al fed into the furnace)	83
	Pilot plant AEB 6-20 mm	% in mass (recovered Al/Al fed into the furnace)	87
	Pilot plant AEB >20 mm	% in mass (recovered Al/Al fed into the furnace)	n.d.
	Multistep unit	% in mass (recovered Al/Al fed into the furnace)	55–65
<i>Manders (2008)</i>	Advanced design	% in mass (recovered Al/Al fed into the furnace)	70
<i>Pruvost (2009)</i>	State of the art in France	% in mass (recovered Al/Al input to the bottom ash treatment plant)	65–70

For aluminium, eddy current separators show an average recovery efficiency of 30% of the aluminium fed into the furnace of the WTE plant, which corresponds to 1% of the bottom ash mass. However, some advanced technologies such as wet eddy current separators (WECS) and Magnus ECS can reach higher recovery rates (up to 70%) by improving the selective separation of small non-ferrous metal particles below 5 mm, as described by Muchova and Rem (2007) and Manders (2008).

The recovery efficiency of ferrous metals is higher than non-ferrous: about 80% of the steel fed into the furnace, i.e. 6% of the bottom ash mass, can be easily recovered. The relatively low recovery yield of aluminium compared to that of ferrous metals is also related to its peculiar behaviour during combustion. The thinner fractions of aluminium, such as foils or light packagings, are subjected to a partial volatilization in the furnace and a consequent concentration on the surface of fly ashes, which leads to an appreciable mass loss, thus affecting the potential recovery from bottom ashes.

Furthermore, even if they are deprived of all the possible impurities, aluminium lumps are always characterized by a partially oxidized surface, as a result of the thermal oxidation processes that occur inside the furnace (see Paragraph 1.6 about corrosion of aluminium in WTE plants). The oxidation level of aluminium lumps is closely connected to their size: the smaller they are, the greater is the surface area exposed to oxidation processes. In addition, the contact with water during the quenching of bottom ash causes the oxide scale to break up very easily because of the strong thermal shock, thus exposing the underlying layer of metallic aluminium to further oxidation and significantly lowering its potential recovery. The presence of aluminium oxide in the scraps promotes the formation of foams during the melting process because the oxide has a lower density than aluminium. As it happens in the production of primary aluminium, foams are removed but, along with them, part of the molten aluminium is inevitably lost. For this reason, aluminium lumps resulting from bottom ash treatment are fed in small percentages into the saline furnaces for the production of secondary aluminium, excluding the material that is too fine in order to avoid dramatic drops in term of recovery yields.

For a more general assessment of the potential aluminium recovery from the residual MSW, the mass balance excerpted from a study conducted in 2009 by the Department of Environmental Engineering of Politecnico di Milano (DIAR) is reported in Figure 1.3.1 (CiAl, 2010).

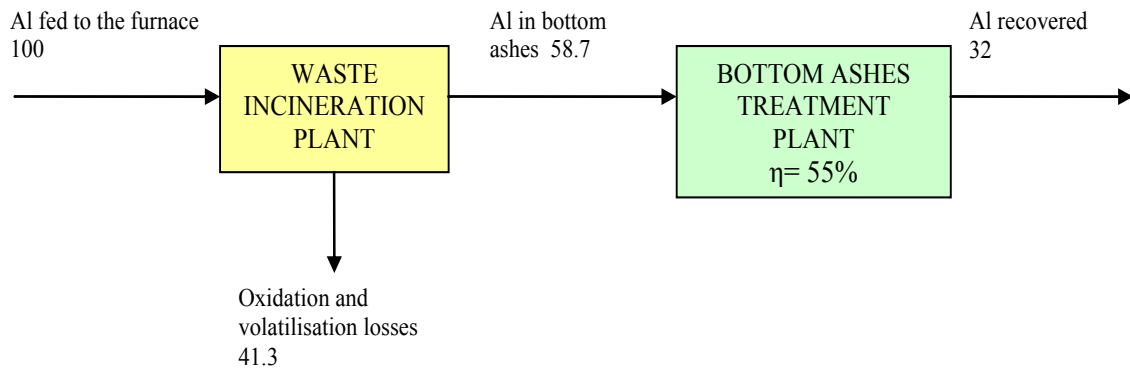


Figure 1.3.1 - Aluminium mass balance excerpted from a study conducted by the Department of Environmental Engineering of Politecnico di Milano in 2009 on aluminium recovery from waste incineration (CiAl, 2010).

Of the total amount of aluminium fed into the WTE plant furnace, approximately 41.3% is lost because of volatilization and oxidation processes, while 58.7% is found in the bottom ashes. Of this, only 32% is actually recovered, assuming an average efficiency of 55% for the bottom ash treatment process.

However, as underlined by the authors of the study, this is only an illustrative mass balance and yet still subject to many uncertainties. In particular, it is precisely the process of volatilization and oxidation of aluminium in the furnace to be less known. The purpose of the present study is to deepen the understanding of those phenomena in order to quantify the loss of aluminium in the incineration furnace and the potential for its recovery from bottom ashes, with particular regards to aluminium packaging.

1.4. Aluminium corrosion in high-temperature oxidizing atmospheres

Alumina (Al_2O_3) is the only thermodynamically stable solid oxide of aluminium. The oxide can exist in various modifications: the most common forms are the γ and the α phases, but also the δ - Al_2O_3 has been identified in scales formed at 900°C . The γ is the stable phase at temperatures below 900 - 950°C and it turns into the α phase when it is heated to high temperatures (above 900 - 1000°C), at which the α phase, called corundum, is the thermodynamically stable modification. The reverse transformation, however, does not take place on cooling. Although Al_2O_3 is the only stable solid oxide of aluminium, the vapour species at high temperatures comprise Al_2O and AlO .

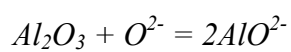
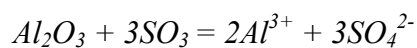
The α -alumina is characterized by a low concentration of electronic and ionic defects and, indeed, the transport through the scale of the reactants forming the oxide (metal cations and oxygen anions) is very slow. Probably this is related to the fact that this oxide has a large band gap (950 - 1050 kJ/mol) and high lattice energy.

With regard to the oxide scale growth, Al_2O_3 scales have constant ionic conductivity in the pressure range 1 - 10^{-15} atm of O_2 , while electronic conductivity predominates at lower oxygen pressures. This suggests that part of the oxide growth is governed by electron transport. However, the growth of alumina scales is more complicated and the transport of the reactants in all probability takes place along grain boundaries. Inward oxygen transport seems to be the principal mechanism for scale growth, however the wrinkling and convolutions of alumina scales suggest that oxide formation takes place also within the scales and that some outward diffusion of aluminium occurs. Furthermore, it is important to note that diffusion in polycrystalline samples is appreciably higher than that in single-crystal specimens.

During the initial stage of oxidation, aluminium develops a transient, metastable scale (γ and δ -alumina), which grows more rapidly than α - Al_2O_3 . The metastable alumina species have lower density than α - Al_2O_3 and their transformation in α - Al_2O_3 is accompanied by a 13% reduction in volume (Young, 2008).

Thanks to the formation of Al_2O_3 protective scale, aluminium is usually used in alloy with other elements such as chromium and silicon, to reduce the effects of corrosion process. Alumina scales generally provide better oxidation resistance and lower oxidation levels than chromia scales, especially at high temperatures. Instead, for temperatures below 800°C the aluminium-forming alloys are more susceptible to corrosion than chromia-forming alloys. This can be explained considering that the transient scales forming on alumina-forming alloys

contain a larger proportion of spinel phase than chromia-forming alloys and, moreover, the alumina formed in this range of temperature does not consist of the highly protective α - Al_2O_3 , but rather of the less protective γ - Al_2O_3 . Alumina does not suffer from oxidative evaporation and alumina-forming alloys can be used at higher temperatures than chromia-forming alloys, from an oxidation point of view. Furthermore, the capacity of alumina of delaying sulphidation is better than that of chromia, but the duration of the protective period also depends on the adhesion and mechanical integrity of the scales and the nature of the sulphidizing environment. In presence of molten Na_2SO_4 , alumina may dissolve through both acid and basic mechanisms, following the reactions:



However, Al_2O_3 is very stable towards basic fluxing and, moreover, for combustion gases at high temperatures, even those containing up to several percentages of SO_2 , the SO_3 level probably never becomes sufficiently high that acid fluxing constitutes an important problem.

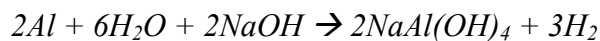
Corrosion of aluminium is also affected by the morphology and the composition of the item/scrap (Soler et al., 2007). The concentration of alloying elements modifies the oxidation behavior of the item/scrap. Certain elements strengthen the protective properties of the oxide film by forming mixed oxides, others, on the contrary, promotes aluminium oxidation. Tenorio and Espinosa (2000) compared the oxidation behaviour of two aluminium alloys used for beverage cans. Lid is made up of the alloy AA5182, which is composed for 4-5% of Mg, for 0.2-0.3% of Mn, for 0.2% of Si and for 0.35% of Fe, whereas the body of the can is made up of the alloy AA3004, composed for 0.8-1.3% of Mg, for 1-1.5 % of Mn, for 0.3% of Si and for 0.7% of Fe. Up to temperatures of 700°C, the oxidation kinetics of the lid material are greater than those of the body alloy due to the higher concentration of Mg, which has a greater affinity with oxygen than aluminium. However, for temperatures higher than 750-800°C the oxidation kinetic of the body changes and becomes linear. This suggests a loss of the initial protective characteristics.

1.5. Aluminium corrosion in aqueous solutions

The fundamental reaction of aluminium corrosion in aqueous media (Vargel, 2004) is:



Aluminium corrosion results in the formation of $Al(OH)_3$, which is insoluble in water and precipitates as white gel, and in the production of hydrogen gas. The corrosion reaction determines the rapid passivation of aluminium, which is recovered with an $Al(OH)_3$ layer (Stockburger et al., 1991). The corrosion process is more aggressive in presence of alkaline solutions. High pH values, in fact, can reduce aluminium surface passivation, enhancing aluminium corrosion. For example, in presence of NaOH the reactions involving aluminium are:



Initially, the hydrogen generation reaction consumes sodium hydroxide, but when the aluminate concentration exceeds the saturation limit, the aluminate undergoes a decomposition reaction that produces a crystalline precipitate of aluminium hydroxide with the regeneration of the alkali. The presence of OH^- ions promotes the dissolution of the oxide layer according to the reaction:



and hence facilitates the reaction between exposed Al and water and improves the corrosion rate (Soler et al., 2009; Pyun and Moon, 2000).

The production of hydrogen can lead to another mechanism of corrosion, named stress corrosion. This type of corrosion results from the combined action of a mechanical stress and a corrosive environment. The formation of an $Al(OH)_3$ layer on the aluminium surface traps water molecules that continue reacting with the metal to produce hydrogen (Ishii et al., 2007), which remains under the passive layer until the pressure of the gas is able to break it. In presence of cracks, the oxide film does not protect aluminium so it reacts with water and releases new hydrogen, which concentrates at grain boundaries and promotes intercrystalline decohesion.

1.6. Aluminium scraps corrosion in WTE plants

Aluminium packaging and other aluminium items contained in the waste fed to WTE plants undergo oxidation processes in the furnace (which represents a typical high temperature oxidizing environment), according to the reactions illustrated in Paragraph 1.4.

Moreover, the amount of aluminium that is not subjected to volatilization processes concentrates in bottom ashes and, when they are quenched in water, it can undergo a further corrosion process. The strong thermal shock can lead to the breakdown of the oxide layer, facilitating a further degradation of the scraps. In addition, the high pH values of the quenching water promote the dissolution of the alumina protective scale. At high pH values, there is a uniform corrosion of aluminium surface because the dissolution rate of the oxide film is greater than its rate of formation. This type of corrosion develops as pits of very small diameter, in the order of a micrometer, and results in a uniform and continuous decrease in thickness over the entire surface area of the metal.

Therefore, the bottom ash discharge method (wet or dry) can strongly influence the oxidation level of aluminium scraps and, as a consequence, their recycling efficiency. Lopez-Delgado et al. (2003) observed that the oxidation level of ferrous scraps recovered from bottom ashes is lower when they are not quenched in water, as in the case of fluidized bed combustion furnaces. This can be extended with a certain probability to non-ferrous scraps.

Laboratory tests carried out by Buekens in 1993 (Pruvost, 2011) show that the oxidation level of aluminium differs from a type of packaging to another and it is included between about 2% and 20%, when the item is exposed to a reducing atmosphere at 500°C for about 30 minutes and then to an oxidizing atmosphere for 30 minutes at 500°C and for other 30 minutes at 1100°C, and between about 0.5% and 40% when the item is exposed for an hour at 800°C with shredding every 10 minutes, as reported in Table 1.6.1. Full-scale tests, carried out on an incineration plant equipped with a dry extraction of bottom ashes, show that 84% of the flexible laminates and 60% of rigid packaging can be recovered in the bottom ashes with an oxidation level around 60% and 26% respectively, as illustrated in Table 1.6.2.

Controlled laboratory pot furnace tests, carried out by Hu et al. (2011) using base household waste with different aluminium packaging types (thin foils, foil containers and beverage cans), produced metallic aluminium recovery yields between 77 wt.% and 93 wt.% (Figure 1.6.1). The recovery yield varies as a function of the type of packaging and it increases with increasing material thickness. In addition, the type of aluminium packaging affects the

resulting size distribution, while the input shape (crumbled or sheet) has only a moderate influence. Furthermore, the oven tests showed that physical, thermal and chemical factors might promote metallic aluminium losses by enhancing the oxidation processes in the furnace. In order of decreasing impact the main factors were the packaging type, combustion temperature, residence time and salt contamination.

Table 1.6.1 - Results of laboratory tests carried out by Buekens (1993) on aluminium packaging.

Material	% Al	½ h 500°C reducing atmosphere ½ h 500°C and ½ h 1100°C oxidizing atmosphere		1h 800°C shredding every 10 min	
		Oxidation %	Thickness oxide µm	Oxidation %	Thickness oxide µm
Yoghurt lid Al 37 µm	93.9	19.4	10.8	8.2	4.6
Cheese pack Al 37 µm PE/EVA 30µm	77.1	13.3	7.4	0.6	0.3
Blister Al 30µm PE 30 µm	74.6	11.2	5.1	10.6	4.8
Biscuit pack Al 7-9 µm Paper 40 µm	28.4	23.6	2.9	42	5.2
Sachet Al 30µm LDPE 30 µm Paper 40 µm	54	3.9	1.8	4.4	2
Household foil Al 7-9 µm	100	n.a.	n.a.	7.8	0.9

Table 1.6.2 - Results of full-scale tests carried out by Buekens (1993) on aluminium packaging.

Residue	Flexible packaging (Al 7m-Paper-PE)		Rigid packaging (aerosol containers)	
	Partitioning %	Oxidation %	Partitioning %	Oxidation %
Bottom ashes	84	60	61	26
Fines under the grate	10	21	39	2
Fly ashes	6	13	0	-

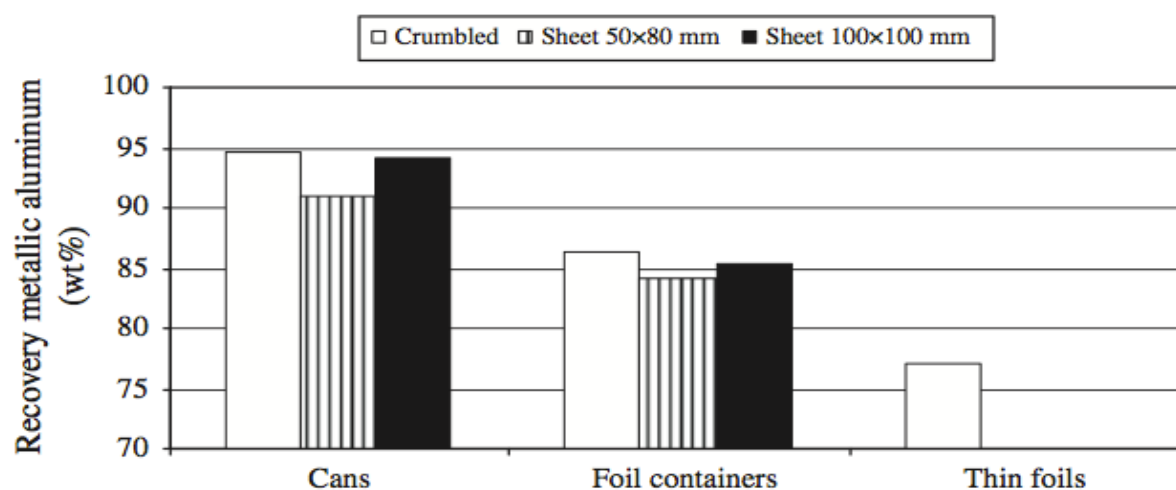


Figure 1.6.1 - Results of laboratory pot furnace tests carried out by Hu et al. (2011) on aluminium packaging.

2. MATERIALS AND METHODS

2.1. Overview of the experimental campaigns

The research project was developed on a full-scale waste incineration plant located in Valmadrera (Province of Lecco, Lombardia, Northern Italy) and was based on two experimental campaigns: during the first, the behaviour of rigid aluminium packaging items was investigated, whereas the second one was devoted to flexible aluminium packaging.

The first campaign (Test 1, Test 2 and Test 3) was carried out from the 6th to the 8th of June 2011. The municipal waste routinely fed to the plant was doped with three different types of rigid aluminium packaging:

- Aluminium beverage cans (Test 1, 6th of June 2011)
- Aluminium trays (Test 2, 7th of June 2011)
- Aluminium spray cans (Test 3, 8th of June 2011)

The second campaign (Test 4) was carried out on the 13th of July 2011. The waste was doped with two different types of flexible aluminium packaging mixed together:

- Aluminium foils
- Aluminium foils poly laminated with paper and plastic

The characteristics of the tested materials are reported in Table 2.1.1: they represent four types among the most widespread and typical items marketed in Italy for what concerns rigid (beverage cans and spray cans), semi-rigid (trays) and flexible (foils and poly laminated foils) aluminium packaging. The aluminium contained in the packaging items is actually made of aluminium alloys. Each alloy contains a small percentage of metals other than aluminium, which are added to increase its mechanical properties. Furthermore, the materials contain other non-metallic components, such as paint (for beverage cans and spray cans), as well as plastic and paper (for poly laminated foils). In addition, the beverage cans used for the experimentation were post-consumer and they probably contained organic and/or inorganic impurities that should be considered in the evaluation of aluminium mass balance. Although using post-consumer materials is the best choice to correctly represent the reality, this is not always possible. For the other tested packaging, in fact, pre-consumer materials were used, due to either safety reasons or technical limitations. Post-consumer spray cans may contain residual pressurised flammable gas, and their feeding in big quantity could cause risks of

explosion in the furnace. For what concerns trays and foils, the limitation was related to the technical impossibility to obtain a sufficient amount of selected post-consumer material from the separated collection, which is largely dominated by cans.

Table 2.1.1 - Tested materials.





Tested material	Characteristics	
Aluminium beverage cans (post-consumer) (Test 1)	volume: 330 ml	
	body alloy: AA3104	
	lid alloy: AA5182	
	body thickness: 0.09 - 0.15 mm	
	lid thickness: 0.22 - 0.25 mm	
	weight: 13.2 g	
Aluminium trays (Test 2)	dimension: 132x107xh30 mm	
	alloy: AA8006	
	body thickness: 0.05 mm	
	weight: 4.28 g	
Aluminium spray cans (Test 3)	dimension: 50x156 mm	
	alloy: AA3000	
	body thickness: 0.32 mm	
	bottom thickness: 0.9 mm	
	crown thickness: 0.44 mm	
	weight: 25 g	
Aluminium packaging foil 1 (Test 4)	alloy: AA1200	
	brown coloured	
	thickness: 12 µm	
Aluminium packaging foil 2 (Test 4)	alloy: AA8079	
	gold coloured	
	thickness: 42 µm	
Aluminium poly laminated packaging foil 1 (Test 4)	alloy: AA1200	
	gold coloured	
	thickness: 10 µm	
	poly laminated with paper 30 gr m ⁻²	
	with glue solvent 2 gr m ⁻²	

Table 2.1.1 (continued) - Tested materials.

Aluminium poly laminated packaging foil 2 (Test 4)	protected aluminium	
	alloy: AA1200	
	thickness: 10 μm	
	poly laminated with paper 20 gr m^{-2} and polyethylene 9 gr m^{-2}	
	with wax 11 gr m^{-2}	
Aluminium poly laminated packaging foil 3 (Test 4)	Triplex foil Alu/PE/Alu	
	alloy: AA1200	
	thickness: 12/60/12 μm	
	with solvent glue 2.5 gr m^{-2} per each side	
Aluminium poly laminated packaging foil 4 (Test 4)	protected aluminium	
	alloy: AA8079	
	thickness: 38 μm	
	poly laminated with polyethylene 45 μm	

2.2. Description of Valmadrera WTE plant

Valmadrera WTE plant consists of two treatment lines, line 1 and line 3, with a throughput of about 6 and 9.5 tonnes per hour of waste, respectively. The feeding includes urban, urban-like non hazardous waste and hospital waste (about 8% of the total waste feed). The plant capacity is based on a nominal lower heating value (LHV) of about 10,500-12,500 kJ kg⁻¹.

The waste bunker has a capacity of 2450 m³ and is equipped with 8 main doors. One of these doors was emptied and used for the doped waste preparation, as it will be explained in the next paragraph.

All tests were conducted on line 3, which is equipped with a forward-acting grate and a wet discharge system for the bottom ashes (Figure 2.2.1). The grate is divided into four sections whose movement can be regulated independently. It is made of moving steps that move back and forth, promoting waste mixing and advance. Furthermore, this movement regulates the thickness of the waste layer above the grate. Primary air is fed from underneath the grate.

At the end of the grate, bottom ashes fall down in a water bath, where they are quenched, extracted by a metallic conveyor belt and then discharged in the bottom ash bunker.

The combustion chamber is designed to prevent the formation of melting slags and ashes deposits on its walls, to limit the quantity of unburned materials in the bottom ashes and to complete the flue gas combustion. The secondary air feeding is regulated to maintain the temperature above 850°C for at least 2 seconds, and the oxygen concentration in the flue gas around 6%. A fraction of the clean flue gas (about 15%) collected downstream the fabric filter is recirculated in the post-combustion chamber, in order to reduce the NO_x formation and to increase the steam production. The plant is equipped with a waste heat boiler for combined heat and power (CHP) production through a steam turbine. The boiler consists of three vertical empty radiant channels, located next to the combustion chamber, and of a downstream horizontal convective heat transfer section, made up of a first evaporator tube, two super heater tubes, a second evaporator tube and two economizer tubes. The boiler provides the production of steam at high pressure (40 bar) and high temperature (400°C) and part of the low-pressure steam is extracted from the turbine and used for auxiliary steam consumptions and hot water production for internal use. The maximum electric energy produced by the plant is equal to 10.5 MWh h⁻¹ and the thermal energy available for district heating is equal to 20 MWh h⁻¹.

The flue gas treatment configuration, depicted in Figure 2.2.2, is based on a dry-wet integrated process design and it includes:

- A dry stage for the removal of acid gases and micro-pollutants with the injection of sodium bicarbonate³ and activated carbon. Fly ashes and neutralization products are separated through a fabric filter (FF), which operates at temperatures around 180°C. The cleaning of the fabric filter is carried out using compressed air jet (pulse-jet method) when the filter is operating. Ashes fall down in heated hoppers and are hydraulically pumped to storage silos;
- A catalytic reactor with ammonia injection for the removal of NO_x, through a selective catalytic reduction process (SCR). The reactor is also designed for the removal of dioxins (DeNO_x-DeDiox);
- A wet scrubber with water and soda injection to complete the removal of acid gases and of the most volatile heavy metals, such as mercury. In particular, line 3 is equipped with a one stage counter-current wet scrubber, filled with plastic elements containing activated carbon particles for dioxin adsorption (Adiox®), in order to prevent the so called “memory effect” (Giugliano et al., 2001).

³ The use of NaHCO₃ is much more widespread in Italy compared to the rest of Europe. Because of stoichiometry, as well as of superior reactivity, the bulk of injected NaHCO₃ is smaller than it would be in the case of hydrated lime, typically used elsewhere. As a consequence, the aluminium in Vamadrea fly ashes is expected to be less diluted and, therefore, more concentrated than usual.

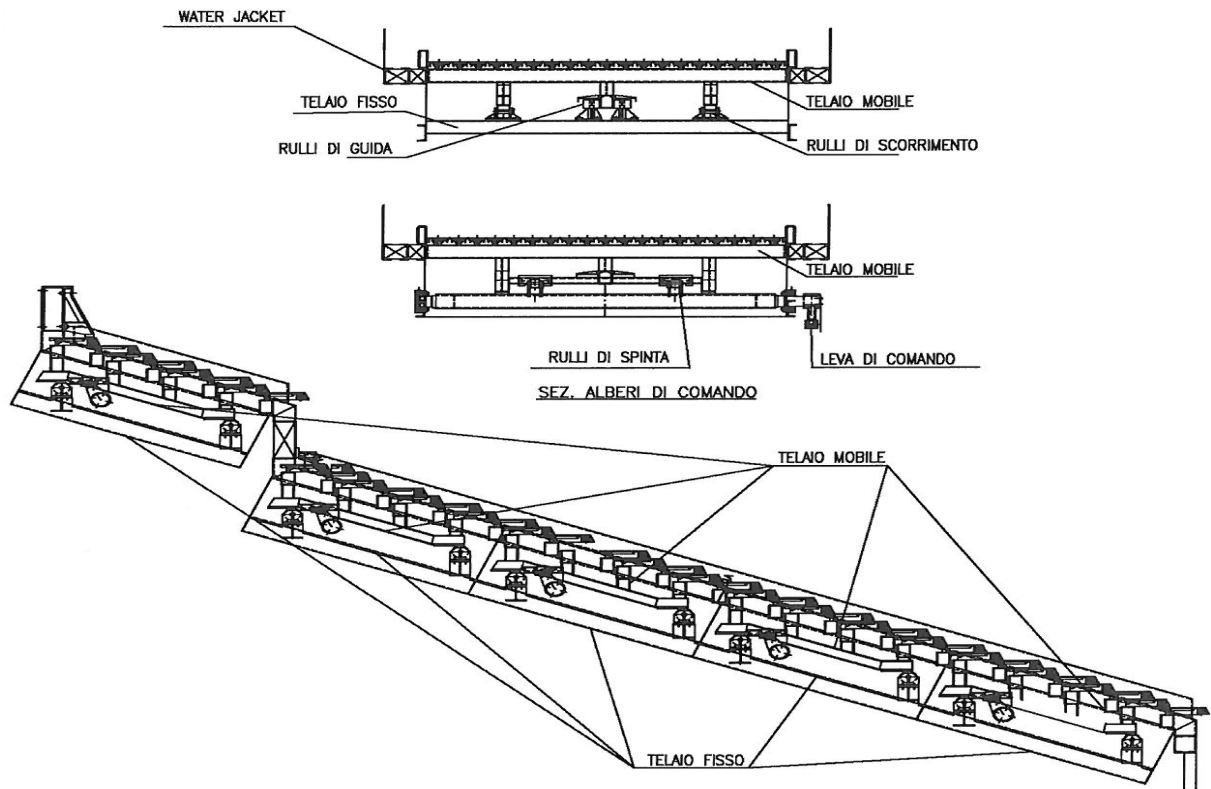


Figure 2.2.1 - Design of the forward-acting grate of line 3 of Valmadrera incineration plant.

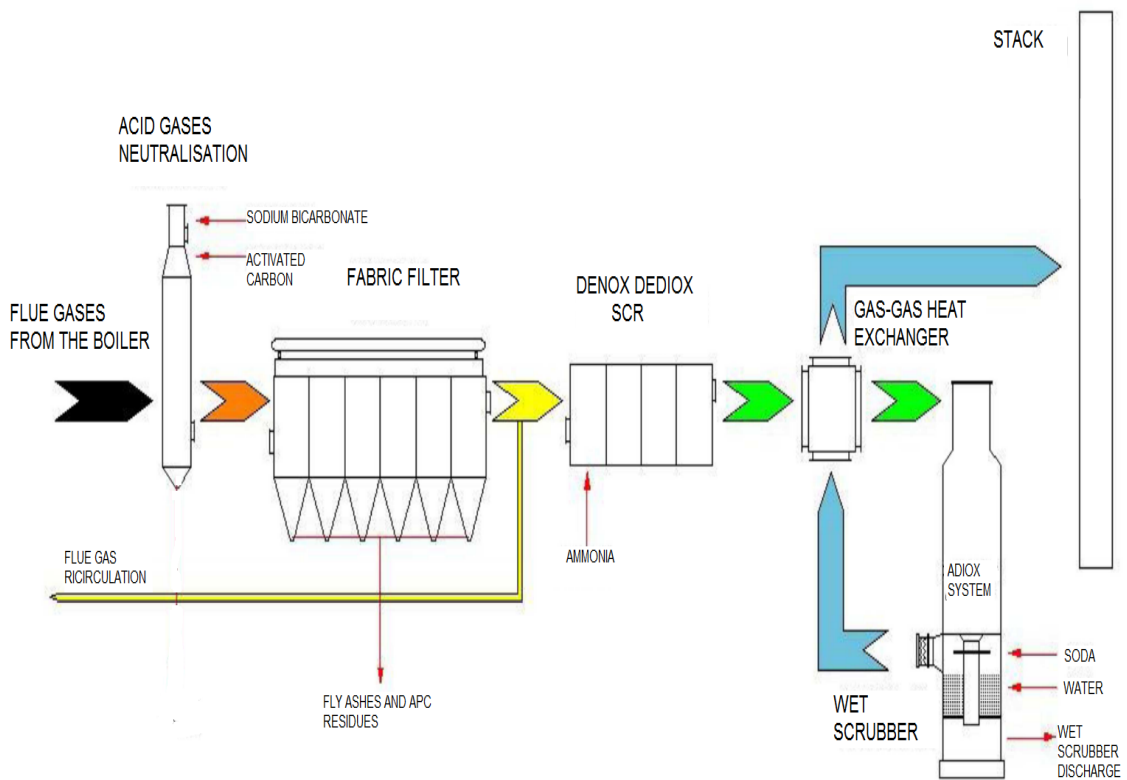


Figure 2.2.2 - Flue gas treatment layout of Valmadrera incineration plant (line 3).

The mass of incinerated waste and the resulting residues generated on average by the plant (line 3 only) are summarized in Table 2.2.1.

Table 2.2.1 - Incinerated waste and related residues produced by line 3 of Valmadrera plant (t year⁻¹).

Waste and residues		2009	2010	2011 (up to April)
MSW	t year ⁻¹	48,481	50,793	12,082
Hospital waste	t year ⁻¹	3,893	4,481	1,038
Bottom ashes	t year ⁻¹	9,860	10,368	2,445
	kg t _{waste} ⁻¹	188	188	186
Fly ashes	t year ⁻¹	1,611	1,648	405
	kg t _{waste} ⁻¹	31	30	31

The main pollutants average concentration in the flue gas at the stack and the operating parameters measured during the experimental campaigns are reported in Table 2.2.2 and 2.2.3. To better understand the fluctuations to which they were subjected during the tests, they are also graphically reported in Figures from 2.2.3 to 2.2.7. The fluctuations in the concentration of the main pollutants in the raw gas are due to the variation of the characteristics related to the waste fed into the furnace. As regards the operating parameters, the differences in the primary air flow rate and in the steam production between the four days of tests highlight the variability of the waste feeding rates and the regime of incineration, which was very low on the 8th of June (Test 3) and markedly higher on the 13th of July (Test 4). This variability certainly had an important influence on the results of the four tests. In general, although the operating conditions were partially different between the four runs and, especially during the tests on aluminium rigid packaging, below the nominal capacity, it is possible to state that the plant always operated in stable conditions.

Table 2.2.2 – Average stack concentrations of the main pollutants during the experimental campaigns.

Average daily concentration		Test 1	Test 2	Test 3	Test 4	Maximum admitted concentration (2000/76/EC)
HCl	mg m _n ⁻³	0.29	0.32	0.16	0.16	10
CO	mg m _n ⁻³	3.83	4.57	4.67	4.54	-
SO₂	mg m _n ⁻³	3.03	5.44	4.03	4.94	50
NOx	mg m _n ⁻³	77.10	73.67	76.67	84.65	200
Total dust	mg m _n ⁻³	0.05	0.08	0.08	0.03	10

Table 2.2.3 - Main operating parameters of the plant during the experimental campaigns.

Average daily concentration		Test 1	Test 2	Test 3	Test 4
HCl raw gas	mg m _n ⁻³	882	1,179	1,137	1,067
CO raw gas	mg m _n ⁻³	2.35	2.96	3.30	2.33
SO ₂ raw gas	mg m _n ⁻³	31.86	95.72	69.58	28.39
NOx raw gas	mg m _n ⁻³	234.49	228.86	219.23	230.25
Flue gas at the stack	m _n ³ h ⁻¹	40,247	41,514	38,447	56,812
O ₂ combustion chamber	%	5.59	5.75	5.45	4.89
Grate T	°C	1,004	1,016	973	1,050
Combustion chamber T	°C	810	826	808	867
Primary air	m ³ h ⁻¹	18,668	19,889	18,126	25,353
Secondary air	m ³ h ⁻¹	9,876	9,390	8,263	10,579
Flue gas recirculation	m ³ h ⁻¹	4,464	3,946	4,904	4,272
Steam P	atm	41.01	41.05	40.94	41.69
Steam T	°C	400.26	399.67	400.17	399.90
Steam flow rate	t h ⁻¹	23.82	24.33	22.77	31.43

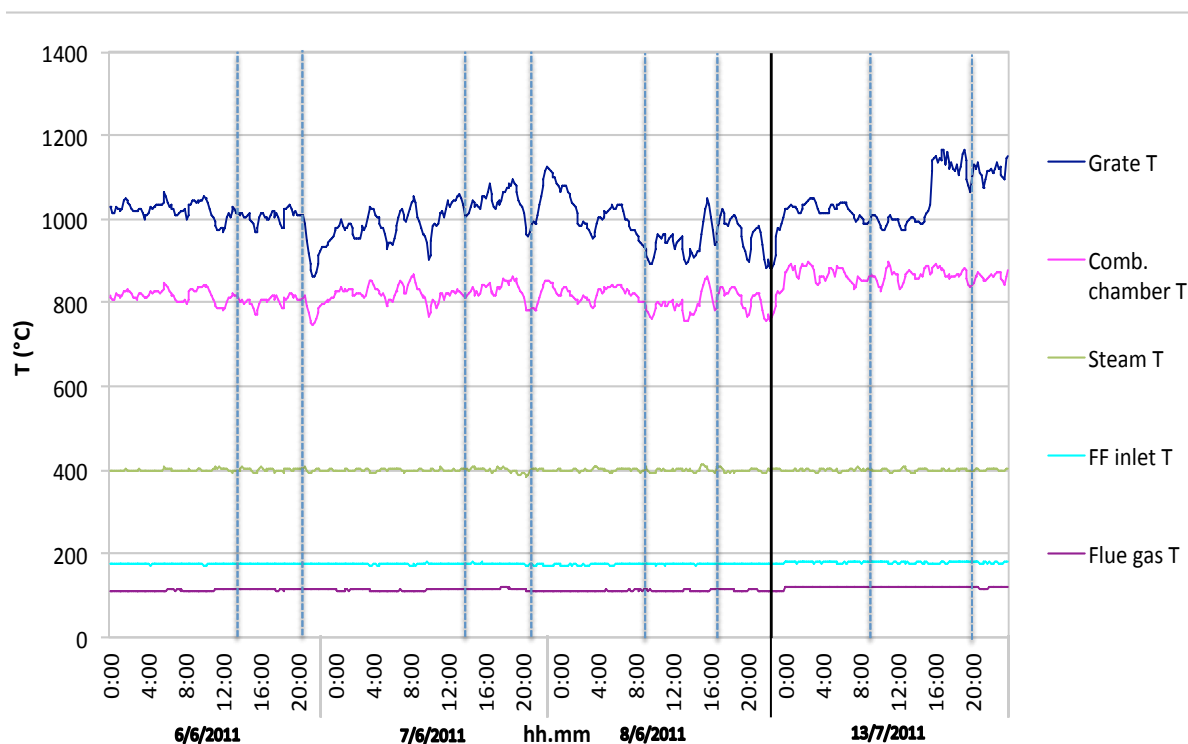


Figure 2.2.3 - Temperatures measured during the days of the experimental campaigns (reported in the x-axis). The sampling period of the residues for each day is delimited by vertical dotted lines.

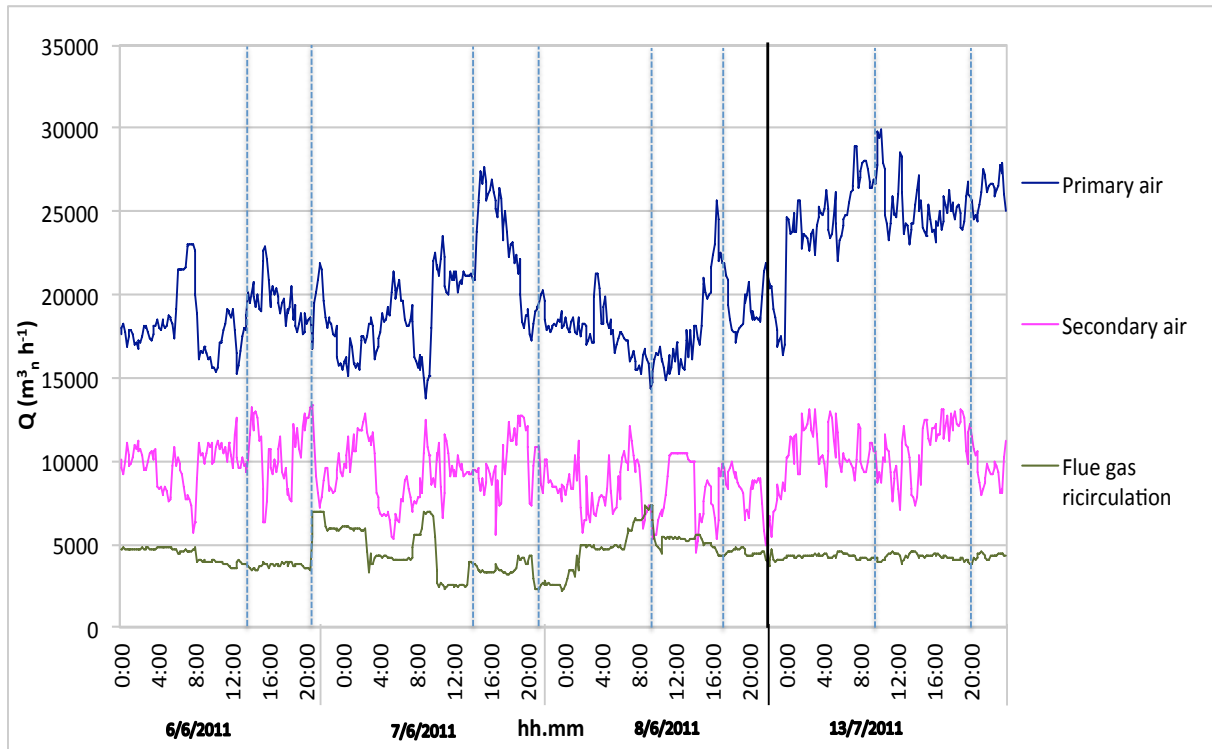


Figure 2.2.4 - Primary, secondary air and flue gas recirculation during the days of the experimental campaigns (reported in the x-axis). The sampling period of the residues for each day is delimited by vertical dotted lines.

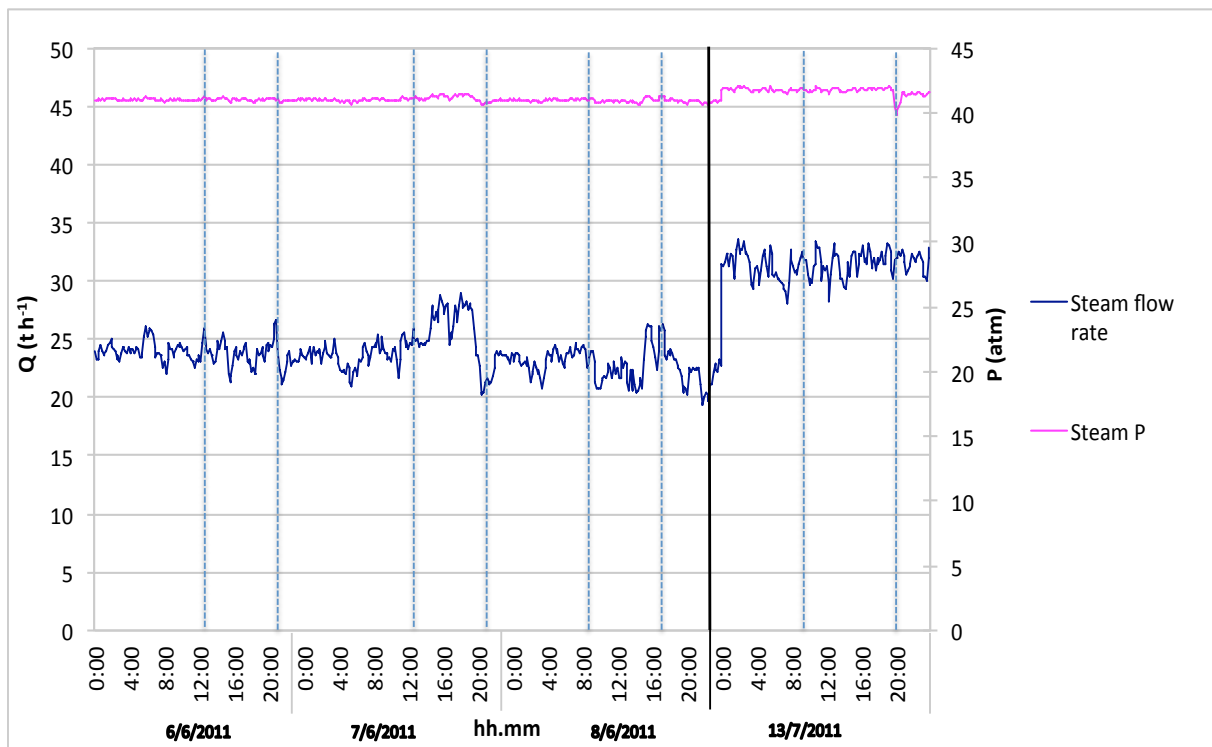


Figure 2.2.5 - Steam flow rate and pressure during the days of the experimental campaigns (reported in the x-axis). The sampling period of the residues for each day is delimited by vertical dotted lines.

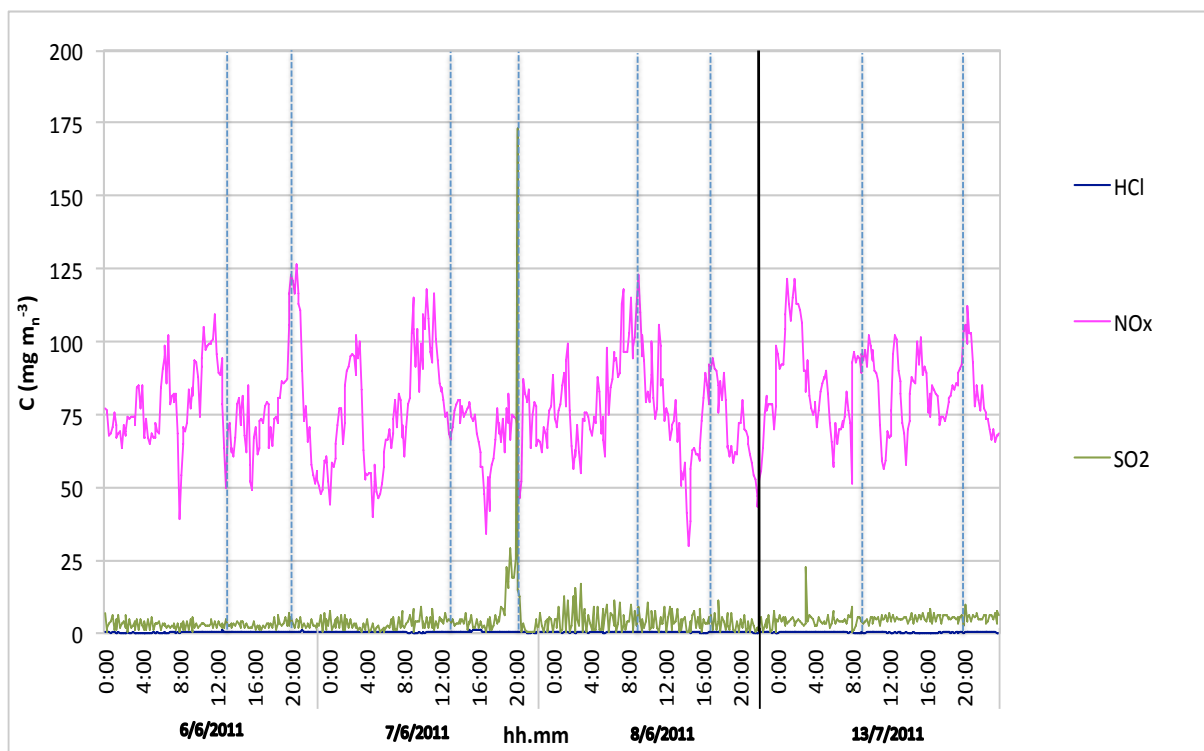


Figure 2.2.6 - Stack concentrations of HCl, NO_x and SO₂ during the days of the experimental campaigns (reported in the x-axis). The sampling period of the residues for each day is delimited by vertical dotted lines.

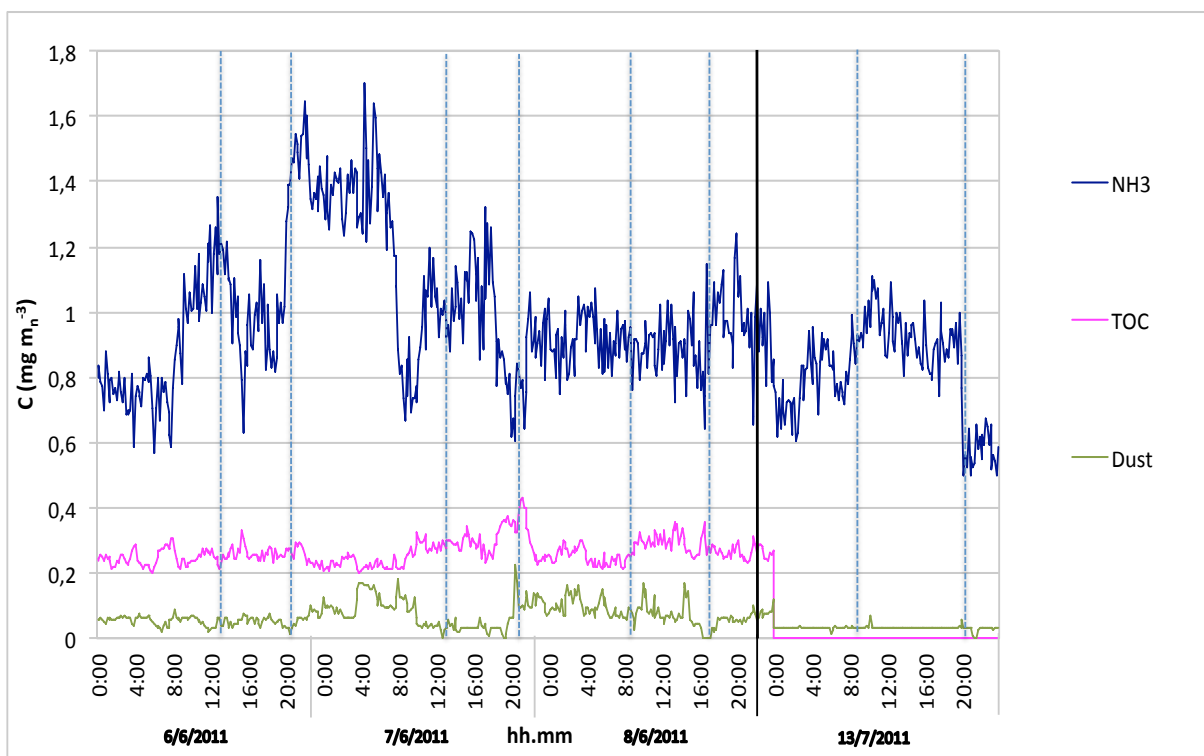


Figure 2.2.7 - Stack concentrations of NH₃, TOC and dust during the days of the experimental campaigns (reported in the x-axis). The sampling period of the residues for each day is delimited by vertical dotted lines.

2.3. Waste charge preparation and feeding

The same sampling procedure was followed in both experimental campaigns. Overall, four doped waste charges were prepared, one for each of the selected aluminium packaging types to be tested.

For what concerns rigid aluminium packaging (beverage cans, trays and spray cans), for each charge about 240 kg were mixed with 400-700 kg of other waste, mainly plastic and paper. This first mixing took place in a waste selection facility located elsewhere from Valmadrera (Seruso material recovery facility, from now on referred to as “Seruso plant”) for mere practical and formal reasons. Then, the aluminium charge was transported to Valmadrera WTE plant where it was mixed with other 7,000-8,000 kg of residual waste ready for incineration. Such second mixing took place in a dedicated bunker section, which was previously emptied. The aluminium charge delivered from Seruso plant and the residual waste were mixed with the help of the grab in order to make the charge as much homogeneous as possible.

For what concerns flexible aluminium packaging (mix of aluminium and poly laminated foils), the quantities prepared at Seruso plant were higher, 979 kg of aluminium-containing packaging and 1000-1100 kg of other waste. It must be specified that the declared weight of aluminium flexible packaging refers to the gross value, thus including the boxes containing the tested material, as they could not be weighted separately to measure their net weight because of technical problems. Nevertheless, the cardboard boxes containing the packaging do not have so much influence on the final tested weight.

Some pictures regarding the doped waste charge preparation are reported in Figures from 2.3.2 to 2.3.4, while the following scheme (Figure 2.3.1) describes the utilized procedure.

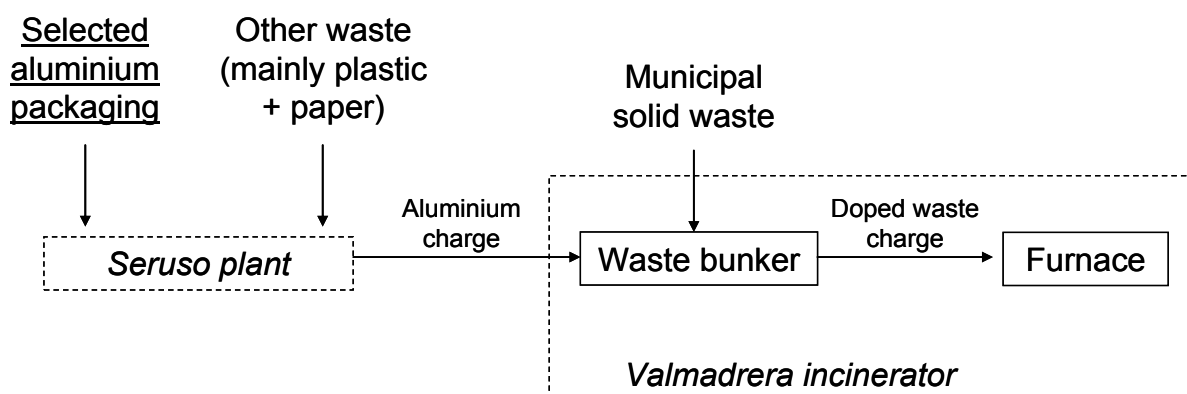


Figure 2.3.1 - Doped waste charge preparation and feeding into the furnace.



Figure 2.3.2 - Doped waste charge preparation: residual waste from Seruso plant (mainly plastic and paper).



Figure 2.3.3 - Doped waste charge preparation: aluminium beverage cans used for Test 1 (6th of June 2011).



Figure 2.3.4 - Doped waste charge preparation: after the second mixing performed through the waste grab, the doped waste is ready to be introduced into the feeding hopper of Valmadrera WTE plant.

Table 2.3.1 shows the amount and the characteristics of the doped waste fed into the furnace. It must be specified that the values reported in this table are probably overestimated compared to what has been actually fed, due to the unavoidable losses occurred during waste mixing operations. During the experimental campaigns, the supply of hospital waste was suspended. Nevertheless, during Test 3 on spray cans there was a temporary breakdown of the loading bucket right at the beginning of the test. In order to prevent the complete emptying of the hopper, the operator was forced to introduce a load of hospital waste right after the beginning of the test. Due to the considerations on the doped waste residence time, it is assumed that this unexpected event had no effect on the results.

Total aluminium content in the doped waste was estimated by considering the contribution of the tested aluminium packaging and the “background” aluminium content in the residual waste. The average composition of the waste flux produced by Seruso plant and of the residual waste incinerated in Valmadrera WTE plant during standard operation is reported in Table 2.3.2.

The doped waste charge was fed into the furnace during approximately one-two hours. Bottom and fly ashes were sampled every 30 minutes on average, depending on the operating

conditions of the plant. The sampling of bottom ashes was intensified during the expected output resulting from the doped waste input.

Table 2.3.1 - Doped waste fed into the furnace during the two experimental campaigns.

Test		Aluminium packaging (kg)	MSW (including Seruso waste) (kg)	Hospital waste (kg)	Total estimated Al content (%)
#1	Beverage cans	240	8,010	0	3.7
#2	Trays	240	9,546	0	3.2
#3	Spray cans	240	7,624	144	3.5
#4	Foils	979	30,236	0	4.0

Table 2.3.2 - Composition of the residual waste incinerated in Valmadrera WTE plant during standard operations (average value based on the analyses of November and December 2010) and of the waste produced by Seruso selection plant (analysis of January 2011).

Waste composition (%)	Residual waste Valmadrera	Waste from Seruso
Aluminium	0.77	0
Paper and paperboard	24.70	25.9
Plastic	21.14	57.3
Ferrous metal	2.12	2.3*
Wood	0.95	4.6
Glass	1.54	0
Laminated	0.84	0
Organic fraction	17.41	0
Green waste	5.79	0
Textile	4.01	9.9
Inert fraction	2.09	0
Undersieve	5.45	0
Other waste (nappies, leather, non-classifiable waste)	12.03	0
Hazardous waste	1.11	0
LHV (kJ kg ⁻¹)	14,966	22,352

* The value includes aluminium.

The residence time of the waste during the whole treatment (from the feeding hopper to the bottom ash extraction system) was initially determined by introducing in the furnace two steel cubic cages (40x40x40 cm, with a mesh of 2x2 cm), one just before the first feeding of the doped waste charge and the second right after the last, each one filled with synthetic waste and some of the packaging items used in the experimentation (Figure 2.3.5). The cages were intended to play the double role of residence time tracer and container for some packaging items properly squeezed, whose surfaces would have been observed at the

microscope to study the oxide scale conformation. The residence time in the feeding hopper and on the furnace grate was evaluated by observing the cages falling down in the quenching water bath from the little window located at the end of the grate (Figure 2.3.6). It resulted significantly variable during the different tests, ranging from 3 to 6 hours, depending on the plant operating conditions. On the other hand, the residence time in the bottom ash extraction system resulted constant in all tests and equal to 20 minutes.



Figure 2.3.5 - Cage before and after the test.



Figure 2.3.6 - Cages in the furnace right before the discharge in the quenching water.

Unfortunately, the two cages underwent damages and breaks during the tests, and the contained material was completely lost. They also failed to be considered reliable tracers for the residence time of the doped waste in the furnace, since their different size and specific weight probably made them roll faster than the waste along the grate, resulting in a possible overrunning and a faster discharge. This conclusion emerged from the examination of aluminium concentration trend in bottom ashes. As an example, the trend of metallic aluminium recovered from bottom ash samples taken during Test 2 with aluminium trays (7th of June 2011) is reported in Figure 2.3.7, where the instants of extraction of the two cages are also indicated.

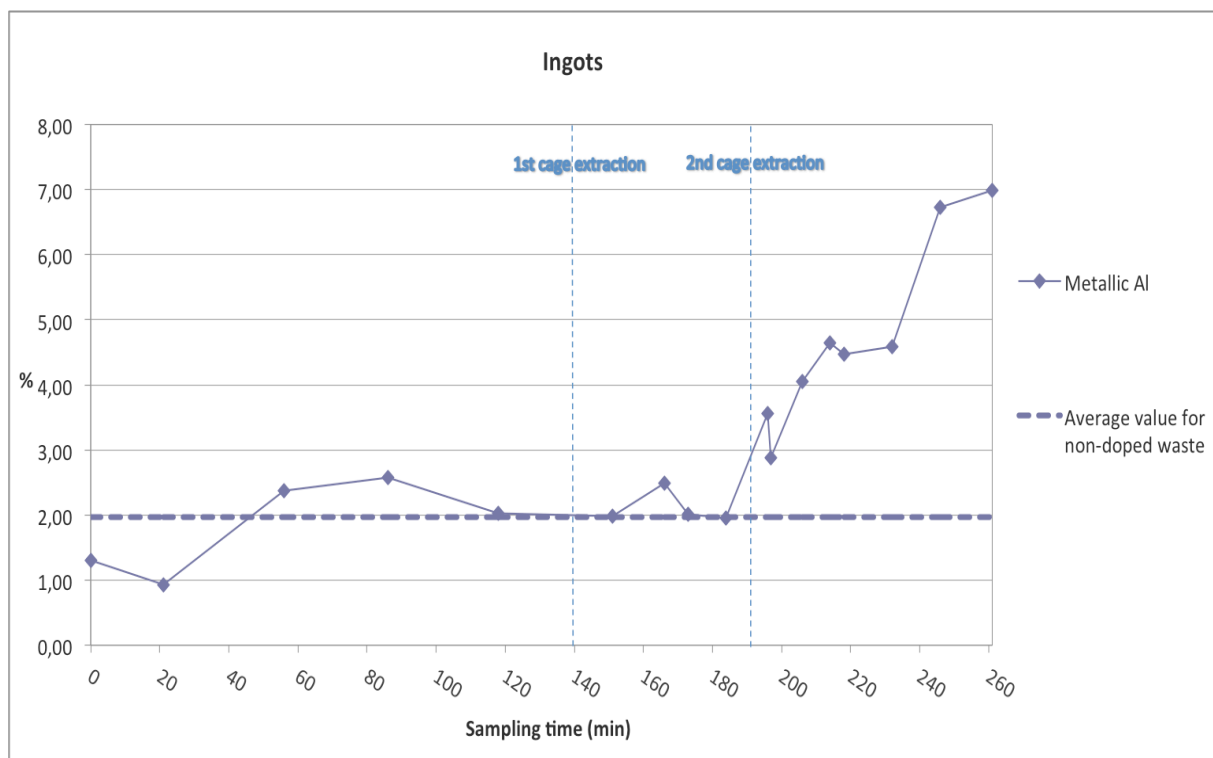


Figure 2.3.7 - Trend of metallic aluminium (mass % on bottom ashes dry weight) recovered from bottom ash samples taken during Test 2 on aluminium trays (7th of June 2011). Dotted lines represent the instants when the two cages were extracted.

As it can clearly be seen, the most pronounced growth trend begins after the extraction of the second cage, meaning that the doped waste was still inside the furnace at that time. The waste residence time evaluated with the cages thus happened to be underestimated. For this reason, during the second experimental campaign (Test 4, 13th of July 2011) only one cage was used as an approximate tracer, and the sampling period of bottom ashes was extended (see Figure 2.4.6 in Paragraph 2.4).

A comparison between the residence time estimated with cages and the one resulting from the analysis of aluminium concentration trend in bottom ashes is reported in Table 2.3.3.

Table 2.3.3 - Residence time of the waste from the feeding hopper to the bottom ash extraction system.

Residence time of the waste on the grate (h)	Test 1	Test 2	Test 3	Test 4
Estimated with cages	4.00	3.50	6.25	4.33
Evaluated from aluminium concentration trend in bottom ashes	6.18	3.70	6.63	4.28

The spread between the values of the 6th (Test 1), 7th of June (Test 2) and 13th of July (Test 4) can be considered normal in MSW incineration, yet the much longer residence time on the 8th of June (Test 3) must be related to a different grate movement. Since no recorded data are available about this specific aspect, it will need to be properly checked and taken into consideration during future campaigns.

Generally speaking, the residence time variability is related to waste availability and its characteristics (e.g. moisture content), besides the specific layout of the WTE plant furnace. It is hard to state what can be regarded as the “normal” residence time. In a recent work carried out on a WTE plant in Denmark (Astrup et al., 2011), it was estimated to be approximately equal to 6 hours. In another study conducted on Roeselare incinerator in 1993 (reported by Pruvost, 2011), it ranged between 1 hour 40 minutes and 4 hours 15 minutes. Without any doubt, the waste residence time in the furnace is one of the most important factors affecting the oxidation of aluminium and its potential recovery from bottom ashes (Hu et al., 2011).

Obviously, the “residence time” of fly ashes⁴ could not be measured with a tracer but it is likely to be much shorter than that of bottom ashes. Indeed, the flue gas released during combustion, which entrains the fly ashes, moves very quickly through the boiler towards the treatment line; moreover, no fly ashes recirculation takes place in the dry absorption system because this is not required when utilizing sodium bicarbonate for the removal of acid gases. In addition, during the experimental campaigns, the boiler surfaces were regularly cleaned in order to minimize fly ashes retention in the system.

⁴ When considering fly ashes, this is not a true residence time, but rather the time elapsed between the introduction of the doped waste in the furnace and the appearance of its effects in the mix of boiler and fabric filter ashes. It can be considered as a “response time” of fly ashes to the doping of the waste.

2.4. Sampling of incineration residues

The layout of the plant, with the indication of sampling points, is reported in Figure 2.4.1. Bottom ashes were sampled from the conveyor belt after quenching using a special shovel (Figure 2.4.2), in a quantity of 2-5 kg per sample. They were collected in plastic buckets of 5 l capacity. This amount was increased to 5-10 kg during the second campaign devoted to aluminium flexible packaging because, following the preliminary results, it turned out to be a critical aspect. Each bucket was identified with the date and the time of sampling, as well as its gross weight. A picture of bottom ash samples is reported in Figure 2.4.3.

Fly ashes were sampled at their discharge in the collecting bags, as shown in Figure 2.4.4. Every sampling operation was carried out very quickly, in order to avoid the dispersion of fine polluted ashes in the atmosphere. The boiler was regularly cleaned every 100 minutes; each cleaning cycle requires about 45 minutes. A picture of fly ash samples is reported in Figure 2.4.5.

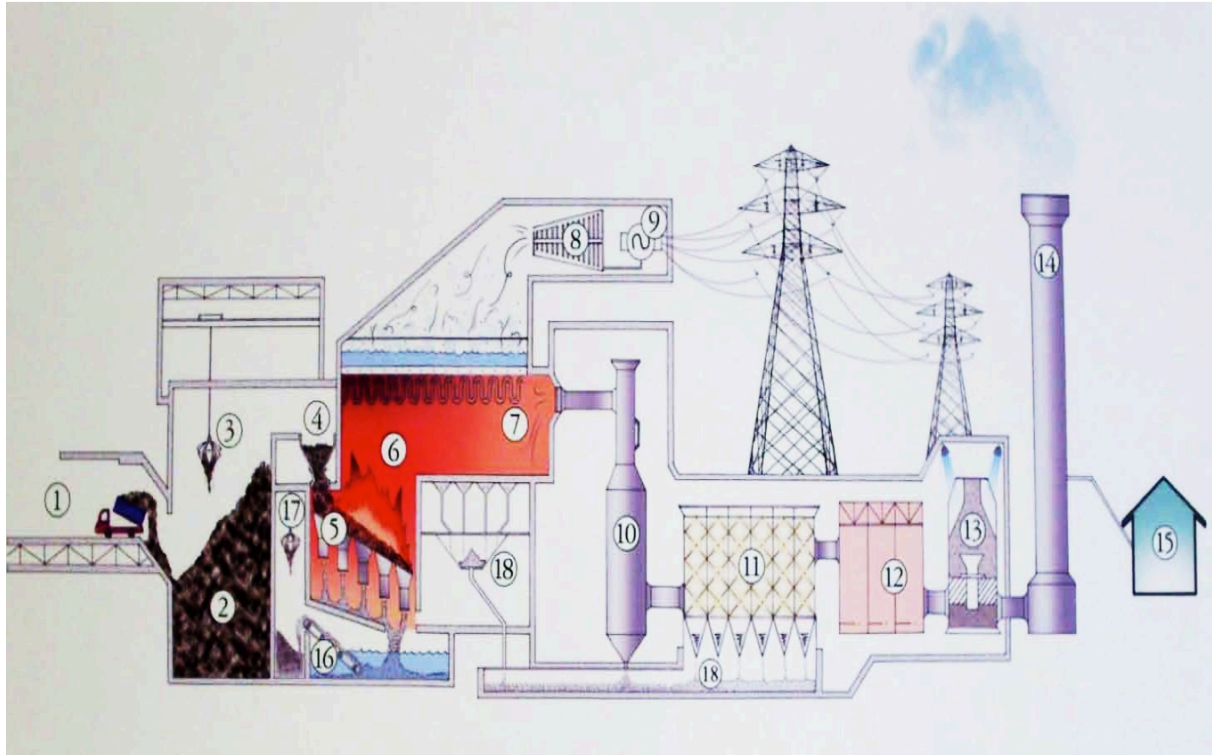
In the calculation of the mass balance, both the amount of aluminium potentially present in the flue gas at the stack and the one deriving from the possible dissolution of metallic aluminium and/or alumina in the bottom ash quenching water have been voluntarily neglected.

Concerning the first aspect, a recent research study focusing on the balance of toxic elements during waste incineration showed that concentrations of aluminium in the flue gas released at the stack are negligible (Stucchi, 2003). According to these results, it was decided not to measure the content of aluminium in the flue gas at the stack. Actually, the doping of the waste might have led to a possible deviation from standard conditions in the furnace and peaks of aluminium concentration might have occurred even for flue gases.

Concerning the second aspect, the sampling of bottom ash quenching water could not be performed because of technical limitations.

With a view to future experimental campaigns, it may be useful to include at least four analysis of aluminium concentration in the flue gas at the stack and in the bottom ash quenching water, two before and two after the doping of the waste.

The detailed time schedule of the experimental campaigns (showing the doped waste input and the sampling of fly and bottom ashes) is reported in Figure 2.4.6.



- | | | |
|-----------------------|-------------------------------|--------------------------------|
| 1) Waste unload yard | 7) Waste heat boiler | 13) Wet Scrubber |
| 2) Waste bunker | 8) Turbine | 14) Stack |
| 3) Waste grab | 9) Alternator | 15) Stack emissions monitoring |
| 4) Feeding hopper | 10) Acid gases neutralization | 16) Bottom ash extractor |
| 5) Furnace grate | 11) Fabric filter (FF) | 17) Bottom ash bunker |
| 6) Combustion chamber | 12) DeNOx - DeDiox | 18) Fly ash collection system |

Figure 2.4.1 - Layout of Valmadrera WTE plant. Bottom ashes and fly ashes sampling points coincide with numbers 16 and 18.



Figure 2.4.2 - Sampling of bottom ashes.



Figure 2.4.3 - Bottom ash samples.



Figure 2.4.4 - Sampling of fly ashes.



Figure 2.4.5 - Fly ash samples.

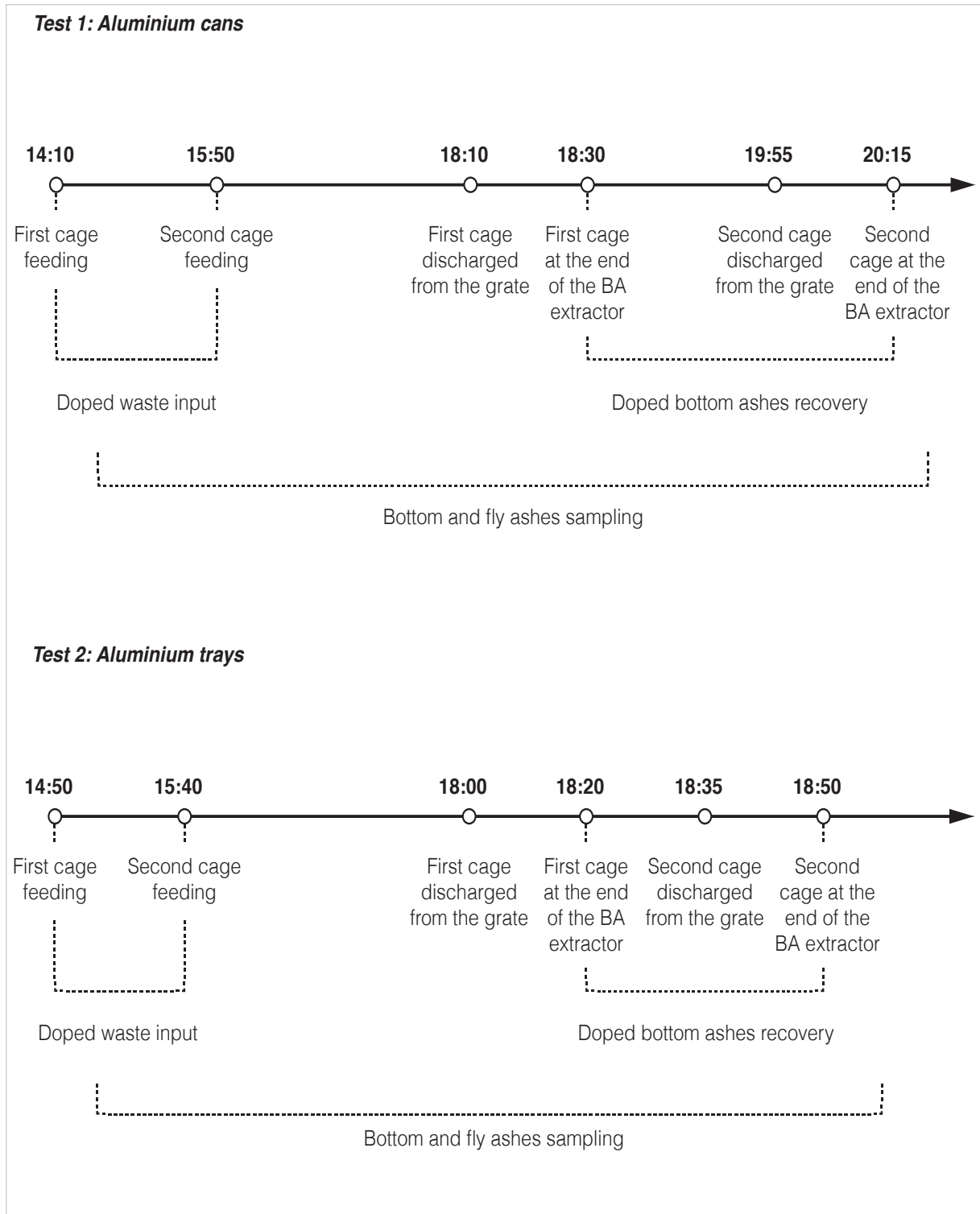


Figure 2.4.6 - Time schedule of the experimental campaigns.

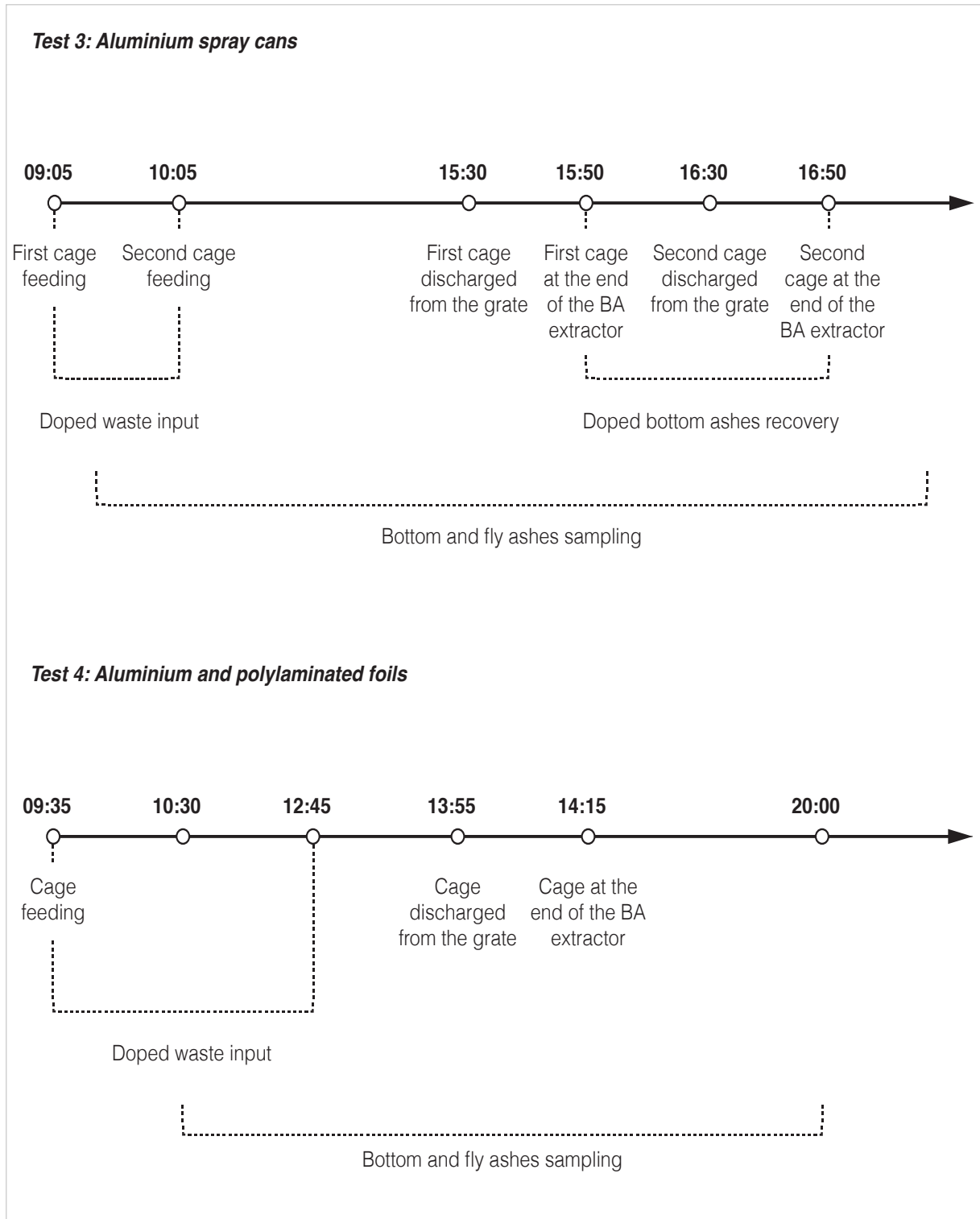


Figure 2.4.6 (continued) – Time schedule of the experimental campaigns.

2.5. Samples treatment and laboratory analysis

2.5.1. Bottom ash samples treatment

All treatments and laboratory analyses were performed at Vedani Carlo Metalli foundry, specialized in the recycling of aluminium scraps and production of aluminium alloys.

Bottom ash samples were properly treated according to the scheme reported in Figure 2.5.1, in order to simulate an advanced system for the recovery of aluminium and to facilitate their subsequent laboratory analysis. The weights were measured after each treatment step by mean of an electronic balance.

Bottom ashes were first dried [1] and then screened at 0.8 mm [2]. The choice of 0.8 mm as cut dimension is due to the recycling capacity of aluminium secondary smelters. Particles bigger than 0.8 mm can generally be recycled, whereas those smaller than 0.8 mm cannot be recovered and determine a loss of material. Iron and inert scraps [3] and aluminium lumps [4] were manually sorted out. The fraction above 0.8 mm was grinded in a grindstone [5] in order to promote metals liberation, and afterwards it was further screened at 0.8 mm [6]. In this way, it was possible to isolate the coarse fraction (above 0.8 mm) enriched of metals, which (unlike the inert material) are not crushed in the grindstone but just flattened.

The two inert fractions below 0.8 mm (before and after the grinding step) were analyzed separately. In these fractions, aluminium is present in low amount and the content of metallic aluminium was detected using the “soda attack” method (see Paragraph 2.5.3). The content of total aluminium was evaluated with X-ray Fluorescence Spectroscopy (XRF, see Paragraph 2.5.4) [7]. The fraction above 0.8 mm resulting from the second screening underwent a magnetic separation with a manual magnet [8] and it was then melted down with salt in the crucible, together with the aluminium lumps manually sorted in the previous steps [9]. The salt dross was analyzed with the same procedure as for the inert fraction of the bottom ashes, whereas the recoverable metal ingot was analyzed through Optic Emission Spectroscopy (OES or quantometer analysis, see Paragraph 2.5.5) in order to evaluate its content of Al (all metallic) [10].

Some modifications in the procedure were introduced for the samples of the second experimental campaign (Test 4 on aluminium flexible packaging); the fraction above 0.8 mm resulting from the second screening, after the magnetic separation, was further screened with a 5 mm mesh screen [11]. The fraction above 5 mm and the manually sorted aluminium

lumps, consisting almost entirely of aluminium and other non-ferrous metals and representing the amount of non-ferrous metals that can be separated with a traditional ECS, were melted together to obtain the metal ingot. The fraction between 0.8 and 5 mm, representing the material that can be recovered only with an advanced ECS specifically calibrated on small grains (eg. high frequency ECS, wet backward ECS, Magnus separator), was melted separately and its dross analyzed with soda attack and XRF for the evaluation of metallic aluminium loss in the crucible. It was possible to apply the procedure of separated melting for the samples taken during this campaign because of the higher amounts of sampled material resulting in the higher quantities of non-ferrous metals recoverable from each fraction. Some pictures illustrating bottom ash samples preparation and the instruments are reported in Figure 2.5.2.

2.5.2. Fly ash samples treatment

Fly ash samples from both experimental campaigns were directly analyzed with soda attack and XRF in order to determine their content of metallic and total aluminium [7], since they did not require any treatment before the analysis.

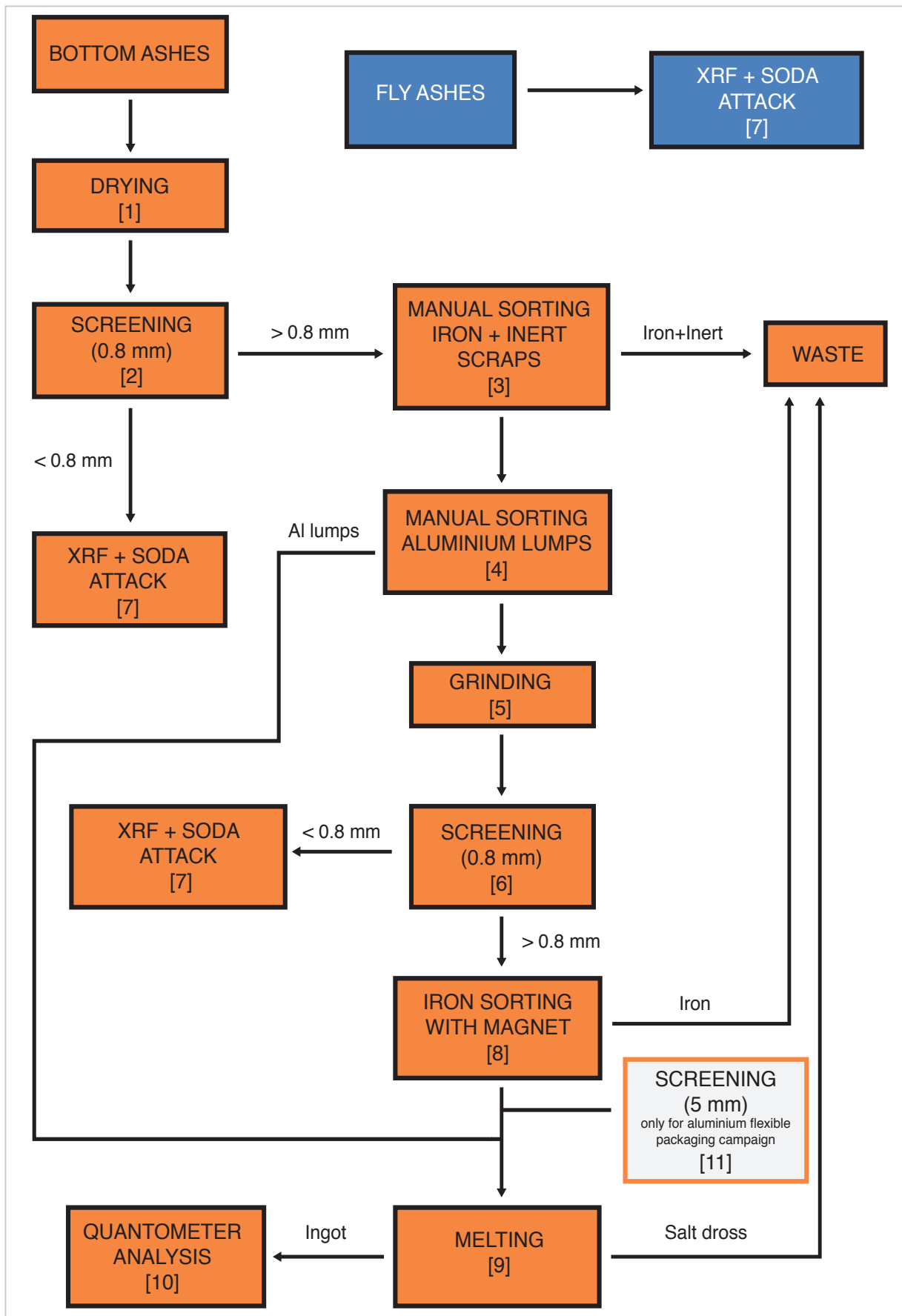


Figure 2.5.1 - Scheme of samples treatment and laboratory analysis.



A) Drying [1] of a bottom ash sample in ambient air, aimed at its preparation for the next treatment steps. It was carried out on a common methane burner.



B) First screening [2] of the bottom ash sample: the fine fraction (below 0.8 mm) was separated from the coarse fraction and sent to laboratory analysis.



C) Manual sorting of large-sized ferrous metals, ceramic and glass scraps [3]. Ceramic and glass negatively affect the melting of the coarse fraction rich in non-ferrous metals, causing significant drops in term of recovery yield. For this reason, they have to be separated as much as possible. The separation of ferrous metals was carried out with the aid of a magnet.



D) Manual sorting of non-ferrous lumps [4], simulating the non-ferrous metals separation with a traditional eddy current separator (ECS). Their size is extremely variable but most of them range between 1 and 5 cm in length.

Figure 2.5.2 - Illustration of bottom ash treatment and preparation for the laboratory analysis.



E) Grinding [5] and second screening [6] of the bottom ash sample. The fraction below 0.8 mm was directly sent to laboratory analysis, whereas the fraction above 0.8 mm was further treated (ferrous metals separation with a manual magnet).



F) Ferrous metals in the coarse fraction (above 0.8 mm after the grinding step) were separated with a manual magnet [8] and flattened non-ferrous metals were manually sorted or screened using a 5 mm mesh screen [11].

Figure 2.5.2 (continued) - Illustration of bottom ash treatment and preparation for the laboratory analysis.



G) The residual material above 0.8 mm (coarse fraction) was melted in a crucible in order to recover the non-ferrous metal content [9].



H) Detail of the casting process: aluminium metal and other non-ferrous metals aggregate into droplets that float above the surface of the molten salts. Therefore, they are easily separated through a casting process that results in the formation of a metal ingot. The remaining salt dross is casted separately in a mould where it cools down and it is conserved for further analysis.



I) The metal ingot resulting from the melting process was weighted and sent to OES analysis in order to assess its aluminium content.



L) The salt dross resulting from the melting process was first grinded and then screened at 0.8 mm. The fraction below 0.8 mm was analyzed with the same procedure as for bottom ash fine fractions. In the dross of several samples it was possible to find aluminium droplets lost during the melting process.

Figure 2.5.2 (continued) - Illustration of bottom ash treatment and preparation for the laboratory analysis.

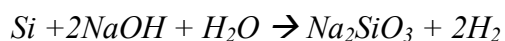
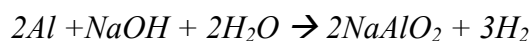
2.5.3. Determination of metallic Al content through “soda attack” method

The laboratory device used to measure the metallic aluminium content in bottom ash and fly ash samples through the “soda attack” method is reported in Figure 2.5.3.



Figure 2.5.3 - Laboratory device used to measure metallic aluminium content with the “soda attack” method.

The principle on which the methodology is based is quite simple: the sample is put in contact with sodium hydroxide under vacuum conditions. Al and Si in the material react with soda causing a development of H_2 according to the reactions:



By measuring the pressure induced by the development of the gas, it is possible to get an indication about the content of Al and Si. Actually, the device detects the total content of metallic aluminium and unbound silicon, thus providing a single result without the possibility of separating the values corresponding to the individual elements. However, in bottom ashes and fly ashes deriving from the incineration process, silicon is found almost exclusively in the bound form of silicate compounds. The content of elemental silicon can therefore be

neglected and, with good approximation, the output data can be considered representative of the sole metallic aluminium content.

The sample must feature a fine grain size that guarantees a ready and complete reaction with soda. For this reason, bottom ash samples were screened at 0.8 mm, while fly ash samples did not require any treatment. The sample must also be free of moisture: the water evaporating during the process increases the gas flow resulting in an overestimation of the actual aluminium content.

Figure 2.5.4 is a scheme showing the laboratory device in all its components. The description of the technical working procedure for the analysis is given immediately below.

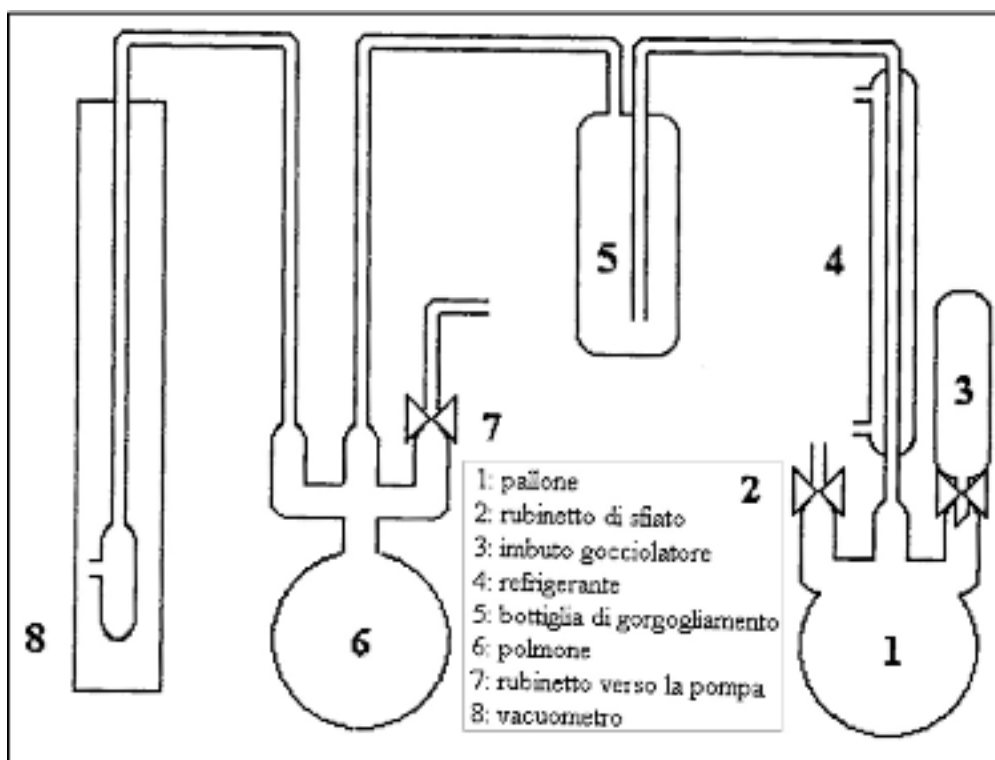


Figure 2.5.4 - Units of the laboratory device used in the measurement of metallic aluminium content through the “soda attack” method.

5 g of fly ashes or bottom ash fractions below 0.8 mm are introduced into the glass ball [1]. The dropping funnel [3] is filled with 100 ml of sodium hydroxide (NaOH 40%), keeping the valve closed until the test is started. In the bubbling bottle [5], 250 ml of sulfuric acid (H₂SO₄ 20%) are placed in order to neutralize ammonia emissions from the sample. Few drops of methyl orange, which has color-turning properties in acidic environments, indicate whether the pH of the solution is increasing and, consequently, when it must be replaced. At this point, vacuum is created inside the unit by activating a pump connected to the device and opening

the appropriate tap [7]: the mercury column inside the gauge capillary slowly begins to rise. Once it has reached about 72 cm in height (assessed using a scale located on the side of the capillary), the tap is closed. The pressure is read on the scale and then the 100 ml of soda are slowly dropped into the glass ball, triggering the reaction. The ball is heated with an electrical resistance to speed up the reaction. The formation of gas, detectable from the development of bubbles inside the bubbling bottle, causes the lowering of the mercury column in the vacuum gauge. At the end of the reaction, when bubbling is no longer detectable, the height reached by the mercury column is annotated. The difference between the initial and the final height of the column expresses the pressure difference between the beginning and the end of the test, given in mm Hg. The percentage content of metallic aluminium can be derived from a comparison with a reference sample. The reference sample consists of 1 g of pure aluminium metal that, under attack with soda, determines a height difference of 17.5 mm Hg. Therefore, the percentage content of aluminium (and, in theory, silicon) can be obtained by using the following formula:

$$\frac{\Delta P(\text{mmHg})}{17.5 \cdot 5} \cdot 100 = (\text{Al} + \text{Si})\%$$

2.5.4. Determination of total Al content through XRF spectroscopy

The determination of total aluminium content (including both the metallic and the oxidized part) in the bottom ash fine fractions and in the fly ashes was performed through X-Ray Fluorescence (XRF) spectroscopy. X-Ray Fluorescence is an analytical technique that uses the interaction of x-rays with a material to determine its elemental composition. It is suitable for solids, liquids and powders, and in most circumstances is non-destructive.

There are two main XRF methodologies: energy dispersive (EDXRF) and wavelength dispersive (WDXRF). Each method has its own advantages and disadvantages. The range of detectable elements varies according to instrument configuration and set up, but typically EDXRF covers all elements from sodium (Na) to uranium (U), while WDXRF can extend this down to beryllium (Be). Concentrations can range from 100% down to ppm and in some cases sub-ppm levels. Limits of detection depend upon the specific element and the sample matrix, but as a general rule, heavier elements will have better detection limits. The XRF spectroscope used to determine total aluminium content in all the samples was an EDXRF.

The principle on which this type of analysis is based can be synthesized as follows: an electron can be ejected from its atomic orbital by the absorption of a light wave (photon) of sufficient energy. The energy of the photon ($h\nu$) must be greater than the energy with which the electron is bound to the nucleus of the atom. When an inner orbital electron is ejected from an atom, an electron from a higher energy level orbital will be transferred to the lower energy level orbital. During this transition, a photon may be emitted from the atom. This fluorescent light is called the characteristic x-ray of the element. The energy of the emitted photon will be equal to the difference in energies between the two orbitals occupied by the electron making the transition. Because the energy difference between two specific orbital shells, in a given element, is always the same (i.e. it is characteristic of a particular element), the photon emitted when an electron moves between these two levels will always have the same energy. Therefore, by determining the energy (wavelength) of the x-ray light (photon) emitted by a particular element, it is possible to determine the identity of that element.

For a particular energy of fluorescent light emitted by an element, the number of photons per unit time (generally referred to as peak intensity or count rate) is related to the amount of that analyte in the sample. The counting rates for all detectable elements within a sample are usually calculated by counting, for a set amount of time, the number of photons that are detected for the various analytes characteristic x-ray energy lines. It is important to note that these fluorescent lines are actually observed as peaks with a semi-Gaussian distribution

because of the imperfect resolution of modern detector technology. Therefore, by determining the energy of the x-ray peaks in a sample spectrum, and by calculating the count rate of the various elemental peaks, it is possible to qualitatively establish the elemental composition of the samples and to quantitatively measure the concentration of these elements.

The procedure requires a preliminary preparation of the sample, which must be compressed into a tablet (Figure 2.5.5): about 2 g of powdered boric acid, which forms the support base of the tablet, is poured inside the mould. Afterwards, few grams of the sample (homogenized in a way that it is representative of the material to be analyzed) are placed inside the mould as well. The mould is then put into a press exerting a pressure of 460 bars for about 10 minutes (Figure 2.5.6). The result is a 3 cm diameter and 1 cm thick cylindrical tablet that can be inserted into the appropriate equipment for the XRF analysis (Figure 2.5.7).



Figure 2.5.6 - Press machine used for the preparation of the tablets.



Figure 2.5.5 - Sample tablets ready for XRF analysis.



Figure 2.5.7 - Equipment for XRF analysis.

It is necessary to highlight the main limitations of this type of analysis, with particular reference to the instrument used for this study, in order to illustrate what can be inferred from the correct interpretation of the obtained results. First of all, a device for XRF analysis is, in general, able to detect only some chemical elements. In this specific case, the instrument could estimate the concentration of the elements characterized by an atomic number equal to or greater than that of sodium ($Z=11$). This implies that it is possible to obtain information only about the inorganic component of the analyzed materials, since carbon has an atomic number equal to 6. Moreover, since the presence of light elements such as oxygen and hydrogen is not detected, the instrument is not able to provide information about water content. For this reason, the material must be properly dried so that the moisture does not affect the results of the analysis. Actually, the problem is more general: if certain elements are excluded from the analysis it follows that the instrument is not able to reconstruct the full composition of the sample. This means that, in theory, the mass balance cannot be closed, thus providing an overestimation of those elements that are detected by the instrument. In practice, this problem can be solved using the data processing software associated with the machine. By changing some parameters, closely related to the type of sample analyzed from time to time, the program is able to arbitrarily assign fictitious concentration of light elements that are not considered for the analysis, thus closing the mass balance.

A second limitation is related to the fact that the machine does detect the content of an element, but it is unable to provide information about its state of aggregation. In a sample, in fact, an element may be present in a free unbound form or as a compound, thus bounded to one or more other elements. For example, in the case of bottom and fly ash, aluminium is present both in the metallic form (Al) and in the oxidized form (Al_2O_3), but the XRF analysis is not able to provide separate measurements of the two forms.

The final limitation is related to the reproducibility of the measurement. The x-ray beam is capable of hitting a very small and limited area compared to the surface of the tablet. Therefore, sample homogenization needs to be carefully evaluated. It is also recommended to perform at least three analyses on the same tablet, but differently orientated (e.g. turning it by 120° each time) and then take the average of the obtained results. Nevertheless, it was not possible to adopt this procedure in the case under study due to the large number of samples to be analyzed.

2.5.5. Determination of metallic Al content through OES

The ingots resulting from the melting process of bottom ash samples were analyzed through a quantometer based on Optical Emission Spectroscopy (OES) to assess their content of metallic aluminium. In the metal ingot there are many other non-ferrous metals than aluminium, which form the alloy resulting from the melting process.

The working principle of the instrument is similar to that previously described for the XRF analysis. Optical emission spectroscopy identifies metals using the frequencies of electromagnetic radiation emitted by a sample when it is heated. The spectrum of radiation emitted by a given element is characteristic of that element. The metal ingot is heated to high temperature through an electrical discharge; the light emitted by the metal atoms in the sample is then passed through a spectrometer, which splits the light up with a prism or a diffraction grating. The pattern of bands cast by the spectrometer can be used to identify the elements that compose the ingot. Software is typically used to help analyze the emission spectra from the sample. A variety of different products are available for this task: in particular, the instrument used in the laboratory (Figure 2.5.8) emits a double electrical discharge from a needle electrode located at a distance of 3 mm from the ingot surface (which must be previously cut to be sure that impurities do not interfere with the analysis, as shown in Figure 2.5.9). The function of the second discharge is to stabilize the sample. In the reaction chamber, pure argon atmosphere is maintained under negative pressure (25 μmHg). The light radiation emitted by the sample is captured by a lens with 1080 facets per millimeter that splits up the incident ray in more beams. These are captured by a multiplier that transforms them into an electrical signal. The signal is then processed by a dedicated software that returns a table reporting the percentage content of each element in the alloy.



Figure 2.5.8 - Quantometer used for the determination of metallic aluminium content in the ingots.



Figure 2.5.9 - Metal ingots after OES analysis.

2.5.6. Measuring precision of XRF spectroscopy and soda attack method

The precision of XRF spectroscopy and soda attack method was evaluated by repeating the analysis several times on few samples of fly and bottom ashes. For XRF, the measuring reproducibility was tested by repeating the analysis three times on three different tablets prepared from the same fly ash and bottom ash sample, changing each time their orientation inside the instrument by rotating them by 120°. The results, reported in Table 2.5.1, show the absolute reliability of the instrument. The obtained standard deviation is included between 0.3% and 3% of the average value, where the highest value refers to samples whose aluminium concentration is very low.

The reproducibility of the soda attack method was evaluated by repeating the analysis three times on 28 fly ash and 10 bottom ash samples. The resulting standard deviation was very variable, from 0% to 72% of the average value (Figure 2.5.10). The method is therefore characterized by low reproducibility and accuracy and this is probably due to the extremely low metallic aluminium concentrations in the samples, too close to the sensitivity limit of the instrument. Indeed, it is very likely that aluminium concentrations were so low that sometimes they fell below the detection limit of the instrument (especially in fly ash samples). Another possible reason is the low precision in reading the pressure difference, as the pressure gague is not digital. This problem occurred repeatedly during the analysis of fly ash samples taken during all the performed tests. For these reasons, we have decided to consider all the results of the analysis concerning fly ashes as general indications only.

Table 2.5.1 - Evaluation of the measuring reproducibility for the XRF spectrometer used in the laboratory analysis.

Sample	Total Al (%)
Tablet 1	11.09
Tablet 2	11.09
Tablet 2 - 120°	11.08
Tablet 2 - 240°	11.00
Tablet 3	11.07
AVERAGE	11.07
STD.DEV.	0.04

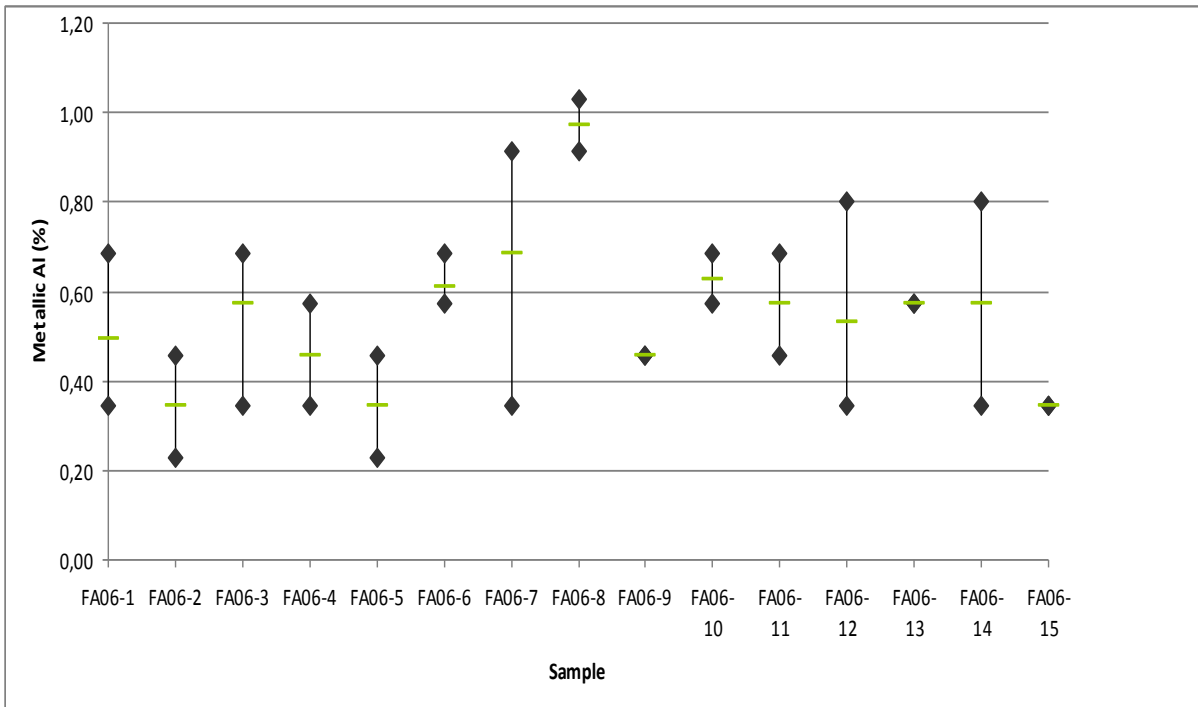


Figure 2.5.10 - Evaluation of sensitivity for the instrument used in the soda attack analysis (fly ash samples taken during Test 1 on aluminium beverage cans).

3. EVALUATION OF THE RESULTS

3.1 Aluminium beverage cans

Results obtained from the analysis of the samples taken during Test 1 on aluminium beverage cans (see Table 2.1.1) are presented in this paragraph. It also illustrates the general criteria and methods chosen for the presentation and interpretation of the results related to all the performed tests; the detailed description of these aspects will then be omitted in the following paragraphs devoted to the other tested packaging.

3.1.1. Bottom ashes

Table 3.1.1 gives an overview of the type and quantity of the sub-fractions obtained from the pre-treatment of bottom ash samples taken during Test 1 on aluminium beverage cans.

Table 3.1.1 - Dry weight, humidity and sub-fractions (expressed as weight percentage on dry samples) obtained from the pre-treatment of bottom ash samples taken during Test 1 on aluminium beverage cans.

Sample*	Time	Dry weight	Humidity	Fraction < 0.8 mm	Fraction < 0.8 mm after grinding	Fraction > 0.8 mm after grinding	Iron+inert scraps
		<i>g</i>	%	%	%	%	%
BA06-1	14:48	935	46	26.74	56.07	5.35	7.49
BA06-2	15:05	2410	28	12.86	48.91	21.99	16.60
BA06-3	15:35	3320	27	10.84	50.77	16.27	20.18
BA06-4	15:55	3675	24	12.52	47.29	20.00	17.82
BA06-5	16:30	2650	29	13.21	50.06	18.49	17.55
BA06-6	17:25	2940	26	11.05	47.12	23.47	18.18
BA06-7	18:00	4205	18	9.04	36.51	28.78	24.97
BA06-8	18:20	4150	15	9.04	25.78	38.07	28.19
BA06-9	18:40	3940	16	7.36	48.02	29.44	13.97
BA06-10	19:00	3490	22	12.89	60.44	11.46	13.97
BA06-11	19:25	3280	24	10.37	47.52	12.50	29.75
BA06-12	19:43	3210	20	9.66	48.10	16.51	25.72
BA06-13	20:16	3310	12	6.04	51.32	19.03	22.02
BA06-14	20:25	3370	13	6.53	56.49	22.55	12.81
BA06-15	20:40	2890	14	6.57	57.90	20.76	14.02
BA06-16	21:05	3890	11	7.46	45.96	19.54	25.44
AVERAGE		3229	22	10.76	48.64	20.26	19.29
ST.DEV.		796	9	4.91	8.32	7.69	6.26

* The reason why the sum of the percentages does not always give 100 is due to the fact that some losses of material occurred during samples pre-treatment, mostly because of the dispersion of dust during screenings and the recovery of material from the grindstone.

The humidity was strongly influenced by samples pre-treatment. Indeed, the drying process did not take place under controlled conditions and it was conducted with the primary purpose of preparing the samples for subsequent treatment steps. Data reported in Table 3.1.1, therefore, do not represent the actual moisture content of the samples but only a rough estimate.

3.1.1.1. Metal ingots from the melting process

Table 3.1.2 shows the yields (%) obtained from non-ferrous metals melting processes, expressed as the ratio between the weight of the metal ingot resulting from melting in the crucible and the total dry weight of the corresponding bottom ash sample. This datum can be regarded as the maximum total efficiency of an advanced bottom ash treatment plant for the recovery of non-ferrous metals. The third column indicates how much of the metal content in the ingot is attributable to manually sorted non-ferrous lumps.

Table 3.1.2 - Yields (%) obtained from non-ferrous metals melting processes and contribution (%) of manually sorted lumps.

Sample	Yield of non-ferrous metals	Contribution of manually sorted lumps
	w% (ingot/dry BA sample)	w% (manually sorted lumps/ingot)
BA06-1	0.56	0.00**
BA06-2	1.25	0.00**
BA06-3	0.00*	0.00**
BA06-4	3.77	57.70
BA06-5	1.52	0.00**
BA06-6	2.59	7.33
BA06-7	1.58	37.63
BA06-8	0.44	109.83***
BA06-9	0.00*	0.00**
BA06-10	1.48	2.24
BA06-11	1.31	32.72
BA06-12	1.07	42.17
BA06-13	2.36	64.81
BA06-14	5.11	37.67
BA06-15	4.19	24.28
BA06-16	6.88	53.09
AVERAGE	2.13	30.72
STD.DEV.	1.94	30.80

*Null values in the second column stand for samples from which it was not possible to extract the metal component during the melting process. For instance, sample BA06-9 was characterized by a very high content of glass that caused problems inside the crucible and affected the melting operation.

**Null values in the third column indicate the impossibility to identify non-ferrous lumps during preliminary sorting.
 ***For sample BA06-8, the weight of manually sorted lumps is higher than the total weight of the ingot, meaning that part of aluminium has been lost and trapped in the salt dross during the melting process.

Figure 3.1.1 shows the trend of metallic aluminium percentage content in the ingots resulting from the melting process. Data were obtained by multiplying the non-ferrous metals yield for each sample by the metallic aluminium concentration given by the OES analysis on the ingots. The percentage content is therefore representative of the actual amount of aluminium recoverable from each bottom ash sample.

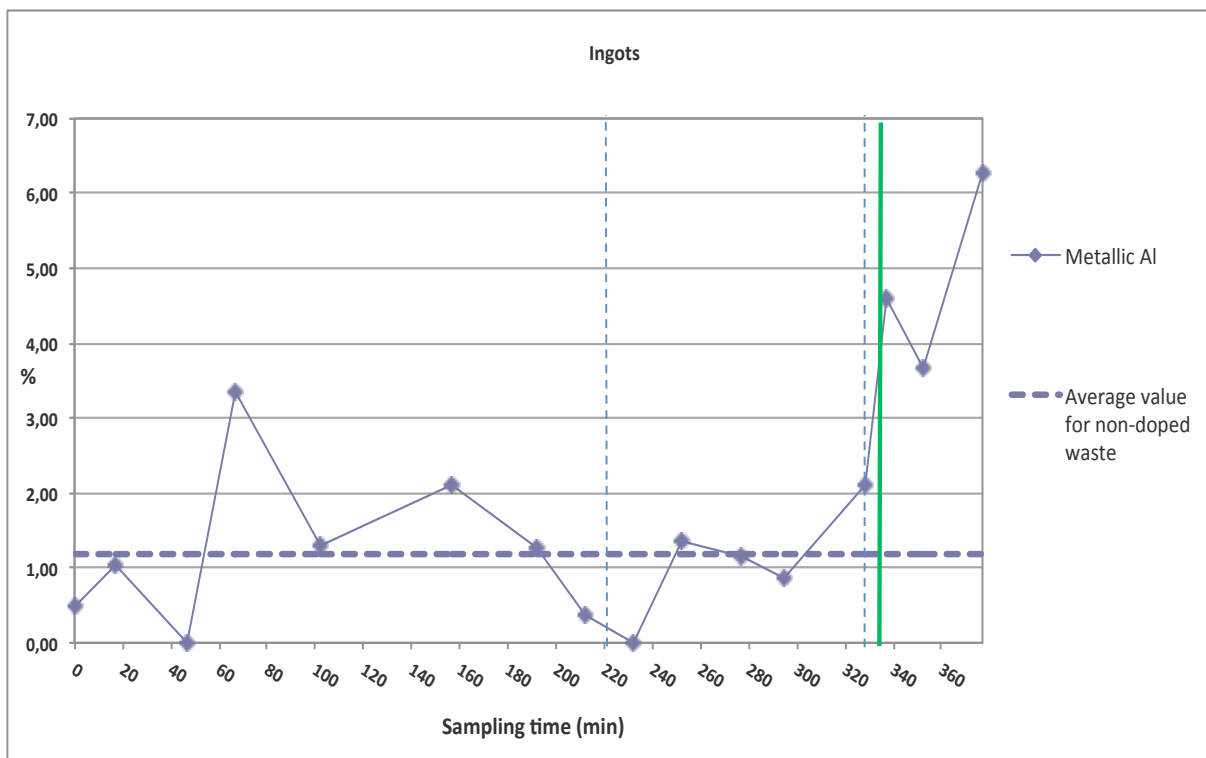


Figure 3.1.1 - Trend of metallic aluminium percentage content (on the dry weight) in the ingots resulting from the melting process. Vertical dotted lines represent the instants when the two cages were extracted. The bold vertical line indicates the beginning of the observed growth trend.

The horizontal dotted line represents the average metallic aluminium content in the ingots for the non-doped waste: it was calculated by averaging the corresponding values obtained by the analysis of the samples representative of the non-doped waste, namely those samples which lay outside the time period during which the effect of doping is clearly visible. The same procedure was repeated for the calculation of all the average values for the non-doped waste throughout this study, both for metallic and total aluminium. In this specific case, the samples representative of the non-doped waste are located between 0 and 328 minutes after the start

of the sampling and the corresponding average value of metallic aluminium is 1.2%. The first peak observed around 60 minutes from the start is probably due to the abnormal presence of a large amount of aluminium in the residual waste incinerated in standard conditions (non-doped waste). Indeed, the percentage content of aluminium drops between 1% and 2% right after that peak. The second peak (around 340 minutes) is located in the middle of a well-defined growth trend. At this stage, it is reasonable to assume that the sampled bottom ashes start to be affected by the doping of the waste.

Based on these results, it is clear that the hypothesis according to which the residence time of the tracers (the metallic cages) can be considered as a reliable estimate of the waste residence time is not validated. Indeed, the growth trend in the aluminium percentage content starts to be well-defined only at the output of the second cage when, in theory, the release of material enriched with aluminium packaging should have already been completed. It is thus possible to estimate the actual waste residence time in the furnace by considering the beginning of the growth trend (bold vertical line in Figure 3.1.1). The first charge of waste enriched with aluminium packaging was introduced into the furnace at 14:14, 34 minutes before the sampling started: being the start of the growth trend 337 minutes after the start of sampling operations, the residence time is approximately equal to 371 minutes. By examining Figure 3.1.1, it follows that only the last three bottom ash samples are affected by the doping of the waste. This information gained from the laboratory analysis has been used to assess the average contribution of aluminium packaging when estimating the final mass balance. This is obtained by calculating the difference between the aluminium content in the doped waste and the background aluminium content in the residual non-doped waste. The former value was estimated by numerical integration of the curve of Figure 3.1.1 for the section between 337 and 377 minutes, where the growth trend is located. The calculation, carried out by using the method of trapezoids, is obviously a partial and rough estimate, as it is not possible to appreciate the overall trend of the curve because the sampling was interrupted right at the beginning of the growth trend. Figure 3.1.2 visually summarizes the utilized method.

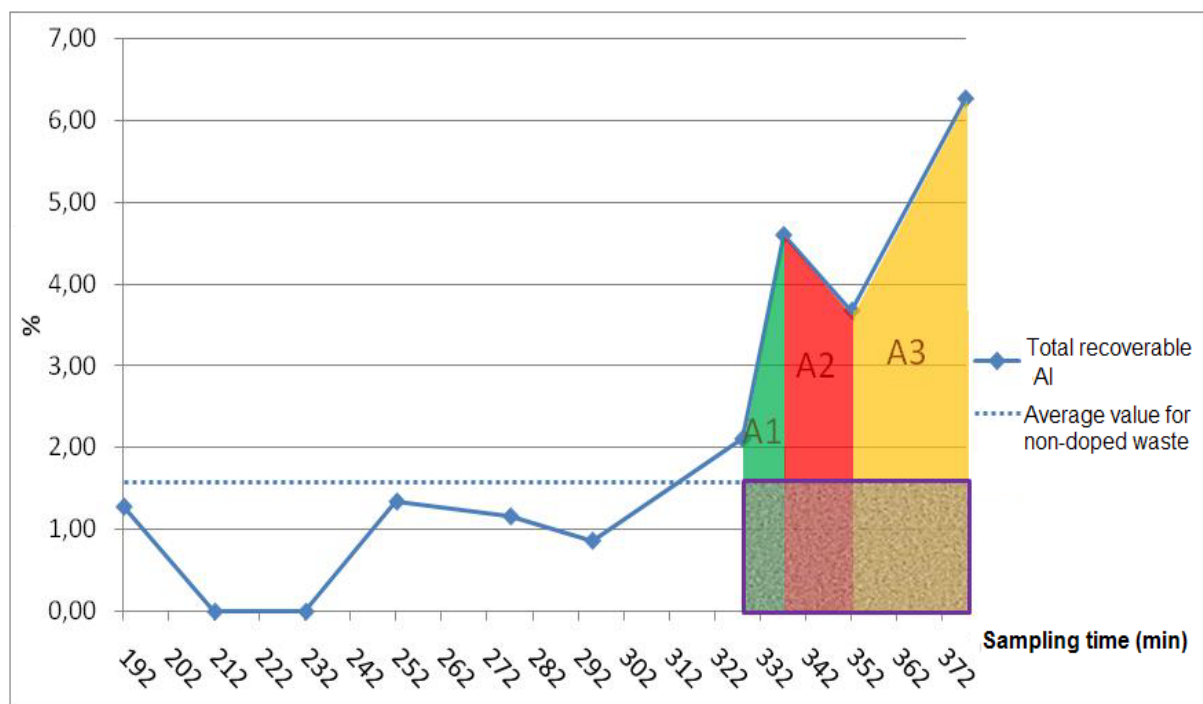


Figure 3.1.2 - Numerical integration of recoverable aluminium curve.

The sum of the trapezoid areas represents the doped waste contribution ($\text{kg}_{\text{Al}} \text{kg}^{-1} \text{bottom ashes min}$). The non-doped waste contribution was calculated by using the average background concentration of metallic aluminium, namely the average concentration corresponding to those samples located outside the growth trend. This value was then multiplied by the integration interval, resulting in the area ($\text{kg}_{\text{Al}} \text{kg}^{-1} \text{bottom ashes min}$) of the rectangle shown in Figure 3.1.2. The fed packaging average contribution, given by the difference between the doped waste contribution and the non-doped waste contribution, will be used in the final paragraph of this section to calculate the final mass balance. Table 3.1.3 gives an overview of the procedure explained above.

Table 3.1.3 - Calculation of fed packaging average contribution in the ingots.

Trapezoid	Area ($\text{kg}_{\text{Al}} \text{kg}^{-1} \text{bottom ashes min}$)
A1	0.30
A2	0.62
A3	1.24
Doped waste contribution A1+A2+A3 ($\text{kg}_{\text{Al}} \text{kg}^{-1} \text{bottom ashes min}$)	2.16
Non-doped waste contribution ($\text{kg}_{\text{Al}} \text{kg}^{-1} \text{bottom ashes min}$)	0.58
Contribution of fed packaging ($\text{kg}_{\text{Al}} \text{kg}^{-1} \text{bottom ashes min}$)	1.58

To complete the discussion on the ingots and fully understand the real potential of aluminium recovery, some samples of the salt dross resulting from the melting process in the crucible were analyzed. In this way it was possible to assess and the extent of metallic aluminium losses during the melting operation in a saline furnace, which is the most commonly used process for secondary aluminium production. Table 3.1.4 shows the results of the analysis, the percentages referring to the total dry weight of bottom ash samples.

Table 3.1.4 - Aluminium percentage content (on the dry weight) in the salt dross samples resulting from the melting process. Samples representative of the doped waste are highlighted in italics.

Sample	Metallic Al (%)	Total Al (%)	Aluminium content in an oxidized form (%)
SS06-9	1.27	2.76	53.99
<i>SS06-13</i>	<i>0.33</i>	<i>0.96</i>	<i>65.63</i>
<i>SS06-14</i>	<i>0.40</i>	<i>1.32</i>	<i>69.70</i>
<i>SS06-15</i>	<i>0.24</i>	<i>0.97</i>	<i>75.26</i>
AVERAGE	0.56	1.50	66.14
STD.DEV.	0.48	0.85	9.01

The salt dross sample SS06-9 shows a high content of aluminium because it was not possible to obtain a metal ingot from the melting operation of the corresponding bottom ash sample: all the metallic aluminium contained in the coarse fraction sent to the crucible was trapped in the salt dross.

Unfortunately, there are not enough data available to draw a general conclusion about the influence of metallic and total aluminium content in the salt dross on the final mass balance. For this reason, the contribution of the salt dross in the estimate of the mass balance was neglected. Table 3.1.5 gives an overview of the losses of metallic aluminium during the melting process in the crucible. The second column shows the sum of metallic aluminium contents analyzed in the ingots and in the salt dross.

Table 3.1.5 - Loss of metallic aluminium during the melting process in the crucible.

Sample	Metallic Al in the fraction > 0.8 mm	Loss of metallic Al in the crucible
	w% (Al/BA fraction > 0.8 mm)	w% (Al in the salt dross/ Al in BA fraction > 0.8 mm)
<i>SS06-13</i>	<i>2.44</i>	<i>13.52</i>
<i>SS06-14</i>	<i>5.00</i>	<i>8.00</i>
<i>SS06-15</i>	<i>3.91</i>	<i>6.14</i>
AVERAGE	3.78	9.22
STD.DEV.	1.28	3.84

3.1.1.2. Fine fractions

Data from the ingots analysis were crucial for the interpretation of the results related to the two bottom ash fine fractions (below 0.8 mm), the first one obtained after the preliminary screening and representing the real fine fraction of the sample, the second one being the result of the screening after grinding. Figures 3.1.3 and 3.1.4 depict the trends of total and metallic aluminium percentage content, both expressed on the total dry weight of the fractions.

A slight growth trend towards the end of the test is visible also for these two fractions, especially for total aluminium, confirming the previous analysis on the ingots. Nevertheless, it is difficult to detect a well-defined growth trend representative of the doped waste.

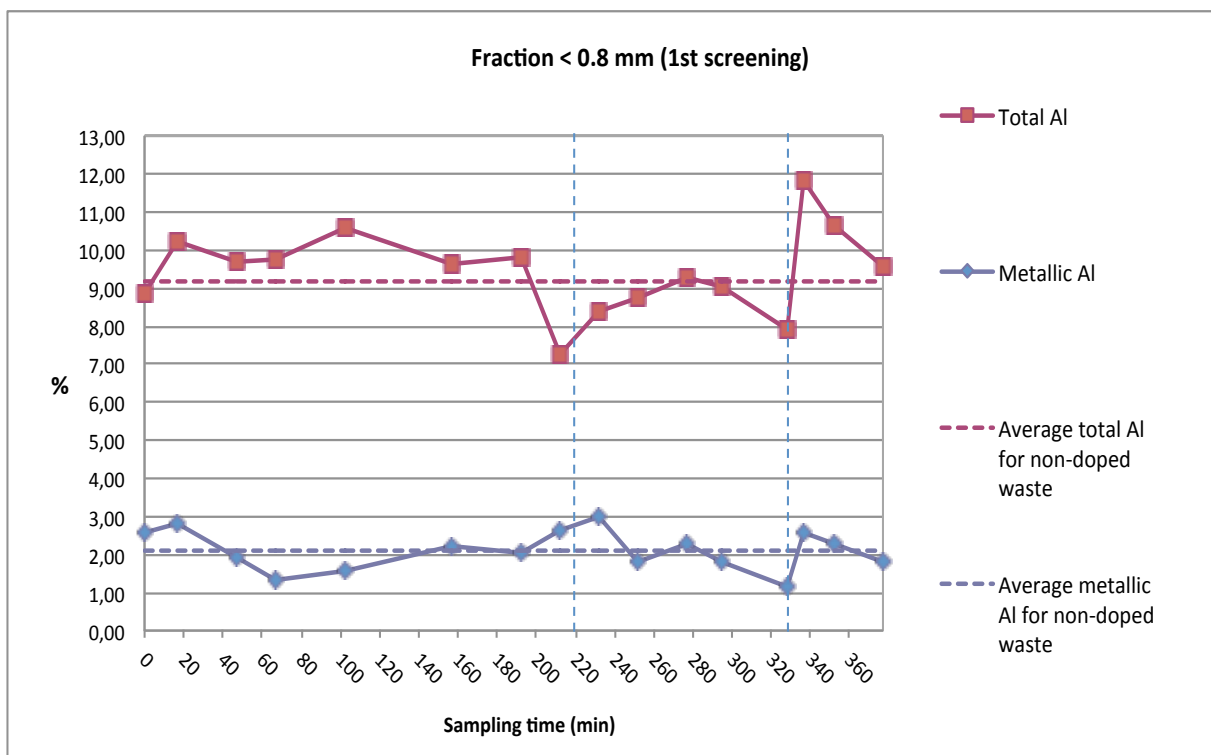


Figure 3.1.3 - Trends of total and metallic aluminium percentage content (on the dry weight) in the fraction below 0.8 mm resulting from the first screening. Vertical dotted lines represent the instants when the two cages were extracted.

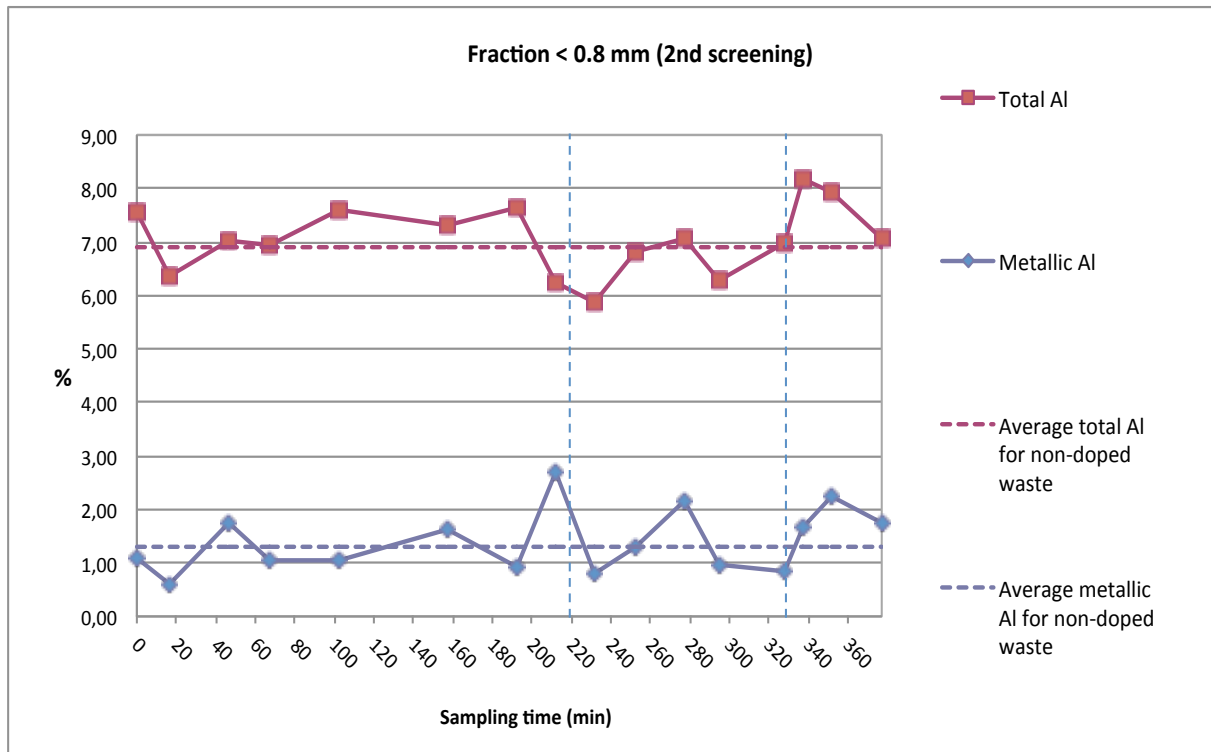


Figure 3.1.4 - Trends of total and metallic aluminium percentage content (on the dry weight) in the fraction below 0.8 mm resulting from the second screening. Vertical dotted lines represent the instants when the two cages were extracted.

Concerning the fine fraction from the first screening, the average contents of total and metallic aluminium in the non-doped waste are 9.2% and 2.1%, respectively. The fine fraction resulting from the second screening after grinding contains, similarly, an average value of 7% for total and 1.3% for metallic aluminium. In both fractions aluminium is mostly present in the oxidized form, as shown in Table 3.1.6.

Table 3.1.6 - Aluminium content in an oxidized form in the bottom ash fine fractions resulting from the first and second screening.

Sample	Aluminium content in an oxidized form (%)	
	Fraction < 0.8 mm (1 st screening)	Fraction < 0.8 mm (2 nd screening)
BA06-1	71.08	85.57
BA06-2	72.58	90.52
BA06-3	79.95	75.38
BA06-4	86.56	84.78
BA06-5	85.46	85.99
BA06-6	76.93	77.65
BA06-7	79.09	87.83
BA06-8	63.74	56.62
BA06-9	64.67	86.06
BA06-10	79.13	80.78
BA06-11	75.34	69.34
BA06-12	79.77	84.81
BA06-13	85.59	87.86
BA06-14	78.26	79.76
BA06-15	78.50	71.69
BA06-16	80.95	75.14
AVERAGE	77.35	79.99
STD. DEV.	6.66	8.81

As already specified, during the determination of metallic aluminium some problems related to the sensitivity of the measuring instrument have been experienced. For this reason, data reported in Table 3.1.6 might be not completely reliable. This aspect will become clear when discussing the results of fly ashes analysis (Paragraph 3.1.2). In any case, Table 3.1.6 does not reveal significant changes in the content of oxidized aluminium due to the doping of the waste. It should also be noted that the content of oxidized aluminium reported in the table refers to all the aluminium in the 3+ oxidation state, regardless of the mineral phase in which it is located (alumina, ettringite, zeolites or other aluminocalcium hydrate compounds).

For the bottom ash fine fractions, the fed packaging average contribution has been calculated using the same procedure as the one described above for the ingots. The curves of Figure 3.1.3 and Figure 3.1.4 were numerically integrated between 337 and 377 minutes with the method of trapezoids and the corresponding average contribution of the non-doped waste was subtracted. Table 3.1.7 shows the results of the calculation.

Table 3.1.7 - Calculation of fed packaging average contribution in the bottom ash fine fractions resulting from the first and second screening.

	Fraction < 0.8 mm (1 st screening)		Fraction < 0.8 mm (2 nd screening)	
	Metallic Al	Total Al	Metallic Al	Total Al
A1	0.17	0.89	0.11	0.68
A2	0.36	1.68	0.29	1.21
A3	0.51	2.53	0.50	1.87
Doped waste contribution (kg_{Al} kg⁻¹_{bottom ashes} min)	1.05	5.10	0.90	3.76
Non-doped waste contribution (kg_{Al} kg⁻¹_{bottom ashes} min)	1.02	4.50	0.64	3.38
Contribution of fed packaging (kg_{Al} kg⁻¹_{bottom ashes} min)	0.02	0.60	0.27	0.38

3.1.2. Fly ashes

Figure 3.1.5 shows the percentage content of total and metallic aluminium detected in fly ash samples.

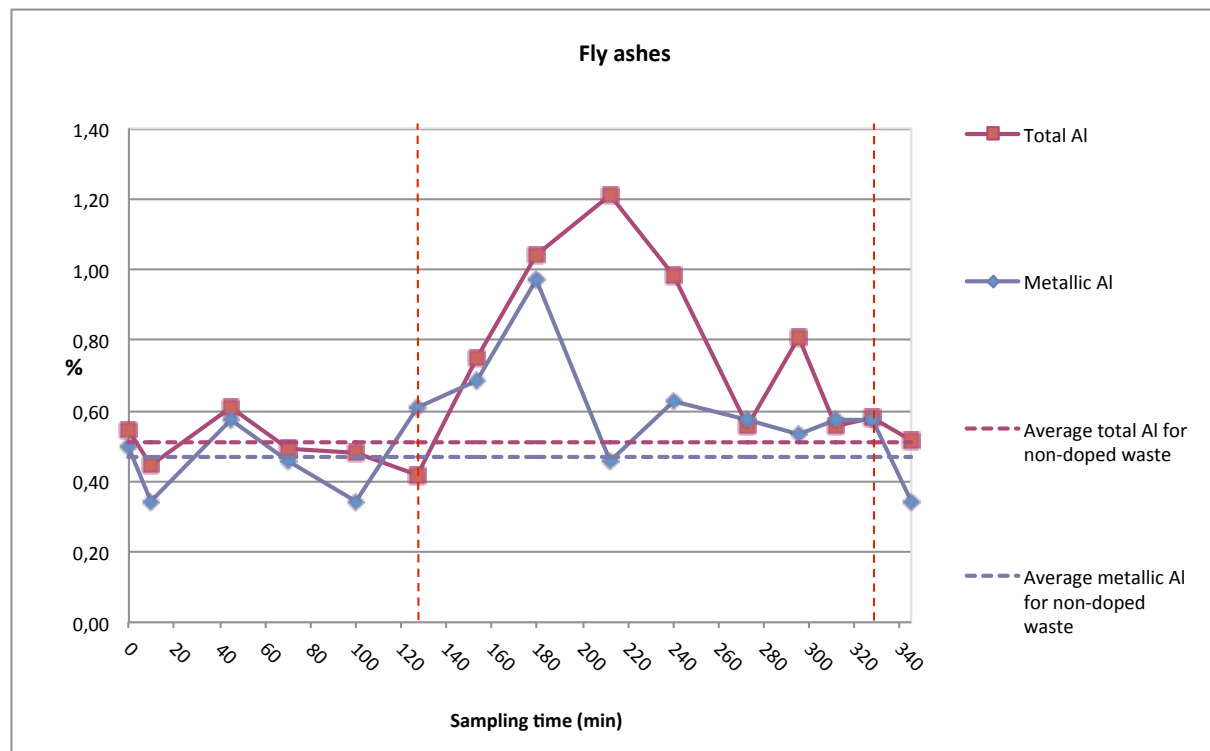


Figure 3.1.5 - Percentage content of total and metallic aluminium measured in fly ash samples. The integration interval used in the calculation of fed packaging average contribution is delimited by dotted lines.

First of all, the response time of fly ashes to the doping of aluminium is very different from that of the waste inside the furnace, as it was expected (see Paragraph 2.1). Whereas for bottom ashes the appearance of doping effects occurred approximately 6 hours after the start of the test, for fly ashes the growth trend appears about 3 hours and 30 minutes after the first doped waste feeding. Furthermore, in this case it is also possible to appreciate the downturn of the curves and hence have a more robust and reliable estimate. The sampling period representative of the doped waste, and the integration interval for the calculation of fed packaging average contribution (delimited by vertical dotted lines in Figure 3.1.5) can be clearly defined.

Secondly, the major problem encountered in the analytical phase (already discussed above) is now emphasized: for two samples, the percentage content of metallic aluminium is higher than the percentage content of total aluminium. This result is obviously illogical and can only be explained by assuming an incorrect evaluation by one of the two instruments used for the analysis: as previously discussed in Paragraph 2.4.6, the problem is evidently related to the measure of metallic aluminium through the soda attack method.

Nevertheless, an estimate of fed packaging average contribution has been provided also for fly ashes, using the same procedure described above. The appearance of the growth trend is located 153 minutes after the start of the sampling. The integration interval used in the calculation is equal to 201 minutes. Table 3.1.8 shows a summary of the calculation.

Table 3.1.8 - Calculation of fed packaging average contribution in fly ashes.

Area	Metallic Al	Total Al
A1	0.17	0.15
A2	0.22	0.24
A3	0.23	0.36
A4	0.15	0.31
A5	0.20	0.25
A6	0.12	0.15
A7	0.09	0.12
A8	0.09	0.09
Doped waste contribution (kg_{Al} kg⁻¹_{fly ashes} min)	1.28	1.67
Non-doped waste contribution (kg_{Al} kg⁻¹_{fly ashes} min)	0.94	1.03
Contribution of fed packaging (kg_{Al} kg⁻¹_{fly ashes} min)	0.34	0.64

3.1.3. Mass balance

In order to assess the distribution of fed aluminium amongst the different types of residues resulting from waste incineration and flue gas cleaning, a final mass balance has been estimated. Table 3.1.9 summarizes the flow rates used in the calculation.

Table 3.1.9 - Waste and residues flow rates used in the calculation of the final mass balance for aluminium beverage cans.

	Flow rate (kg h ⁻¹)	Flow rate (% on waste flow rate)
Waste	6320	100
Fly ashes	193	3
Wet bottom ashes	1184	19
Dry bottom ashes	929	15
Bottom ash fraction < 0.8 mm (1st screening)	100	2
Bottom ash fraction < 0.8 mm (2nd screening)	452	7

The waste flow rate was estimated by dividing the total weight of the fed waste by the period of time during which the test was carried out. As starting point it was considered the first sampling time deprived of the waste residence time in the furnace and in the bottom ash discharge system. The end of the test was determined by subtracting the response time of fly ashes to the last sampling time. Concerning fly ash flow rate, the value was obtained by multiplying the average annual specific production of the WTE plant (kg_{fly ashes} t_{MSW}⁻¹) by the waste flow rate (t_{MSW} h⁻¹). The same procedure was used to calculate the flow rate of wet bottom ashes. The corresponding dry flow rate was estimated by taking into account the average moisture content in bottom ashes reported in Table 3.1.1. The flow rates of bottom ash fine fractions (after the first and second screening) were obtained by multiplying the total dry flow rate by the average weight percentages reported in Table 3.1.1.

Table 3.1.10 shows the results of the final mass balance, obtained by multiplying the fed packaging average contribution in each fraction (kg_{Al} kg_{residue}⁻¹ min) by its corresponding flow rate converted to kg min⁻¹.

Table 3.1.10 - Mass balance related to Test 1 on aluminium beverage cans (June 6th, 2011).

	Total Al (kg)	Partitioning of recovered total Al in the residues (%)	Metallic Al (kg)	Metallic/Total Al (%)
INPUT				
Fed aluminium	228		228	
OUTPUT				
<i>Fly ashes</i>	2.1	6.8	1.1	52.7
<i>Bottom ash fraction < 0.8 mm before grinding</i>	1.0	3.3	0.04	3.8
<i>Bottom ash fraction < 0.8 mm after grinding</i>	2.9	9.4	2.0	70.4
<i>Ingots</i>	24.5	80.5	24.5	100.0
Total recovered aluminium	30.5		27.7	90.8

The actual amount of aluminium fed to the furnace (228 kg) is lower than the amount of fed packaging (240 kg) because of aluminium alloys composition. In this specific case, beverage cans are made of two different alloys: AA5182 containing 94% of aluminium and AA3004 containing about 96% of aluminium. The average of the two percentage contents, multiplied by the amount of fed packaging, gives the actual weight of aluminium placed in the furnace. It must be specified that only a part of the prepared packaging was introduced into the furnace. During feeding operation, in fact, part of the material has inevitably slipped out of the grab grip, settling at the bottom of the waste pit. It would have been necessary to consider this aspect through an appropriate correction factor, but the impossibility to quantify the exact loss advised against its use.

The mass balance shows that only the 13% of aluminium fed into the furnace was recovered in the incineration residues (30.5 out of 227.8 kg). By examining the information previously obtained, three hypotheses can be advanced to explain this result:

- The first is related to the sampling interval. The residence time of the waste during the test was significantly higher than the one theoretically expected and estimated with tracers. Consequently, the sampling did not cover the entire period during which the appearance of bottom ashes representative of the doped waste took place. The evidence is provided by Figure 3.1.1: after an initial growth phase of the curve, a similar downturn should follow. However, it is not possible to appreciate its overall trend because the sampling stops right at the highest measured value.
- The second is linked to the specific characteristics of the incineration process and, in particular, to the type of plant. During combustion, aluminium subjected to temperatures

above 650°C melts and percolates through the grate mesh. In the sub-grate section the temperature drop causes the solidification of the metal, which can form lumps or alternatively stick to the surrounding surfaces; it follows that the metal is trapped within the grate itself or its moving mechanisms. A confirmation was given by Valmadrera plant operators, who reported that during temporary plant shutdowns for maintaining operations it is possible to recover a certain amount of aluminium from the sub-grate section.

- The third hypothesis regards the dissolution of aluminium metal and alumina in the extremely alkaline environment characterizing the bottom ash quenching water, according to the reactions and the mechanisms already illustrated in Paragraph 1.5 and 1.6.

Despite the poor closure of the final mass balance, data from Table 3.1.10, which show the partitioning of total and metallic aluminium recovered in the incineration residues, provide ground for interesting considerations.

More specifically, it has to be noted that, out of the total aluminium recovered from the residues (30.5 kg), about 80% (24.5 kg) comes from the ingots resulting from the melting process. This fraction is representative of the real amount of recoverable metal since it only consists of metallic aluminium.

Actually, the calculated partitioning percentages are partially distorted by the different relationship between the residence time and the sampling time of the incineration residues. For fly ashes the sampling covered the entire period during which the material representative of the doped waste was discharged. It was then possible to reconstruct the overall trend of the curve (Figure 3.1.5) and evaluate the total contribution of the packaging. This is not true for bottom ashes, the sampling of which enabled to recover only a small part of the introduced material. Therefore, the percentage value of aluminium partitioning in bottom ashes (and consequently in the ingots) is underestimated.

Concerning the metallic content of aluminium recovered in the residues, a very low amount (4%) is contained in the bottom ash fine fraction before grinding: it means that, in this residue, aluminium is almost all oxidized. In contrast, most of the aluminium in the fine fraction after grinding is metallic (70%). Fly ashes contain about half of the aluminium in the metallic form (53%), while metal ingots contain only metallic aluminium by definition.

3.2. Aluminium trays

Results obtained from the analysis of the samples taken during Test 2 on aluminium trays (see Table 2.1.1) are presented in this paragraph.

3.2.1 Bottom ashes

Table 3.2.1 gives an overview of the type and quantity of the sub-fractions obtained from the pre-treatment of bottom ash samples taken during Test 2 on aluminium trays.

Table 3.2.1 - Dry weight, humidity and sub-fractions (expressed as weight percentage on dry samples) obtained from the pre-treatment of bottom ash samples taken during Test 2 on aluminium trays.

Sample	Time	Dry weight	Humidity	Fraction < 0.8 mm	Fraction < 0.8 mm after grinding	Fraction > 0.8 mm after grinding	Iron+inert scraps
		<i>g</i>	<i>%</i>	<i>%</i>	<i>%</i>	<i>%</i>	<i>%</i>
BA07-1	15:19	2800	18	10.71	57.97	11.07	20.00
BA07-2	15:40	2770	13	7.94	55.08	15.02	22.53
BA07-3	16:15	2230	15	7.62	59.47	14.80	17.49
BA07-4	16:45	2510	14	5.58	54.35	23.11	15.94
BA07-5	17:17	3170	11	4.73	53.36	23.03	18.30
BA07-6	17:50	2730	17	6.59	55.66	13.92	23.08
BA07-7	18:05	2170	23	8.29	59.74	12.90	19.35
BA07-8	18:12	2840	17	8.80	52.34	18.31	20.07
BA07-9	18:23	1340	21	7.46	65.20	10.45	17.16
BA07-10	18:35	1980	24	10.10	66.05	9.60	13.64
BA07-11	18:36	2150	15	6.05	67.20	12.09	14.88
BA07-12	18:45	2290	12	5.68	64.96	12.23	17.03
BA07-13	18:53	1960	16	8.16	60.57	15.82	15.31
BA07-14	18:57	2370	25	13.50	56.44	15.19	13.92
BA07-15	19:11	2730	14	6.96	53.85	12.82	26.01
BA07-16	19:25	2600	20	13.08	56.89	13.46	16.92
BA07-17	19:40	2420	26	19.42	69.67	14.46	19.01
AVERAGE		2415	18	8.86	59.34	14.60	18.27
STD.DEV.		433	5	3.67	5.41	3.82	3.36

Compared to Test 1 on aluminium beverage cans, there is a slight increase of the fine fraction resulting from the second screening (after grinding) at the expense of the coarse fraction sent to the crucible.

3.2.1.1 Metal ingots from the melting process

Table 3.2.2 shows the yields (%) obtained from non-ferrous metals melting processes, expressed by the ratio between the weight of the metal ingot resulting from melting in the crucible and the total dry weight of the corresponding bottom ash sample (second column). The metal content in the ingot that is attributable to manually sorted non-ferrous lumps is reported in the third column.

Table 3.2.2 - Yields (%) obtained from non-ferrous metals melting processes and contribution (%) of manually sorted lumps.

Sample	Yield of non-ferrous metals w% (ingot/dry BA sample)	Contribution of manually sorted lumps w% (manually sorted lumps/ingot)
BA07-1	1.42	41.28
BA07-2	1.21	0.00*
BA07-3	2.74	61.77
BA07-4	2.77	34.99
BA07-5	2.27	36.20
BA07-6	2.17	31.19
BA07-7	2.74	34.10
BA07-8	2.22	16.07
BA07-9	2.48	11.43
BA07-10	3.82	41.97
BA07-11	3.23	8.12
BA07-12	4.37	15.14
BA07-13	5.25	19.12
BA07-14	4.80	7.17
BA07-15	4.99	35.25
BA07-16	7.48	42.48
BA07-17	7.52	48.64
AVERAGE	3.62	28.53
DEV. STD.	1.88	17.02

*Null values in the third column indicate that it was not possible to identify non-ferrous lumps during the preliminary sorting.

Again, there is an increase in the yields of non-ferrous metal corresponding to the last samples but, compared to Test 1 on aluminium beverage cans, the growth appears more gradual and well-defined. Figure 3.2.1 shows the trend of metallic aluminium percentage content in the ingots resulting from the melting process.

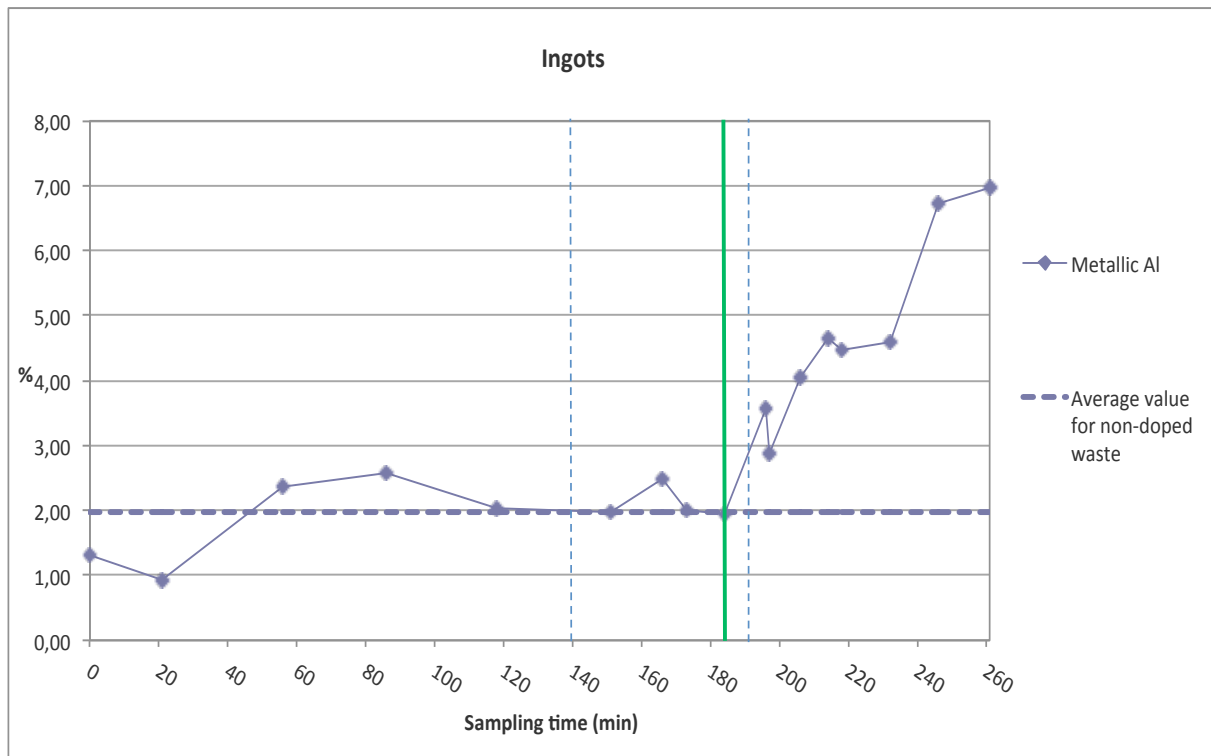


Figure 3.2.1 - Trend of metallic aluminium percentage content (on the dry weight) in the ingots resulting from the melting process. Vertical dotted lines represent the moments when the two cages were extracted. The bold vertical line indicates the beginning of the observed growth trend.

The curve is still increasing at the end of the sampling period, meaning that even in this case the downturn cannot be observed. A precise indication of the waste residence time and a reliable value about the contribution of the doped waste cannot be gathered. The results, however, allow for a better interpretation of the test compared to those obtained for beverage cans. First of all, there is a good distribution of the non-doped waste samples around their average value, equal to 1.96%, without unexpected peaks as it happened for beverage cans. Secondly, the increase in the percentage content of aluminium is distributed over multiple samples, thus providing a better assessment of the packaging contribution.

The first charge of waste enriched with aluminium packaging was introduced into the furnace at 14:53, 26 minutes before the sampling started: being the start of the growth trend located at 196 minutes after the start of sampling operations, the residence time is thus approximately equal to 222 minutes. The integration of the curve has been calculated from 196 minutes after the start of the sampling (beginning of the growth trend) to the end of the sampling period, resulting in an integration interval of 65 minutes. The methodology used for the calculation of fed packaging average contribution has already been described in paragraph 3.1.1.1 of this chapter. Table 3.2.3 summarizes the results of calculation.

Table 3.2.3 - Calculation of fed packaging average contribution in the ingots.

Trapezoid	Area ($\text{kg}_{\text{Al}} \text{kg}^{-1} \text{bottom ashes min}$)
A1	0.33
A2	0.03
A3	0.31
A4	0.35
A5	0.18
A6	0.63
A7	0.79
A8	1.03
Doped waste contribution ($\text{kg}_{\text{Al}} \text{kg}^{-1} \text{bottom ashes min}$)	3.66
Non-doped waste contribution ($\text{kg}_{\text{Al}} \text{kg}^{-1} \text{bottom ashes min}$)	1.51
Contribution of fed packaging ($\text{kg}_{\text{Al}} \text{kg}^{-1} \text{bottom ashes min}$)	2.15

Results of the analysis on some salt dross samples resulting from the melting process in the crucible are reported in Table 3.2.4. Percentages of metallic and total aluminium refer to the total dry weight of bottom ash samples, as usual.

Table 3.2.4 - Aluminium percentage content (on the dry weight) in some salt dross samples resulting from the melting process. Samples representative of the doped waste are highlighted in italics.

Sample	Metallic Al (%)	Total Al (%)	Aluminium content in an oxidized form (%)
SS07-2	0.44	0.98	55.10
SS07-3	0.34	0.86	60.47
SS07-6	0.37	0.84	55.95
SS07-8	0.59	1.37	56.93
<i>SS07-13</i>	<i>0.29</i>	<i>0.88</i>	<i>67.05</i>
<i>SS07-15</i>	<i>0.26</i>	<i>0.50</i>	<i>48.00</i>
<i>SS07-16</i>	<i>0.19</i>	<i>0.40</i>	<i>52.50</i>
<i>SS07-17</i>	<i>0.06</i>	<i>0.10</i>	<i>40.00</i>
AVERAGE	0.32	0.74	54.50
STD.DEV.	0.16	0.39	8.09

Four samples of salt dross were selected as representative of the non-doped waste, and four of the doped waste (in italics in Table 3.2.4). There is a significant decrease in aluminium content in the transition from the non-doped waste salt dross to the doped waste salt dross. To better appreciate this variation, Table 3.2.5 reports the loss of metallic aluminium during the melting process in the crucible.

Table 3.2.5 - Loss of metallic aluminium during the melting process in the crucible. Samples representative of the doped waste are highlighted in italics.

Sample	Metallic Al in the fraction > 0.8 mm	Loss of metallic Al in the crucible
	w% (Al/BA fraction > 0.8 mm)	w% (Al in the salt dross/ Al in BA fraction > 0.8 mm)
SS07-2	1.37	32.12
SS07-3	2.72	12.50
SS07-6	2.36	15.68
SS07-8	2.61	22.61
<i>SS07-13</i>	<i>4.94</i>	<i>5.87</i>
<i>SS07-15</i>	<i>4.85</i>	<i>5.36</i>
<i>SS07-16</i>	<i>6.92</i>	<i>2.75</i>
<i>SS07-17</i>	<i>7.04</i>	<i>0.85</i>
AVERAGE	4.10	12.22
STD.DEV.	2.15	10.84

Losses decrease dramatically in the transition from the non-doped to the doped waste. This effect is related to the characteristics of the melting process itself: the greater the amount of aluminium contained in the fraction above 0.8 mm, the easier the melting process because the operator is favoured in the separation of the metal from the molten salt cake. In contrast, when aluminium concentration is too low, the operator is forced to add large quantities of salt to manage the removal of impurities. The salt increases the residues volume and, consequently, the phenomena of molten aluminium capture in the dross. Due to the extremely low content of aluminium, the contribution of the salt dross in the calculation of fed packaging average contribution for the doped waste has been considered negligible.

3.2.1.2. Fine fractions

Figures 3.2.2 and 3.2.3 depict the trends of total and metallic aluminium percentage content (on the dry weight) in the bottom ash fine fractions.

The bold vertical line corresponding to 184 minutes shows the instant when the samples begin to be affected by the doping of the waste, as it has emerged from the analysis of metallic aluminium recovered in the crucible. Looking at those figures, a peculiarity can be noticed: the increase of total and metallic aluminium concentrations in the two fractions takes place before the appearance of the corresponding growth trend in the ingots. This aspect is probably due to the characteristics of the incineration plant and, more specifically, to the

grate structure. During combustion, the finest fractions of the waste may already fall underneath the grate in its first sections, passing through the holes designed for the supply of combustion air. There might be, in other words, a sort of bypass, with the finest material sometimes reaching the quenching water bath and the extraction system much earlier than the corresponding coarse fraction, forced to move along the grate in its entire length. This explanation is only valid for the fraction separated through the first screening, since it is representative of the real bottom ash fine material. The second screening, in fact, takes place after the grinding of the coarse fraction. Actually, the 0.8 mm mesh screen is very selective and retains, during the first screening, a large amount of the material that may possibly fall into the sub-grate. It might also happen that a part of the fine fraction is trapped in the coarse size of inert material when discharged in the water bath and this may explain the anticipation of the growth trend also for the fraction below 0.8 mm separated through the second screening.

The described phenomenon affects the estimate of the average packaging contribution. As a final result of this consideration, the integration of the curves of total and metallic aluminium content cannot be based on the same time interval considered for the ingots. In this case, the growth trend begins 118 minutes after the start of the sampling. For this reason, the vertical line has been moved at the beginning of the growth trend observed for the two fine fractions.

The peculiarity above explained was not observed during the analysis of bottom ash fine fractions related to Test 1 on beverage cans, probably because of the different structures characterizing the two packaging types. Indeed, aluminium from trays tends to migrate much more easily in the finer fractions of bottom ashes than aluminium from cans does, as it will be further discussed in Paragraph 3.2.3.

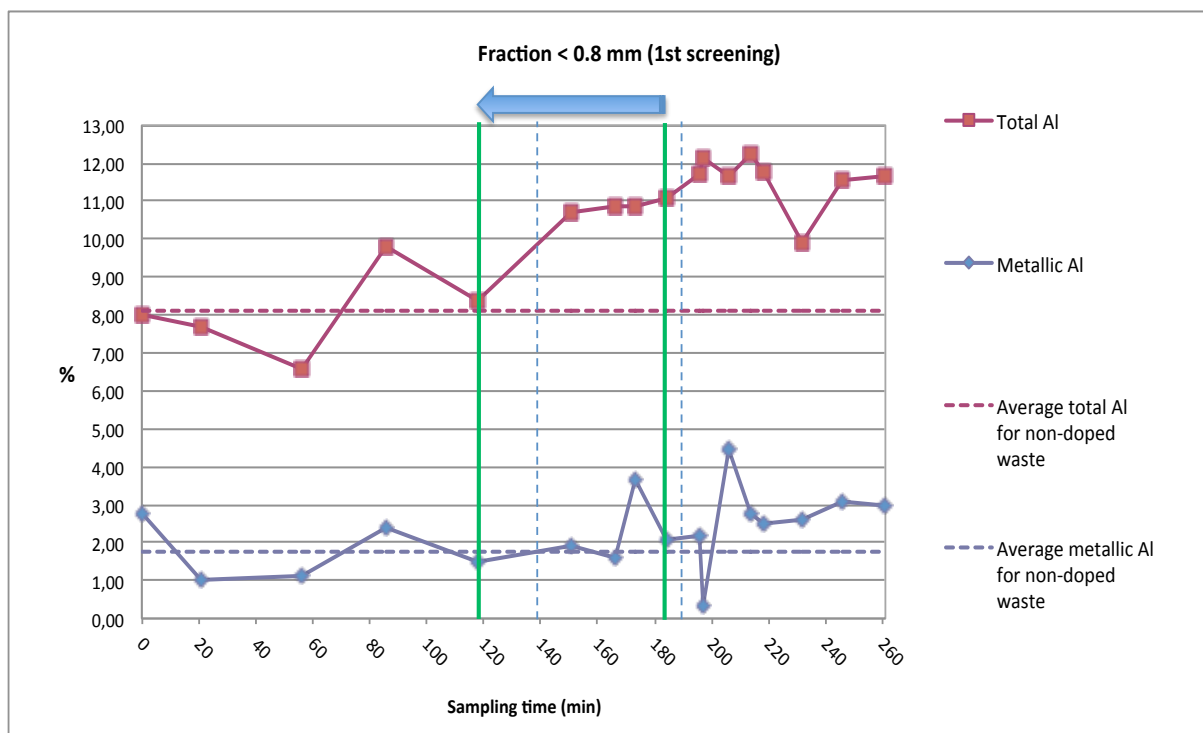


Figure 3.2.2 - Trends of total and metallic Al percentage content (on the dry weight) in the fraction below 0.8 mm resulting from the first screening. Vertical dotted lines represent the instants when the two cages were extracted. The vertical lines indicate the beginning of the growth trend according to the analysis on metallic Al content in the ingots (line on the right) and in the fine fractions (line on the left).

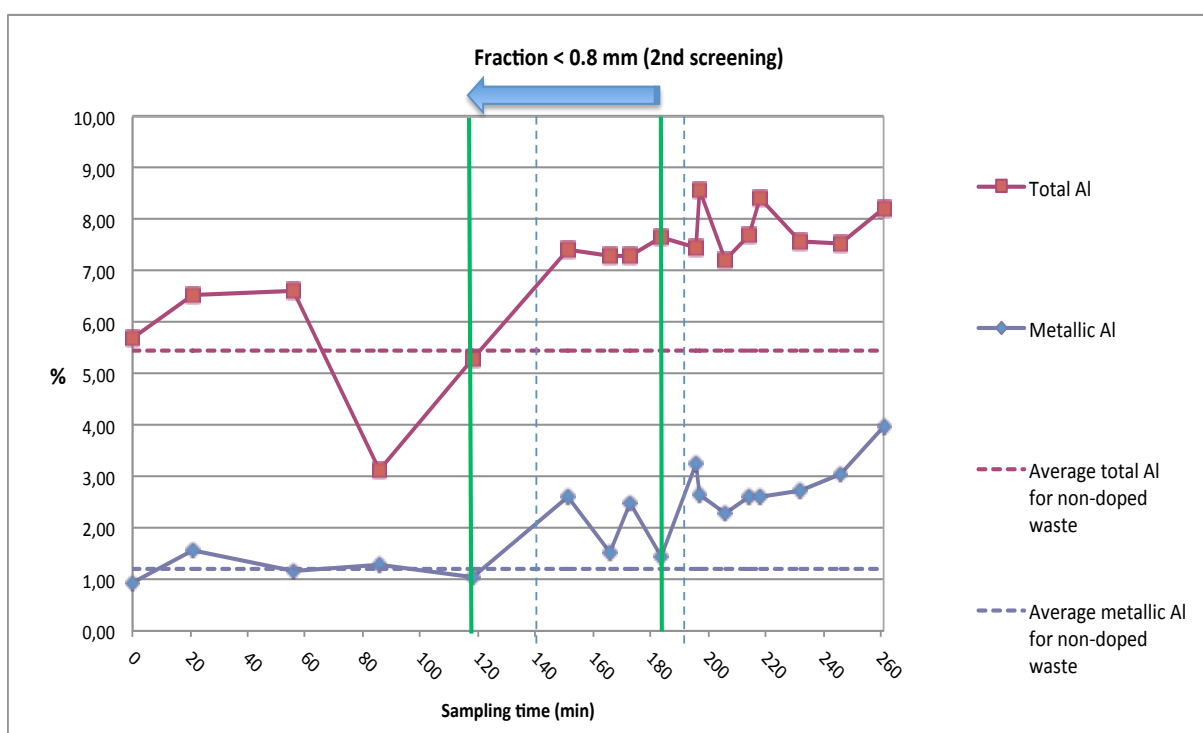


Figure 3.2.3 - Trends of total and metallic Al percentage content (on the dry weight) in the fraction below 0.8 mm resulting from the second screening. Vertical dotted lines represent the instants when the two cages were extracted. The vertical lines indicate the beginning of the growth trend according to the analysis on metallic Al content in the ingots (line on the right) and in the fine fractions (line on the left).

The time horizon considered in the numerical integration is therefore equal to 143 minutes. Dotted horizontal lines indicate the average values of total and metallic aluminium percentage content calculated for the non-doped waste. Concerning the fine fraction resulting from the first screening, the average total aluminium content is 8.1%, while the average metallic aluminium content is 1.8%. For the fine fraction resulting from the second screening, the average percentage contents are equal to 5.4% and 1.2%, respectively.

Table 3.2.6 reports the calculation of fed packaging average contribution. Table 3.2.7 shows the aluminium content in an oxidized form in the two bottom ash fine fractions. It does not reveal any significant change due to the doping of the waste.

Table 3.2.6 - Calculation of fed packaging average contribution in the bottom ash fine fractions resulting from the first and second screening.

	Fraction < 0.8 mm (1 st screening)		Fraction < 0.8 mm (2 nd screening)	
	Metallic Al	Total Al	Metallic Al	Total Al
A1	0.57	3.15	0.61	2.09
A2	0.53	1.62	0.31	1.10
A3	0.37	0.76	0.14	0.51
A4	0.63	1.21	0.22	0.82
A5	0.51	1.37	0.28	0.90
A6	0.03	0.12	0.03	0.08
A7	0.43	1.07	0.22	0.71
A8	0.58	0.96	0.20	0.60
A9	0.21	0.48	0.10	0.32
A10	0.72	1.52	0.37	1.12
A11	0.80	1.50	0.40	1.06
A12	0.91	1.74	0.53	1.18
Doped waste contribution (kg_{Al} kg⁻¹_{bottom ashes} min)	6.27	15.48	3.41	10.50
Non-doped waste contribution (kg_{Al} kg⁻¹_{bottom ashes} min)	2.52	11.58	1.72	7.79
Contribution of fed packaging (kg_{Al} kg⁻¹_{bottom ashes} min)	3.76	3.90	1.70	2.71

Table 3.2.7 - Aluminium content in an oxidized form in the bottom ash fine fractions resulting from the first and second screening.

Sample	Aluminium content in an oxidized form (%)	
	Fraction < 0.8 mm (1 st screening)	Fraction < 0.8 mm (2 nd screening)
BA07-1	65.84	83.50
BA07-2	86.62	76.30
BA07-3	82.60	82.20
BA07-4	75.56	59.18
BA07-5	82.27	79.87
BA07-6	81.84	64.64
BA07-7	85.31	79.02
BA07-8	66.39	65.86
BA07-9	81.41	81.16
BA07-10	81.44	56.23
BA07-11	97.17	68.96
BA07-12	61.77	68.25
BA07-13	77.55	65.93
BA07-14	78.62	69.19
BA07-15	73.45	64.04
BA07-16	73.31	59.68
BA07-17	74.47	51.49
AVERAGE	77.98	69.15
STD.DEV.	8.59	9.75

3.2.2. Fly ashes

Figure 3.2.4 shows the percentage content of total and metallic aluminium measured in fly ash samples.

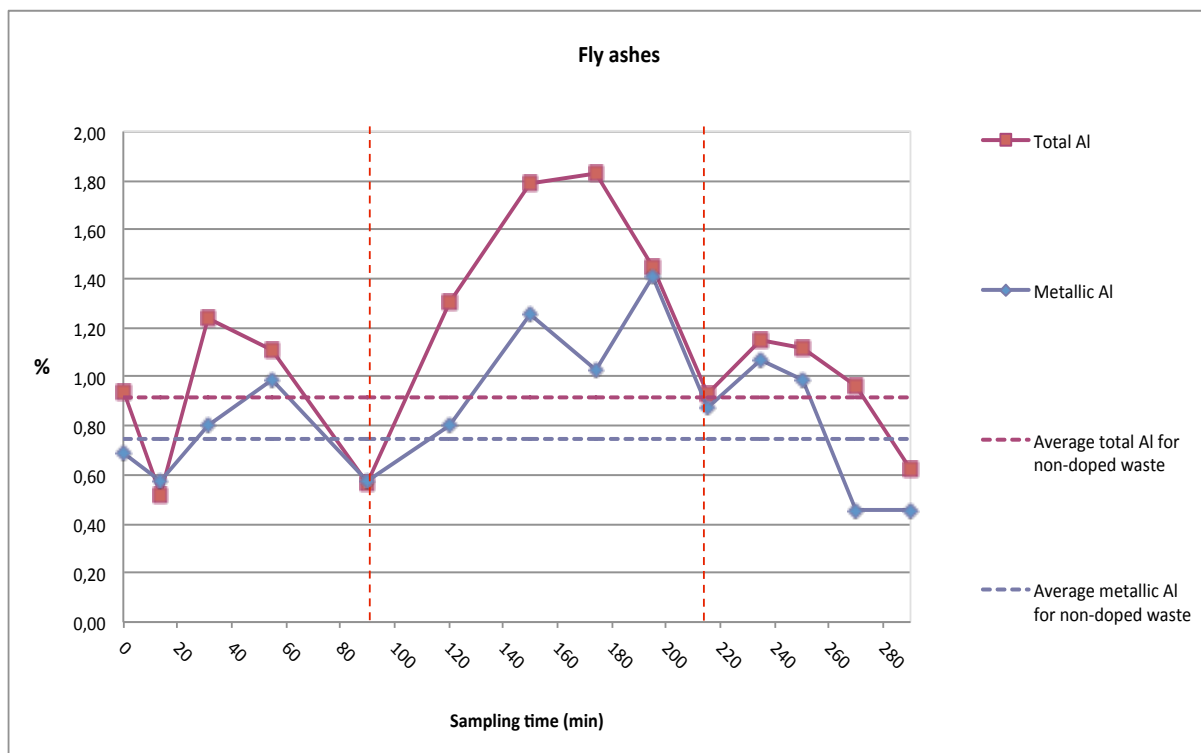


Figure 3.2.4 - Percentage content of total and metallic aluminium measured in fly ash samples. The integration interval used in the calculation of fed packaging average contribution is delimited by vertical dotted lines.

It is important to underline that the values of metallic aluminium are affected by the limitations of the measuring instruments described in Paragraph 2.4.6. The curves reproduce the same trend appreciated in Figure 3.1.5 concerning Test 1 on beverage cans. The growth trend appears around 120 minutes after the start of the sampling. Considering that the first charge of doped waste was introduced into the furnace at 14:53 and fly ash sampling started at 15:00, the estimate of the response time amounts to 127 minutes. The integration interval, identified by vertical dotted lines, is equal to 125 minutes and corresponds to the period during which fly ash samples representative of the doped waste were taken. Table 3.2.8 shows the results of the numerical integration, carried out in the usual way.

Table 3.2.8 - Calculation of fed packaging average contribution in fly ashes.

Area	Metallic Al	Total Al
A1	0.21	0.28
A2	0.31	0.46
A3	0.27	0.43
A4	0.26	0.34
A5	0.23	0.24
Doped waste contribution (kg_{Al} kg⁻¹_{fly ashes} min)	1.27	1.76
Non-doped waste contribution (kg_{Al} kg⁻¹_{fly ashes} min)	0.93	1.15
Contribution of fed packaging (kg_{Al} kg⁻¹_{fly ashes} min)	0.34	0.62

3.2.3. Mass balance

Table 3.2.9 lists all the flow rates considered in the estimate of the final mass balance.

Table 3.2.9 - Waste and residues flow rates used in the calculation of the final mass balance for aluminium trays.

	Flow rate (kg h ⁻¹)	Flow rate (w% on waste flow rate)
Waste	6210	100
Fly ashes	189	3
Wet bottom ashes	1164	19
Dry bottom ashes	958	15
Bottom ash fraction < 0.8 mm (1st screening)	85	1
Bottom ash fraction < 0.8 mm (2nd screening)	569	9

All the flow rates have been calculated according to the method reported in Paragraph 3.1.3. Table 3.2.10 shows the results of the final mass balance, obtained by multiplying the fed packaging average contribution in each fraction by the corresponding flow rate converted to kg min⁻¹.

Table 3.2.10 - Mass balance related to Test 2 on aluminium trays (June 7th, 2011).

	Total Al (kg)	Partitioning of recovered total Al in the residues (%)	Metallic Al (kg)	Metallic/Total Al (%)
INPUT				
Fed aluminium	232		232	
OUTPUT				
<i>Fly ashes</i>	1.9	2.9	1.1	55.2
<i>Bottom ash fraction < 0.8 mm before grinding</i>	5.5	8.2	5.3	96.2
<i>Bottom ash fraction < 0.8 mm after grinding</i>	25.7	38.0	16.1	62.7
<i>Ingots</i>	34.3	50.9	34.3	100.0
Total recovered aluminium	67.4		55.7	82.6

Once again, the composition of the alloy was taken into account in determining the amount of fed aluminium. Trays are made of AA8006 alloy, which contains 96.7% aluminium on average.

About 30% of the aluminium introduced with the packaging has been recovered (67.4 out of 232 kg). This result shows a significant improvement concerning the material recovered from all the incineration residues, in comparison to Test 1 performed on beverage cans. The explanation lies in two main factors:

- The first is connected with the waste residence time and, implicitly, with the conditions that occurred during the combustion process. During this test, the movement of the waste inside the furnace was faster, as confirmed by the analysis of process parameters in Paragraph 2.2. Therefore, it was possible to increase the number of samples taken after the exit of the second cage, hence representative of the doped waste. Consequently, a better reconstruction of the curves representing recoverable aluminium in the ingots and metallic and total aluminium in the two fine fractions could be implemented.
- The second factor regards the specific packaging type. Aluminium trays are characterized by a lower weight and thickness compared to beverage cans. The number of single units introduced into the furnace is therefore much larger (around 50,000), despite the total mass is exactly the same. This implies a better mixing of the packaging within the waste but also the possible formation of small-sized lumps because of their thinner structure. This is partly confirmed by the significant increase in the aluminium content registered in the bottom ash fine fractions. As explained above, this increase is probably attributable to

the material that fell underneath the grate, to which trays may have contributed in relevant quantities.

Although there is a greater recovery of aluminium from the incineration residues, even for trays the closure of the final mass balance is far from being achieved. The reasons lie once again in the incompleteness of the sampling, in the entrapment of molten metal inside the furnace grate during the combustion process and in the possible dissolution of aluminium in the bottom ash quenching water. Consequently, even for trays the contribution of bottom ashes in the aluminium mass balance happens to be underestimated. All these aspects have already been discussed in Paragraph 3.1.3.

Concerning the metallic content of aluminium recovered in the residues, there is a considerable difference from Test 1 on beverage cans. Aluminium is almost entirely in the metallic form (96%) in the “real” bottom ash fine fraction, while fly ashes contain about half of the aluminium (55%) as a metal, as it was also observed for beverage cans.

3.3 Aluminium spray cans

Results obtained from the analysis of the samples taken during Test 3 on aluminium spray cans (see Table 2.1.1) are presented in this paragraph.

3.3.1 Bottom ashes

Table 3.3.1 gives an overview of the type and quantity of the sub-fractions obtained from the pre-treatment of bottom ash samples taken during Test 3 on aluminium spray cans.

Table 3.3.1 - Dry weight, humidity and sub-fractions (expressed as weight percentage on dry samples) obtained from the pre-treatment of bottom ash samples taken during Test 3 on aluminium spray cans.

Sample	Time	Dry weight	Humidity	Fraction < 0.8 mm	Fraction < 0.8 mm after grinding	Fraction > 0.8 mm after grinding	Iron+inert scraps
		<i>g</i>	%	%	%	%	%
BA08-1	9.50	2190	18	7.76	67.12	12.33	12.79
BA08-2	10.13	2040	20	7.84	64.09	13.73	14.22
BA08-3	10.45	2210	11	4.98	72.91	7.69	14.03
BA08-4	11.30	2440	28	14.34	57.70	9.84	18.03
BA08-5	13.15	1530	25	7.84	69.93	11.76	10.46
BA08-6	14.30	2300	20	6.52	73.61	8.26	11.74
BA08-7	15.30	3780	24	10.58	55.74	17.06	16.54
BA08-8	15.50	2910	15	4.81	63.46	4.47	27.15
BA08-9	15.53	1350	25	13.33	63.29	14.07	9.63
BA08-10	16.00	2410	24	7.05	63.71	17.01	12.45
BA08-11	16.10	1690	27	10.65	66.27	11.24	11.83
BA08-12	16.16	3690	25	11.38	54.65	22.49	11.38
BA08-13	16.23	1520	33	16.45	59.74	9.87	13.82
BA08-14	16.30	1250	31	12.80	73.19	8.80	4.80
BA08-15	16.35	2030	18	8.37	66.73	9.85	15.27
BA08-16	16.45	3370	17	9.50	61.21	15.73	13.65
BA08-17	16.52	3510	14	8.55	60.58	21.37	9.69
BA08-18	17.00	3480	19	11.21	50.97	23.28	14.66
AVERAGE		2428	22	9.67	63.61	13.27	13.45
STD.DEV.		839	6	3.20	6.48	5.32	4.52

Compared to Test 1 on beverage cans and Test 2 on trays, there is a further increase in the fine fraction separated through the second screening.

3.3.1.1 Metal ingots from the melting process

Table 3.3.2 shows the yields (%) obtained from non-ferrous metals melting processes, expressed as the ratio between the weight of the metal ingot resulting from melting in the crucible and the total dry weight of the corresponding bottom ash sample (second column). The metal content in the ingots attributable to manually sorted non-ferrous lumps is reported in the third column.

Table 3.3.2 - Yields (%) obtained from non-ferrous metals melting processes and contribution (%) of manually sorted lumps.

Sample	Yield of non-ferrous metals w% (ingot/dry BA sample)	Contribution of manually sorted lumps w% (manually sorted lumps/ingot)
BA08-1	3.32	72.66
BA08-2	1.38	15.28
BA08-3	1.09	33.95
BA08-4	1.77	40.39
BA08-5	5.19	83.38
BA08-6	1.70	57.80
BA08-7	2.17	65.35
BA08-8	1.27	54.53
BA08-9	5.42	85.66
BA08-10	0.93	70.89
BA08-11	3.71	78.95
BA08-12	2.61	59.85
BA08-13	0.30	622.22*
BA08-14	2.96	55.81
BA08-15	1.31	48.30
BA08-16	4.42	58.29
BA08-17	4.50	64.30
BA08-18	6.61	53.91
AVERAGE	2.81	90.09
DEV. STD.	1.81	133.94

* The total weight of manually sorted lumps is higher than the weight of the ingot. This means that part of aluminium had been trapped in the salt dross during the melting process causing a loss of recoverable material.

The results indicate that most of the aluminium was trapped in the salt dross during the melting process, as it is confirmed by the low non-ferrous metal yields. In general, a moderate increase is detectable for the last three samples. These data can be better evaluated by looking to Figure 3.3.1, which shows the trend of metallic aluminium percentage content in the ingots from the melting process expressed as a function of the sampling time.

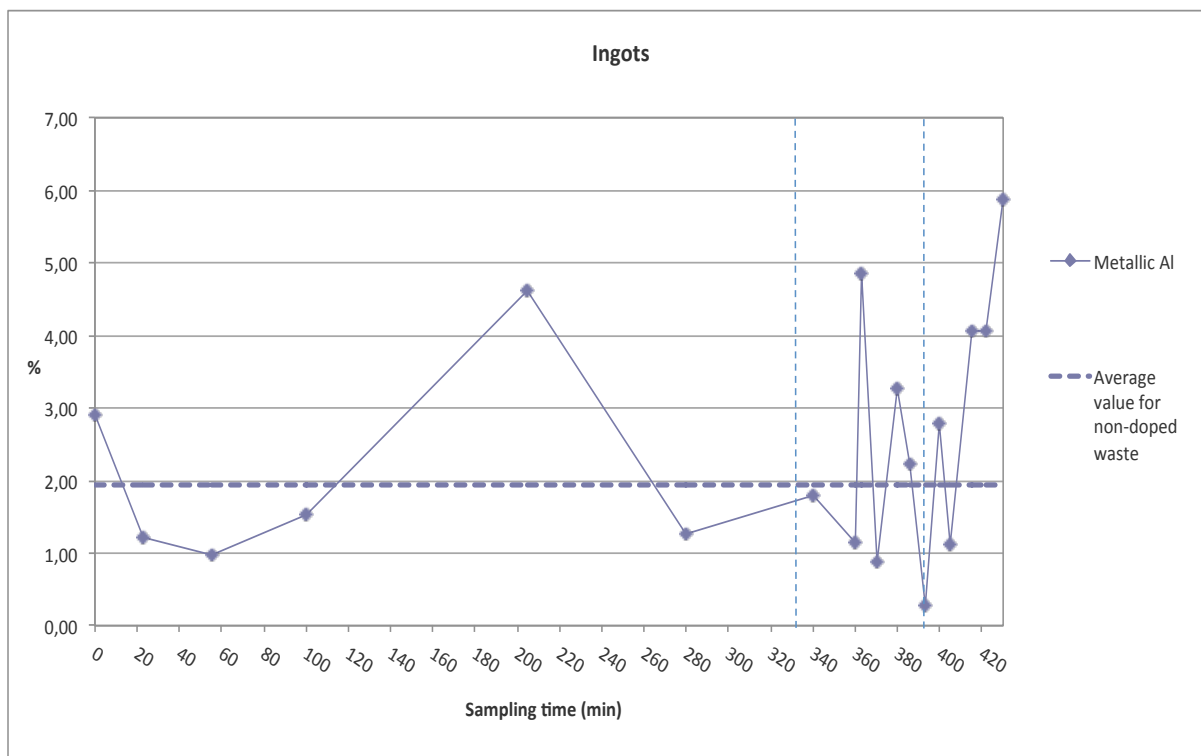


Figure 3.3.1 - Trend of metallic aluminium percentage content (on the dry weight) in the ingots resulting from the melting process. Vertical dotted lines represent the moments when the two cages were extracted.

The curve presents a very irregular trend and many points of local maximum and minimum, which are hardly referable to a specific phenomenon. This implies that it is difficult to estimate a waste residence time more reliable than the one provided by the tracers; the definition of a time interval for the numerical integration of the curve is thereby quite complex. This experimental session is affected, more markedly than for the other tests, by the lack of data relating to the period which follows the extraction of the second cage. The few available values are not sufficient to reconstruct the full curve pattern and see whether the growth trend detectable for the last three samples is really due to the doping of the waste or to the natural variability of the test. In order to obtain relevant information for the interpretation of Figure 3.3.1 and the consequent definition of the integration interval for the ingots, the study of aluminium concentration in the bottom ash fine fractions will be crucial.

Results of the analysis on few salt dross samples resulting from the melting process in the crucible are reported in Table 3.3.3. Percentages refer to the total dry weight of bottom ash samples, as usual.

Table 3.3.3 - Aluminium percentage content (on the dry weight) in some salt dross samples resulting from the melting process. Samples representative of the doped waste are highlighted in italics.

Sample	Metallic Al (%)	Total Al (%)	Aluminium content in an oxidized form (%)
SS08-1	0.27	0.64	57.81
SS08-2	0.36	0.52	30.77
SS08-4	0.39	0.93	58.06
SS08-5	0.35	0.74	52.70
<i>SS08-15</i>	<i>0.13</i>	<i>0.36</i>	<i>63.89</i>
<i>SS08-16</i>	<i>0.05</i>	<i>0.16</i>	<i>68.75</i>
<i>SS08-17</i>	<i>0.42</i>	<i>0.73</i>	<i>42.47</i>
<i>SS08-18</i>	<i>0.20</i>	<i>0.47</i>	<i>57.45</i>
AVERAGE	0.27	0.57	53.99
STD.DEV.	0.13	0.24	12.15

Significant differences are observed between the samples, while the variation in the transition from the non-doped to the doped waste is less evident compared to what happened for the other types of packaging. This aspect is confirmed by the analysis of metallic aluminium loss during the melting process in the crucible, as reported in Table 3.3.4.

Table 3.3.4 - Loss of metallic aluminium during the melting process in the crucible. Samples representative of the doped waste are highlighted in italics.

Sample	Metallic Al (%) in the fraction > 0.8 mm	Loss of metallic Al in the crucible (%)
SS08-1	3.17	8.52
SS08-2	1.57	22.93
SS08-4	1.92	20.31
SS08-5	4.97	7.04
<i>SS08-15</i>	<i>1.26</i>	<i>10.32</i>
<i>SS08-16</i>	<i>4.12</i>	<i>1.21</i>
<i>SS08-17</i>	<i>4.49</i>	<i>9.35</i>
<i>SS08-18</i>	<i>6.09</i>	<i>3.28</i>
AVERAGE	3.45	10.37
STD.DEV.	1.76	7.62

3.3.1.2. Fine fractions

Figure 3.3.2 and Figure 3.3.3 depict the trends of total and metallic aluminium percentage content (on the dry weight) in the bottom ash fine fractions.

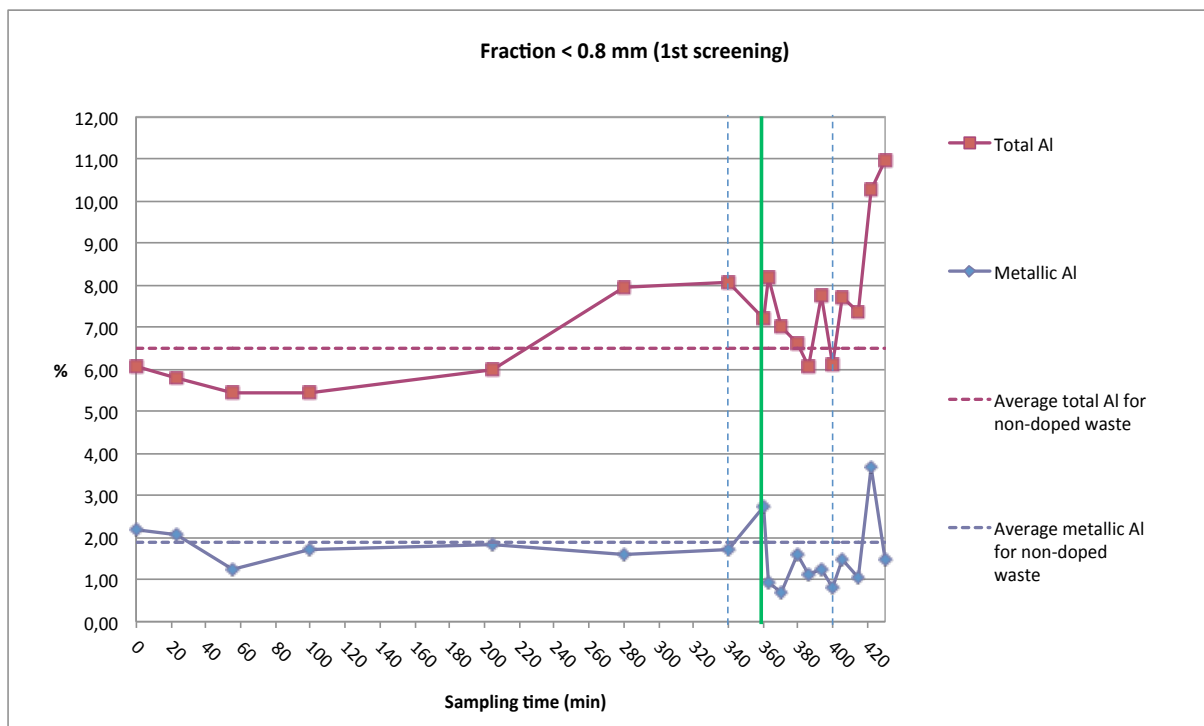


Figure 3.3.2 - Trends of total and metallic aluminium percentage content (on the dry weight) in the fraction below 0.8 mm resulting from the first screening. Vertical dotted lines represent the instants when the two cages were extracted. The vertical line indicates the beginning of the growth trend observed for these fractions.

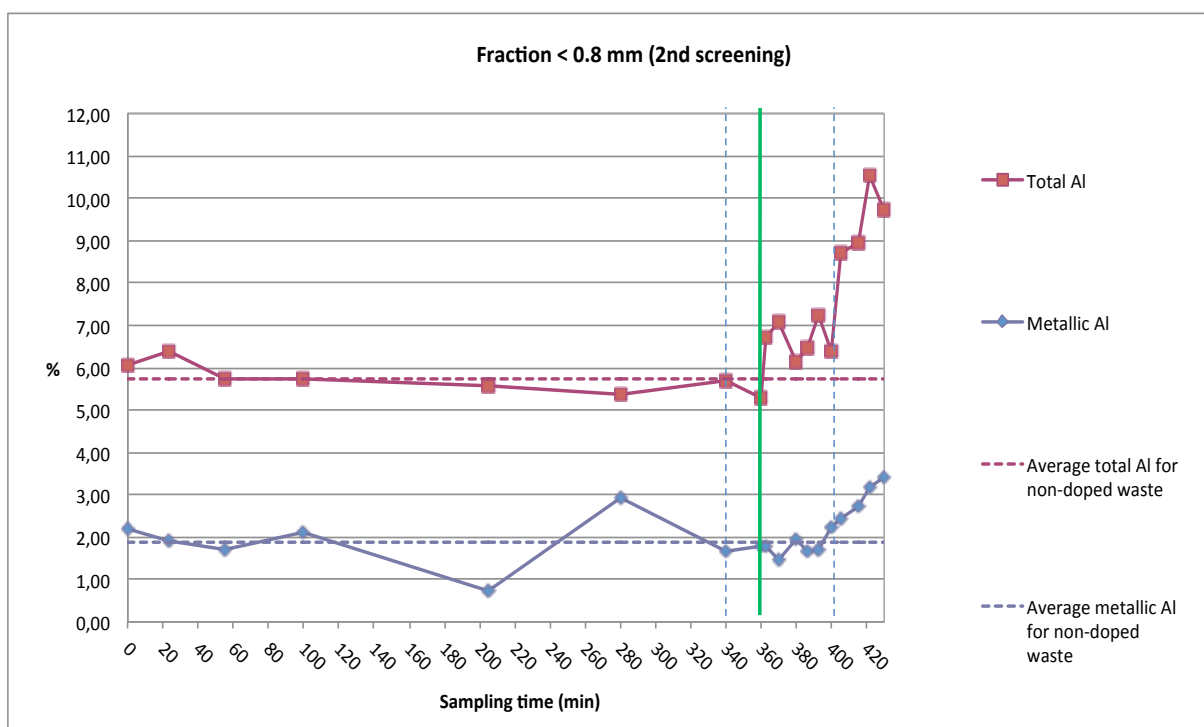


Figure 3.3.3 - Trends of total and metallic aluminium percentage content (on the dry weight) in the fraction below 0.8 mm resulting from the second screening. Vertical dotted lines represent the instants when the two cages were extracted. The vertical line indicates the beginning of the growth trend observed for these fractions.

Both fractions show a well-defined growth trend starting from a specific time. In particular, the fine fraction from the second screening (after grinding) shows a clear increase in the percentage of total aluminium content starting from 360 minutes after the beginning of the test. It has been decided to take this time as a reference also for the fine fraction from the first screening and for the coarse fraction sent to the crucible. From this data it is also possible to estimate the waste residence time, which is approximately equal to 398 minutes. The integration interval is therefore assumed equal to 67 minutes. The horizontal dotted lines identify the average percentage content of total and metallic aluminium for the non-doped waste. Concerning the fraction from the first screening, the average content of total aluminium is 6.5% while that of metallic aluminium is about 1.9%. For the fraction obtained from the second screening, the average percentage contents are respectively 5.7% and 1.9%. Table 3.3.5 reports the calculation of fed packaging average contribution.

Table 3.3.5 - Calculation of fed packaging average contribution in the bottom ash fine fractions resulting from the first and second screening.

	Fraction < 0.8 mm (1 st screening)		Fraction < 0.8 mm (2 nd screening)	
	Metallic Al	Total Al	Metallic Al	Total Al
A1	0.11	0.23	0,05	0.18
A2	0.11	0.53	0.12	0.48
A3	0.23	0.68	0.17	0.66
A4	0.16	0.38	0.11	0.38
A5	0.17	0.48	0.12	0.48
A6	0.14	0.49	0.14	0.48
A7	0.11	0.35	0.12	0.38
A8	0.25	0.75	0.26	0.88
A9	0.33	0.62	0.21	0.68
A10	0.41	0.85	0.26	0.81
Doped waste contribution (kg_{Al} kg⁻¹_{bottom ashes} min)	2.03	5.36	1.55	5.41
Non-doped waste contribution (kg_{Al} kg⁻¹_{bottom ashes} min)	1.32	4.55	1.32	4.01
Contribution of fed packaging (kg_{Al} kg⁻¹_{bottom ashes} min)	0.71	0.82	0.23	1.40

The analysis on fine fractions has supplied the necessary information for the interpretation of the results concerning the coarse fraction sent to the melting process in the crucible. Figure 3.3.4 shows again the trend of recoverable aluminium in the ingots, marking the instant when the material begins to be representative of the doped waste according to the analysis on fine fractions.

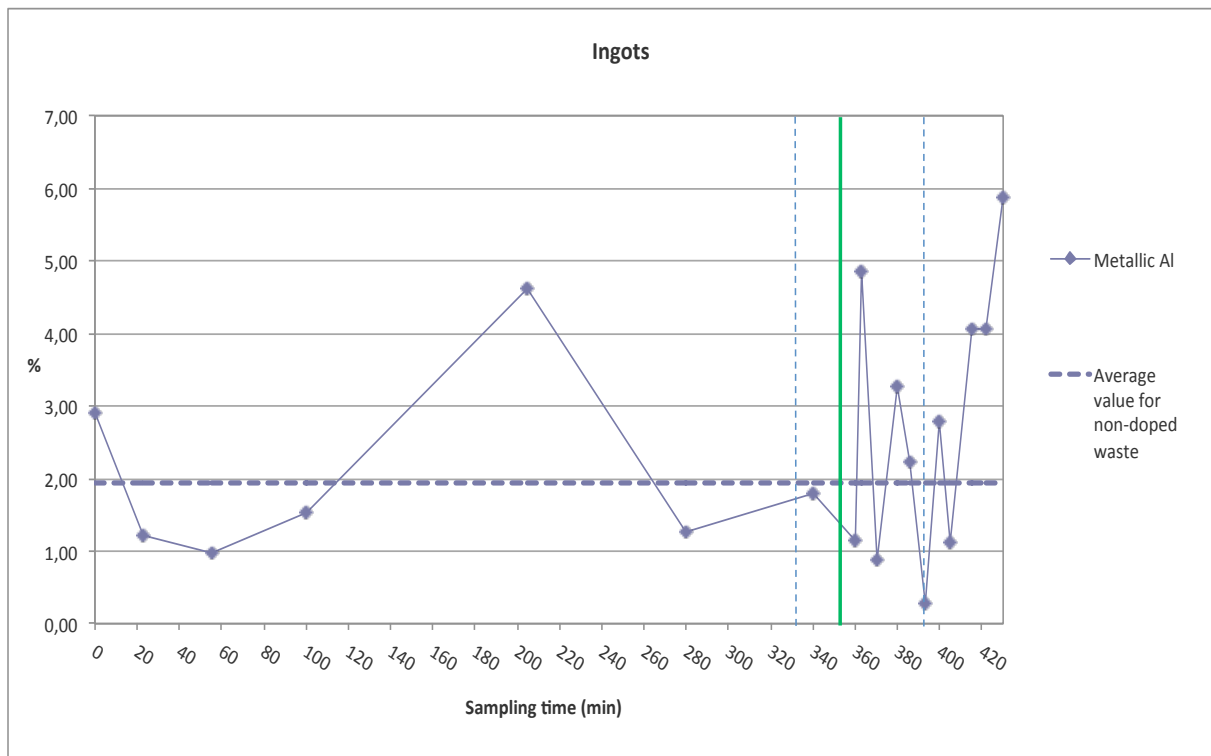


Figure 3.3.4 - Trend of metallic aluminium percentage content (on the dry weight) in the ingots resulting from the melting process. Vertical dotted lines represent the instants when the two cages were extracted. The bold vertical line indicates the beginning of the observed growth trend according to the analysis on total aluminium content in the fine fraction from the second screening.

It can be noticed how the alternation between local maximum and minimum starts right at the marked time (vertical line), excluding the first peak at 200 minutes probably due to an unusual aluminium concentration in the non-doped waste. It is quite difficult to explain this trend. A possible interpretation is linked to the type of tested packaging. Spray cans are heavier (25 g) than beverage cans (13.2 g) and trays (4.3 g), leading to a smaller number of single units (9,600) introduced with the waste in the furnace. Lumps formed during the combustion process are therefore bigger but not homogeneously distributed within the sampled material: hence, the loss of a single lump during sampling operations strongly affects the results of the analysis (see Paragraph 3.3.3 for further details).

Nevertheless, the curve has been integrated in order to obtain an estimate of fed packaging average contribution. The integration interval is the same as the one considered for the fine fractions and hence equal to 67 minutes. The results of the calculation are reported in Table 3.3.6. Table 3.3.7 shows the aluminium content in an oxidized form measured in the bottom ash fine fractions resulting from the first and second screening.

Table 3.3.6 - Calculation of fed packaging average contribution in the ingots.

Trapezoid	Area ($\text{kg}_{\text{Al}} \text{kg}^{-1}_{\text{bottom ashes min}}$)
A1	0.09
A2	0.20
A3	0.21
A4	0.16
A5	0.09
A6	0.11
A7	0.10
A8	0.26
A9	0.28
A10	0.40
Doped waste contribution ($\text{kg}_{\text{Al}} \text{kg}^{-1}_{\text{bottom ashes min}}$)	1.90
Non-doped waste contribution ($\text{kg}_{\text{Al}} \text{kg}^{-1}_{\text{bottom ashes min}}$)	1.35
Contribution of fed packaging ($\text{kg}_{\text{Al}} \text{kg}^{-1}_{\text{bottom ashes min}}$)	0.55

Table 3.3.7 - Aluminium content in an oxidized form in the bottom ash fine fractions resulting from the first and second screening.

Sample	Aluminium content in an oxidized form (%)	
	Fraction < 0.8 mm (1 st screening)	Fraction < 0.8 mm (2 nd screening)
BA08-1	64.17	63.85
BA08-2	64.59	70.22
BA08-3	76.89	70.15
BA08-4	68.43	63.20
BA08-5	69.37	86.84
BA08-6	79.90	45.58
BA08-7	78.73	70.70
BA08-8	62.01	66.05
BA08-9	88.84	73.13
BA08-10	90.23	79.09
BA08-11	75.87	68.20
BA08-12	81.20	74.28
BA08-13	83.80	76.61
BA08-14	86.93	64.86
BA08-15	80.71	72.16
BA08-16	86.02	69.40
BA08-17	64.39	69.84
BA08-18	86.44	65.04
AVERAGE	77.14	69.40
STD.DEV.	9.42	8.36

3.3.2 Fly ashes

Figure 3.3.5 shows the percentage content of total aluminium measured in fly ash samples. Metallic aluminium content is not reported since most of the values were above their corresponding total aluminium values due to the measuring problems already discussed in Paragraph 2.5.6. These problems seemed to have a greater impact on this test compared to the others.

In this case, no growth trend representative of the doped waste can be observed. Moreover, the time intervals calculated for bottom ashes cannot be used because the residence times of the two residues are significantly different. Furthermore, the comparison with fly ash residence times estimated during the other tests is not recommendable because operating conditions were too different during the four experimental sessions. As a result, the curve of total aluminium content in fly ashes cannot be integrated; therefore, the fed packaging average contribution has been considered equal to zero.

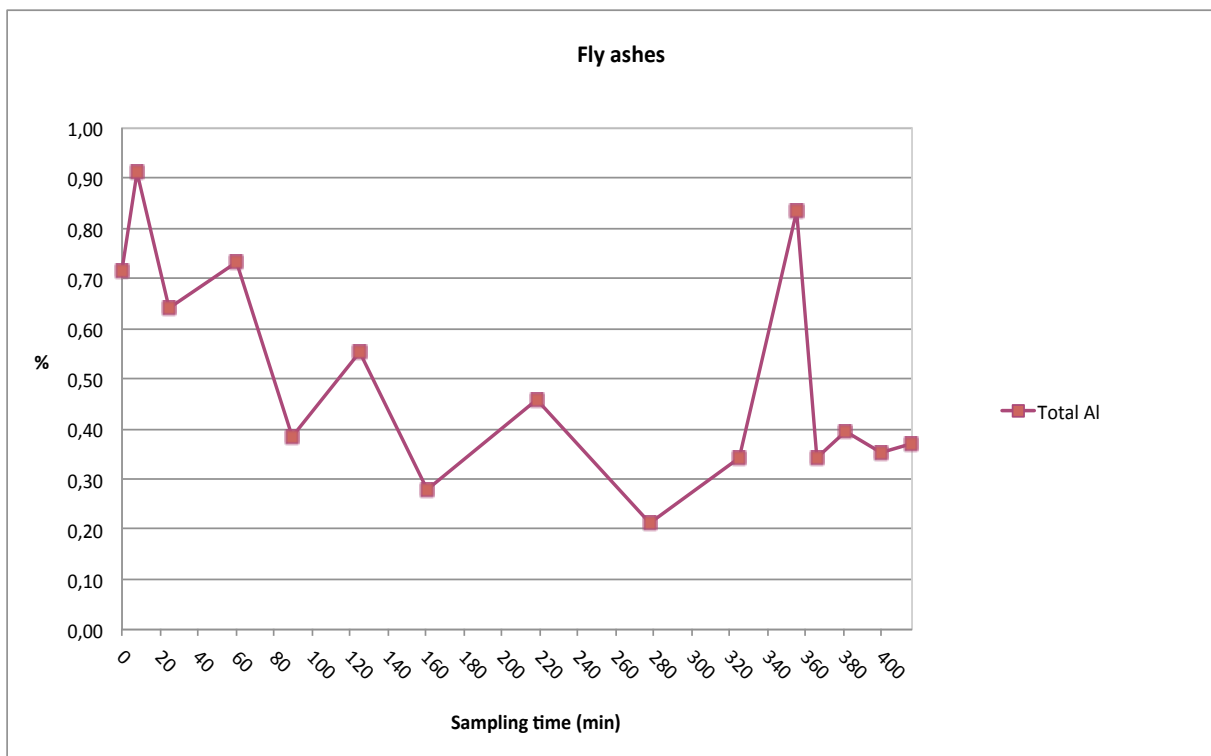


Figure 3.3.5 - Percentage content of total aluminium measured in fly ash samples.

3.3.3 Mass balance

Table 3.3.8 lists all the flow rates considered in the calculation of the final mass balance.

Table 3.3.8 - Waste and residues flow rates used in the calculation of the final mass balance for aluminium spray cans.

	Flow rate (kg h ⁻¹)	Flow rate (w% on waste flow rate)
Waste	5939	100
Fly ashes	181	3
Wet bottom ashes	1113	19
Dry bottom ashes	870	15
Bottom ash fraction < 0.8 mm (1st screening)	84	1
Bottom ash fraction < 0.8 mm (2nd screening)	553	9

All the flow rates have been calculated according to the method reported in paragraph 3.1.3. Table 3.3.9 shows the results of the final mass balance, obtained by multiplying the fed packaging average contribution in each fraction by the corresponding flow rate converted to kg min⁻¹.

Table 3.3.9 - Mass balance related to Test 3 on aluminium spray cans (June 8th, 2011). Data concerning fly ashes are not available.

	Total Al (kg)	Partitioning of recovered total Al in the residues (%)	Metallic Al (kg)	Metallic/Total Al (%)
INPUT				
Fed aluminium	231		231	
OUTPUT				
<i>Fly ashes</i>	n.a.	n.a.	n.a.	n.a.
<i>Bottom ash fraction < 0.8 mm before grinding</i>	1.1	5.2	1.0	87.2
<i>Bottom ash fraction < 0.8 mm after grinding</i>	12.9	58.7	2.2	16.7
<i>Ingots</i>	7.9	36.1	7.9	100.0
Total recovered aluminium	22.0		11.1	50.4

Once again, the composition of the alloy has been taken into account in determining the amount of fed aluminium. Spray cans are made of the AA3000 series alloy, which contains 96.4% aluminium on average.

Only the 9.5% of the aluminium introduced with the packaging has been recovered (22.0 out of 231 kg). Through the analysis of aluminium partitioning in the incineration residues it is

possible to observe that the metal found in the ingots makes up only the 36% of the total recovered amount. This percentage, as already specified, is representative of the actual amount of aluminium recoverable through an advanced treatment of bottom ashes followed by a melting process in the saline furnace. However, the estimate of this parameter is affected by all problems related to the packaging type already discussed in Paragraphs 3.3.1.1 and 3.3.1.2. In addition, such a difference in term of results between beverage cans and spray cans might be explained as follows. Both beverage and spray cans are thicker compared to the other tested materials and this results in the formation of bigger aluminium lumps. When aluminium is present in small-sized lumps, the loss of a single lump or fragment during the sampling does not significantly alter its average concentration. However, if lumps are big and limited in number, the loss of a single unit during sampling substantially alters the results. On the 8th of June, the day of Test 3 on spray cans, sampling conditions of bottom ashes were extremely harsh⁵ and it is very likely that several lumps were lost during sampling operations, thus affecting the results of the analysis. Therefore, in order to fully understand the behaviour of spray cans, further investigations are needed.

Concerning the metallic content of aluminium recovered in the residues, in the bottom ash fine fraction resulting from the second screening it is lower (17%) than for the other types of packaging. As already said, data referred to fly ashes are not available.

Because of all the issues raised and discussed above, the results obtained for spray cans are not considered reliable from a scientific point of view and hence they will not be further mentioned in the conclusions of this study.

⁵ A huge amount of vapours from the bottom ash pit prevented to have a clear view of the material during sampling operations.

3.4 Aluminium and polylaminated foils

Results obtained from the analysis of the samples taken during Test 4 on aluminium and polylaminated foils (see Table 2.1.1) are presented in this paragraph.

3.4.1 Bottom ashes

Table 3.4.1 gives an overview of the type and quantity of the sub-fractions obtained from the pre-treatment of bottom ash samples taken during Test 4 on aluminium and polylaminated foils.

Table 3.4.1 - Dry weight, humidity and sub-fractions (expressed as weight percentage on dry samples) obtained from the pre-treatment of bottom ash samples taken during Test 4 on aluminium and polylaminated foils.

Sample	Time	Dry weight	Humidity	Fraction < 0,8 mm	Fraction < 0,8 mm after grinding	Fraction > 0,8 mm after grinding	Iron+inert scraps
		g	%	%	%	%	%
BA13-1	11:30	2330	18	8.58	70.55	6.87	13.30
BA13-2	11:40	7050	15	7.52	50.07	23.69	19.01
BA13-3	12:10	7320	23	10.25	53.83	17.62	18.31
BA13-4	13:30	6960	25	12.79	52.10	22.70	12.36
BA13-5	13:55	5500	27	14.00	54.45	13.82	17.64
BA13-6	14:20	6930	30	13.71	45.66	22.51	18.18
BA13-7	14:50	7210	24	8.32	57.69	15.95	17.34
BA13-8	15:25	4890	24	11.45	49.29	17.79	22.49
BA13-9	15:45	2910	38	19.59	57.38	7.56	14.78
BA13-10	16:15	6350	27	12.60	58.96	16.22	12.44
BA13-11	16:45	7880	24	9.90	42.34	22.34	22.46
BA13-12	17:15	7310	22	9.71	46.33	16.96	26.95
BA13-13	17:45	7240	23	10.22	54.74	17.68	17.40
BA13-14	18:15	8920	36	19.51	44.03	24.44	11.66
BA13-15	19:00	6990	24	11,30	51.98	27.18	10.73
BA13-16	19:40	6750	25	12.89	50.18	18.37	18.52
BA13-17	20:00	6680	11	4.64	54.15	22.31	19.01
AVERAGE		6425	24	11.59	52.57	18.47	17.21
STD.DEV.		1676	7	3.84	6.68	5.55	4.34

The dry weights of the samples taken during this experimental campaign are significantly higher compared to those of tests on rigid packaging because larger amounts of material were sampled in order to increase representativeness.

3.4.1.1 Metal ingots from the melting process

Table 3.4.2 shows the yields (%) obtained from non-ferrous metals melting processes, expressed by the ratio between the weight of the metal ingot resulting from melting in the crucible and the total dry weight of the corresponding bottom ash sample (second column). The metal content in the ingots attributable to non-ferrous manually sorted lumps is reported in the third column.

Table 3.4.2 - Yields (%) obtained from non-ferrous metals melting processes and contribution (%) of manually sorted lumps. The table refers to the total yield, considering both the 0.8 - 5 mm and > 5 mm sub-fractions sent to the crucible.

Sample	Yield of non-ferrous metals w% (ingot/dry BA sample)	Contribution of manually sorted lumps w% (manually sorted lumps/ingot)
BA13-1	2.15	58.34
BA13-2	1.50	141.57*
BA13-3	2.34	77.95
BA13-4	1.88	77.68
BA13-5	0.98	77.48
BA13-6	2.76	89.40
BA13-7	2.81	70.48
BA13-8	3.24	66.15
BA13-9	2.27	57.90
BA13-10	3.31	72.79
BA13-11	2.00	70.06
BA13-12	2.77	94.60
BA13-13	3.65	75.25
BA13-14	4.76	148.59*
BA13-15	2.78	126.11*
BA13-16	3.16	64.49
BA13-17	1.91	82.16
AVERAGE	2.60	85.35
STD.DEV.	0.89	27.51

* The weight of manually sorted lumps is higher than the total weight of the ingot, meaning that part of aluminium had been trapped in the salt dross during the melting process, causing a loss of recoverable material.

The yields of non-ferrous metals are comparable with those obtained from the other tested materials, while contributions of manually sorted lumps are generally higher. This result is rather unusual considering the packaging structure and it is probably due to the thick layers of uncombusted aluminium and poly laminated foils found during the preliminary manual sorting in some samples (especially between BA13-10 and BA13-16), suggesting a poor mixing of the fed packaging within the waste. As already specified in Paragraph 2.5.1, for this test it was decided to split the coarse fraction resulting from the second screening into two sub-fractions (0.8 - 5 mm and > 5 mm) by mean of an additional 5 mm mesh screening step. These two sub-fractions were separately melted in the crucible in order to simulate the possibility of aluminium recovery using a traditional ECS (dealing with a grain size larger than 5 mm) and evaluate the benefit from the application of a high-frequency ECS specifically calibrated on the 0.8 - 5 mm size range. Figure 3.4.1 shows the trend of metallic aluminium percentage content in the ingots resulting from the separate melting of the two sub-fractions and the total corresponding value, expressed as functions of the sampling time.

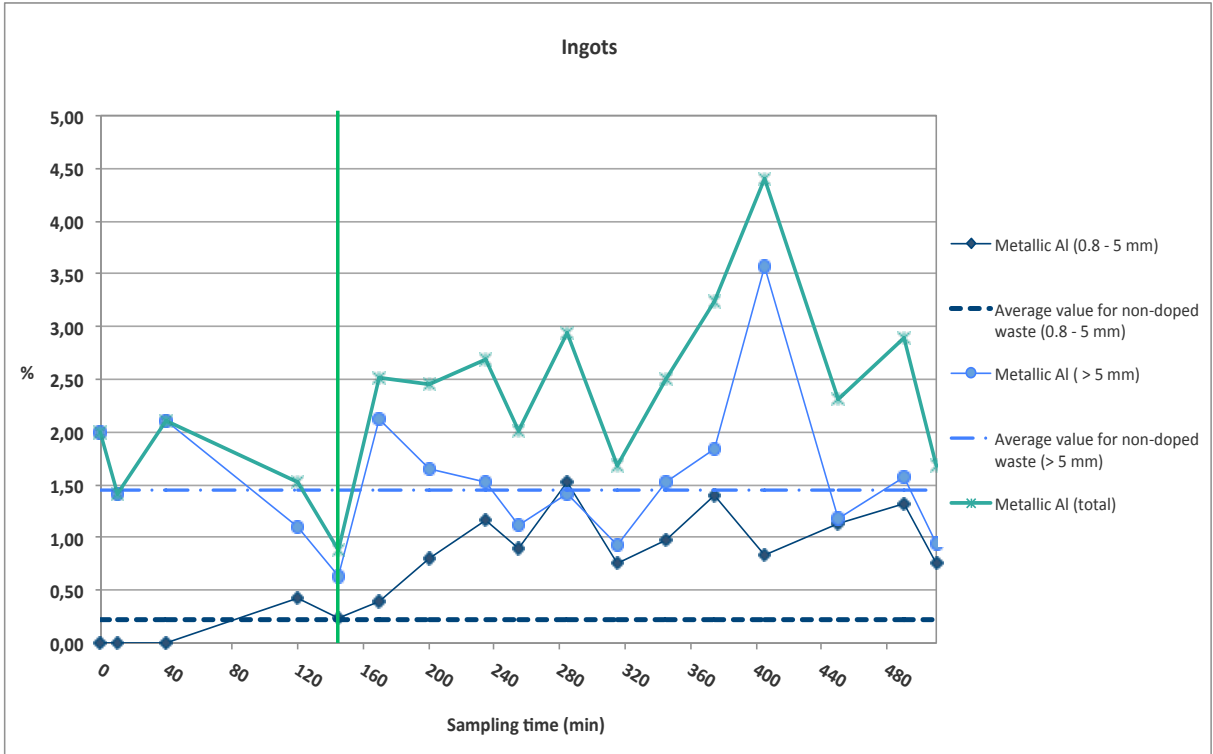


Figure 3.4.1 - Trend of metallic aluminium percentage content (on the dry weight) in the ingots resulting from the melting process of the 0.8 - 5 mm and > 5 mm sub-fractions. The vertical line indicates the beginning of the observed growth trend, also taking into account the growth trend observed in the fine fractions (see Paragraph 3.4.1.2).

The percentage content of metallic aluminium in the ingots obtained from the sub-fraction above 5 mm presents an irregular trend, and no clear growth trend linked to the doping of the waste can be observed. In the 0.8 - 5 mm sub-fraction, in contrast, there is an evident increase attributable to the doping of the waste, starting around 170 minutes after the beginning of sampling operations. This result was expected considering the thickness of the tested packaging (10 - 42 μm range) and it underlines the importance of an advanced ECS separation system to maximize aluminium recovery in this specific situation. To better appreciate this aspect, Table 3.4.3 reports the total recovery of metallic aluminium from the two sub-fractions (expressed as a percentage on the dry weight of the initial bottom ash sample) and the corresponding contribution of the 0.8 - 5 mm sub-fraction. It is important to keep in mind that these values include the background aluminium concentration of the non-doped waste, so they do not correspond to the sole fed packaging contribution of the 0.8 - 5 mm sub-fraction.

Table 3.4.3 - Total recovery of metallic aluminium from the two coarse sub-fractions and contribution of the 0.8-5 mm sub-fraction.

Sample	Total recovery of metallic Al	Contribution of 0.8 - 5 mm sub-fraction
	w% (referred to dry BA sample)	w% (referred to metallic Al in the ingot)
BA13-1	1.99	n.a.*
BA13-2	1.41	0.00**
BA13-3	2.11	n.a.*
BA13-4	1.53	27.92
BA13-5	0.87	27.32
BA13-6	2.52	15.92
BA13-7	2.46	32.96
BA13-8	2.69	43.45
BA13-9	2.01	44.66
BA13-10	2.93	51.85
BA13-11	1.69	45.22
BA13-12	2.51	39.18
BA13-13	3.24	43.41
BA13-14	4.41	18.87
BA13-15	2.32	48.93
BA13-16	2.90	45.80
BA13-17	1.69	44.56
AVERAGE	2.31	35.34
STD.DEV.	0.82	14.65

* The separated melting of the two sub-fractions was not possible because of technical problems.

** The 0.8 - 5 mm sub-fraction did not contain recoverable aluminium so its contribution is equal to zero.

3. EVALUATION OF THE RESULTS

The time corresponding to the beginning of the growth trend has been used to estimate the waste residence time and the integration intervals for the calculation of fed packaging average contribution related to the two sub-fractions. The vertical line in Figure 3.4.1, corresponding to 145 minutes, indicates the beginning of the growth trend observed for metal ingots.

Considering that the first charge of doped waste was put in the feeding hopper at 9:38, 110 minutes before the start of sampling operations, the estimated residence time is approximately equal to 255 minutes.

The integration of the two curves was calculated starting from 145 minutes after the beginning of the sampling to the end of the sampling period, resulting in an integration interval of 365 minutes. Although the integration interval is much longer compared to the other tests, the fed packaging average contribution is again affected by the lack of a complete evolution of the curve, since the final decreasing phase towards the average values of the non-doped waste is still missing. Table 3.4.4 summarizes the results of the calculation for both the sub-fractions.

Table 3.4.4 - Calculation of fed packaging average contribution in the ingots.

Trapezoid	Area ($\text{kg}_{\text{Al}} \text{kg}^{-1}_{\text{bottom ashes}} \text{min}$)		
	Sub-fraction 0.8 - 5 mm	Sub-fraction >5 mm	Total
A1	0.08	0.34	0.42
A2	0.18	0.56	0.75
A3	0.35	0.55	0.90
A4	0.21	0.26	0.47
A5	0.36	0.38	0.74
A6	0.34	0.35	0.69
A7	0.26	0.37	0.63
A8	0.36	0.50	0.86
A9	0.34	0.81	1.15
A10	0.44	1.07	1.51
A11	0.49	0.55	1.04
A12	0.21	0.25	0.46
Doped waste contribution ($\text{kg}_{\text{Al}} \text{kg}^{-1}_{\text{bottom ashes}} \text{min}$)	3.62	6.01	9.63
Non-doped waste contribution ($\text{kg}_{\text{Al}} \text{kg}^{-1}_{\text{bottom ashes}} \text{min}$)	0.81	5.29	5.78
Contribution of fed packaging ($\text{kg}_{\text{Al}} \text{kg}^{-1}_{\text{bottom ashes}} \text{min}$)	2.81	0.72	3.85

Results of the analysis on the salt dross resulting from the melting process of the 0.8 - 5 mm sub-fraction are reported in Table 3.4.5. For the sub-fraction above 5 mm, no dross has been produced since it consisted of non-ferrous lumps (from preliminary sorting and 5 mm mesh screening) nearly without any impurity. Percentages refer to the total dry weight of bottom ash samples, as usual.

Table 3.4.5 - Aluminium percentage content (on the dry weight) in the salt dross resulting from the melting process of the 0.8 - 5 mm sub-fraction. Samples representative of the doped waste are highlighted in italics.

Sample	Metallic Al (%)	Total Al (%)	Aluminium content in an oxidized form (%)
SS13-1*	0.39	0.68	42.25
SS13-2	0.43	2.06	79.23
SS13-3*	0.24	0.43	43.10
SS13-4	0.33	1.16	71.56
<i>SS13-5</i>	<i>0.30</i>	<i>0.78</i>	<i>61.67</i>
<i>SS13-6</i>	<i>0.30</i>	<i>0.70</i>	<i>56.81</i>
<i>SS13-7</i>	<i>0.24</i>	<i>0.53</i>	<i>54.06</i>
<i>SS13-8</i>	<i>0.36</i>	<i>0.78</i>	<i>53.27</i>
<i>SS13-9</i>	<i>0.42</i>	<i>0.78</i>	<i>45.38</i>
<i>SS13-10</i>	<i>0.32</i>	<i>0.84</i>	<i>62.15</i>
<i>SS13-11</i>	<i>0.19</i>	<i>0.57</i>	<i>66.78</i>
<i>SS13-12</i>	<i>0.19</i>	<i>0.49</i>	<i>61.28</i>
<i>SS13-13</i>	<i>0.26</i>	<i>0.39</i>	<i>31.88</i>
<i>SS13-14</i>	<i>0.49</i>	<i>1.26</i>	<i>61.36</i>
<i>SS13-15</i>	<i>0.20</i>	<i>0.86</i>	<i>76.40</i>
<i>SS13-16</i>	<i>0.18</i>	<i>0.65</i>	<i>72.41</i>
<i>SS13-17</i>	<i>0.49</i>	<i>0.88</i>	<i>44.55</i>
AVERAGE	0.31	0.81	57.89
STD.DEV.	0.10	0.40	13.33

*The analysis refers to the salt dross resulting from the melting process without separation into two sub-fractions.

No significant differences are observed between the non-doped and the doped waste, as confirmed by Table 3.4.6 reporting the loss of metallic aluminium during the melting process in the crucible.

Table 3.4.6 - Loss of metallic aluminium during the melting process in the crucible. Samples representative of the doped waste are highlighted in italics.

Sample	Metallic Al (%) in the fraction > 0.8 mm	Loss of metallic Al in the crucible (%)
SS13-1*	<i>2.38</i>	<i>16.52</i>
SS13-2	1.84	23.30
SS13-3*	<i>2.36</i>	<i>10.33</i>
SS13-4	1.86	17.72
<i>SS13-5</i>	<i>1.17</i>	<i>25.46</i>
<i>SS13-6</i>	<i>2.82</i>	<i>10.69</i>
<i>SS13-7</i>	<i>2.70</i>	<i>9.03</i>
<i>SS13-8</i>	<i>3.05</i>	<i>11.91</i>
<i>SS13-9</i>	<i>2.43</i>	<i>17.40</i>
<i>SS13-10</i>	<i>3.25</i>	<i>9.81</i>
<i>SS13-11</i>	<i>1.88</i>	<i>10.11</i>
<i>SS13-12</i>	<i>2.70</i>	<i>7.05</i>
<i>SS13-13</i>	<i>3.50</i>	<i>7.50</i>
<i>SS13-14</i>	<i>4.90</i>	<i>9.97</i>
<i>SS13-15</i>	<i>2.52</i>	<i>8.07</i>
<i>SS13-16</i>	<i>3.08</i>	<i>5.83</i>
<i>SS13-17</i>	<i>2.18</i>	<i>22.45</i>
AVERAGE	2.62	13.13
STD.DEV.	0.83	6.14

* The analysis refers to the salt dross resulting from the melting process without separation into two sub-fractions.

3.4.1.2 Fine fractions

Figures 3.4.2 and 3.4.3 depict the trends of total and metallic aluminium percentage content (on the dry weight) in the bottom ash fine fractions.

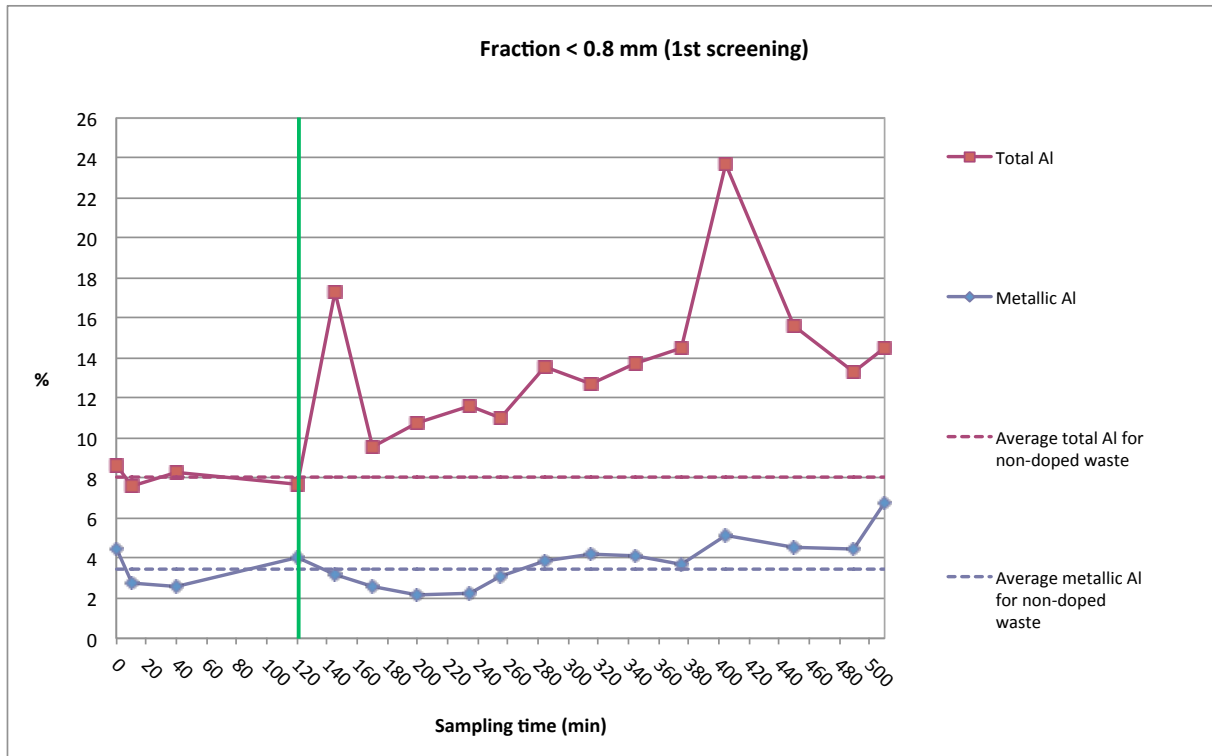


Figure 3.4.2 - Trends of total and metallic aluminium percentage content (on the dry weight) in the fraction below 0.8 mm resulting from the first screening. The vertical line indicates the beginning of the growth trend observed for these fractions.

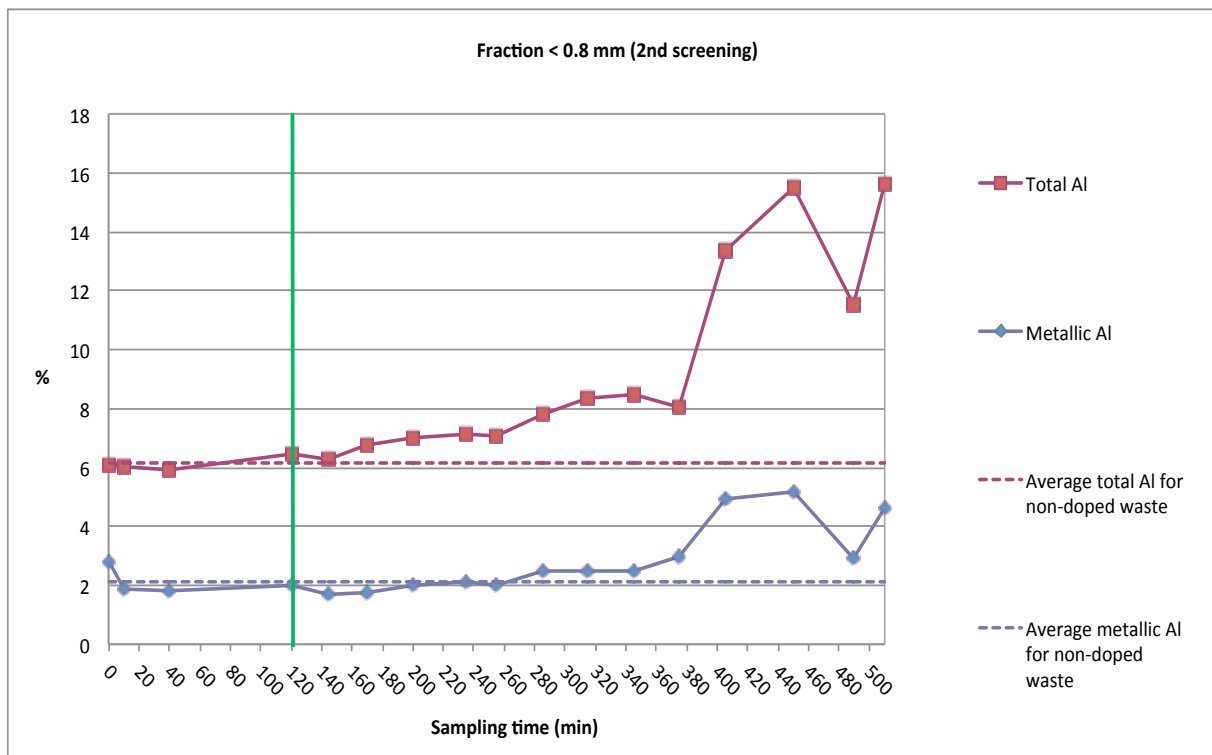


Figure 3.4.3 - Trends of total and metallic aluminium percentage content (on the dry weight) in the fraction below 0.8 mm resulting from the second screening. The vertical line indicates the beginning of the growth trend observed for these fractions.

Both fractions show an established growth trend (more evident for total aluminium) due to the doping of the waste, starting around 120 minutes after the beginning of sampling operations. Nevertheless, the trend of aluminium in the fine fractions confirms what emerged from the analysis on ingots: the impossibility to appreciate the complete evolution of the curve and, in particular, its decreasing phase towards the average values of the non-doped waste.

The time horizon considered in the numerical integration starts from 120 minutes after the beginning of the sampling and it is hence equal to 390 minutes. Compared to the one used for the ingots, it has been modified and adapted to the growth trend observed for the fine fractions, which starts one sample earlier, probably because of the so called “bypass effect” already mentioned in paragraph 3.2.1.2. Table 3.4.7 reports the results of calculation.

Table 3.4.7 - Calculation of fed packaging average contribution in the bottom ash fine fractions resulting from the first and second screening.

	Fraction < 0.8 mm (1 st screening)		Fraction < 0.8 mm (2 nd screening)	
	Metallic Al	Total Al	Metallic Al	Total Al
A1	0.90	3.12	0.46	1.60
A2	0.73	3.36	0.43	1.63
A3	0.72	3.05	0.56	2.07
A4	0.78	3.91	0.72	2.48
A5	0.54	2.26	0.41	1.42
A6	1.05	3.69	0.67	2.23
A7	1.22	3.94	0.74	2.42
A8	1.25	3.97	0.74	2.52
A9	1.17	4.25	0.82	2.48
A10	1.32	5.73	1.19	3.21
A11	2.19	8.83	2.27	6.49
A12	1.81	5.78	1.61	5.40
A13	1.12	2.78	0.76	2.72
Doped waste contribution (kg_{Al} kg⁻¹_{bottom ashes} min)	14.78	54.67	11.38	36.68
Non-doped waste contribution (kg_{Al} kg⁻¹_{bottom ashes} min)	13.48	31.41	8.21	23.92
Contribution of fed packaging (kg_{Al} kg⁻¹_{bottom ashes} min)	1.29	23.26	3.17	12.76

Dotted horizontal lines in Figures 3.4.3 and 3.4.4 indicate the average values of total and metallic aluminium percentage content calculated for the non-doped waste. Concerning the fine fraction resulting from the first screening, the average total aluminium content is 8.1%,

while the average metallic aluminium content is equal to 3.5%. For the fine fraction from the second screening, the average percentage contents are equal to 6.1% and 2.1%, respectively. Table 3.4.8 shows the aluminium content in an oxidized form in both the fine fractions. It does not reveal any significant change due to the doping of the waste.

Table 3.4.8 - Aluminium content in an oxidized form in the bottom ash fine fractions (below 0.8 mm) resulting from the first and second screening.

Sample	Aluminium content in an oxidized form (%)	
	Fraction < 0.8 mm (1 st screening)	Fraction < 0.8 mm (2 nd screening)
BA13-1	48.47	54.60
BA13-2	63.86	68.90
BA13-3	68.22	69.60
BA13-4	48.12	69.50
BA13-5	81.49	73.47
BA13-6	72.59	73.91
BA13-7	79.84	71.72
BA13-8	80.28	70.49
BA13-9	72.05	71.60
BA13-10	71.34	68.34
BA13-11	66.68	70.55
BA13-12	70.12	70.66
BA13-13	74.85	62.75
BA13-14	78.25	63.11
BA13-15	70.71	66.72
BA13-16	66.46	74.74
BA13-17	53.37	70.35
AVERAGE	68.63	68.88
STD.DEV.	10.28	4.92

3.4.2 Fly ashes

Figure 3.4.4 shows the percentage content of total and metallic aluminium measured in fly ash samples.

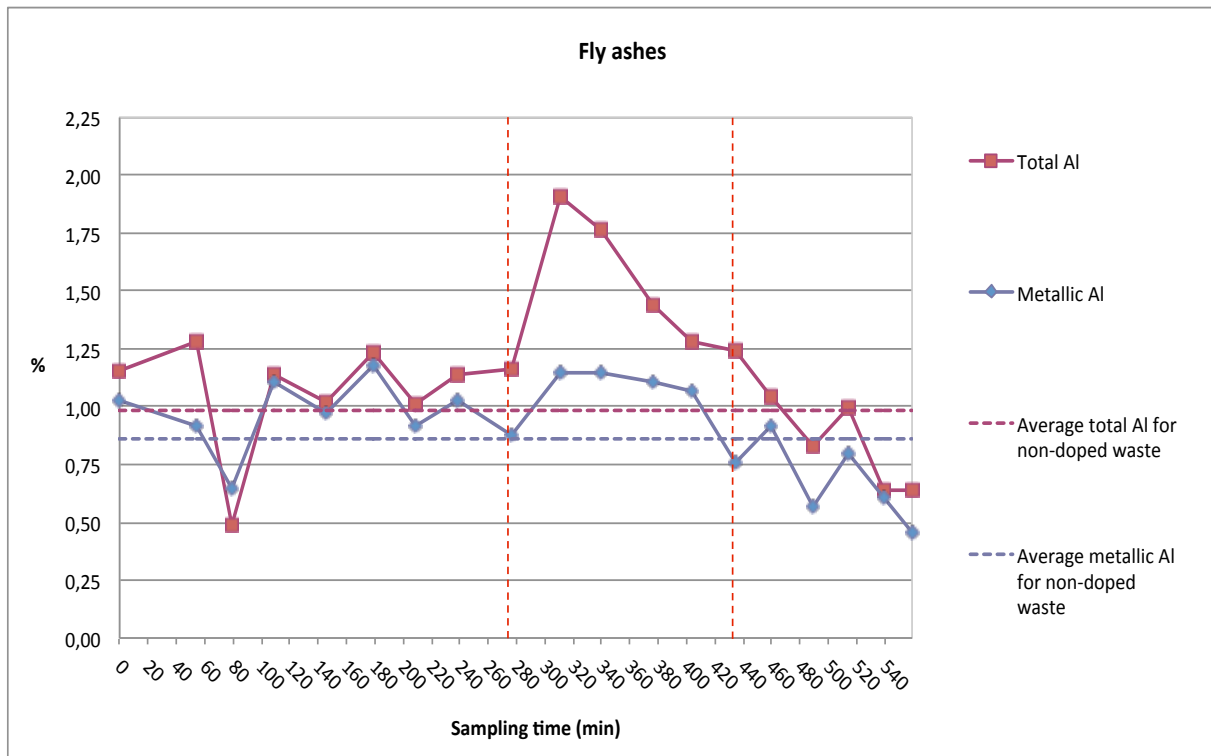


Figure 3.4.4 - Percentage content of total and metallic aluminium measured in fly ash samples. The integration interval used in the calculation of fed packaging average contribution is delimited by vertical dotted lines.

The curves reproduce the same trends observed in the tests on beverage cans and trays, showing an increase and a subsequent decrease located in a time interval clearly representative of the doped waste sampling. As for the previous tests, problems of instrumental sensitivity affected this analysis on fly ashes. The growth trend appears 311 minutes after the start of the sampling, which in turn took place 53 minutes after the first doped waste feeding: the estimated residence time of these residues therefore amounts to 364 minutes. This value is about twice as much as the one estimated during the first experimental campaign, confirming the high variability of the WTE plant operating conditions. The integration interval, identified by vertical dotted lines, is equal to 183 minutes and corresponds to the period during which fly ash samples representative of the doped waste were taken. Table 3.4.9 shows the results of calculation, carried out in the usual way.

Table 3.4.9 - Calculation of fed packaging average contribution in fly ashes.

Area	Metallic Al	Total Al
A1	0.35	0.54
A2	0.32	0.51
A3	0.42	0.59
A4	0.30	0.38
A5	0.27	0.38
A6	0.21	0.29
Doped waste contribution (kg_{Al} kg⁻¹_{fly ashes} min)	1.88	2.69
Non-doped waste contribution (kg_{Al} kg⁻¹_{fly ashes} min)	1.57	1.80
Contribution of fed packaging (kg_{Al} kg⁻¹_{fly ashes} min)	0.31	0.89

3.4.3 Mass balance

Table 3.4.10 lists all the flow rates considered in the calculation of the final mass balance.

Table 3.4.10 - Waste and residues flow rates used in the calculation of the final mass balance for aluminium and poly laminated foils.

	Flow rate (kg h ⁻¹)	Flow rate (w% on waste flow rate)
Waste	8394	100
Fly ashes	256	3
Wet bottom ashes	1573	19
Dry bottom ashes	1188	14
Bottom ash fraction < 0.8 mm (1st screening)	138	2
Bottom ash fraction < 0.8 mm (2nd screening)	625	7

Table 3.4.11 shows the results of the final mass balance, obtained by multiplying the fed packaging average contribution in each fraction by the corresponding flow rate converted to kg min⁻¹.

Once again, the actual amount of aluminium fed to the furnace (616 kg) is not equal to the amount of fed packaging (979 kg). The packaging introduced into the furnace consists of aluminium and poly laminated foils. Concerning aluminium thin foils, they are made of 98-99% aluminium so their total weight matches almost exactly that of fed aluminium. On the

other hand, the determination of the aluminium amount introduced with poly laminated foils required the consideration of their specific structure and composition⁶.

Table 3.4.11 - Mass balance related to Test 4 on aluminium and poly laminated foils (July 13th, 2011).

	Total Al (kg)	Partitioning of recovered total Al in the residues (%)	Metallic Al (kg)	Metallic/Total Al (%)
INPUT				
Fed aluminium	616		616	
OUTPUT				
<i>Fly ashes</i>	3.8	1.5	1.3	34.4
<i>Bottom ash fraction < 0.8 mm before grinding</i>	53.4	20.5	3.0	5.6
<i>Bottom ash fraction < 0.8 mm after grinding</i>	132.9	51.1	33.0	24.8
<i>Ingots from 0.8 - 5 mm sub-fraction</i>	55.6	21.4	55.6	100.0
<i>Ingots from > 5 mm sub-fraction</i>	14.2	5.5	14.2	100.0
Total recovered aluminium	259.8		107.1	41.2

The mass balance shows that about 42% of the aluminium introduced into the furnace has been recovered in the incineration residues (260 out of 616 kg). In this regard, a great improvement in aluminium recovery is observed in comparison to the tests on rigid packaging, essentially because of two different factors:

- The first one regards the faster movement of the waste inside the furnace (compared to the first experimental campaign), allowing more material to be taken during the test.
- The second is related to the extension of bottom ash sampling period, thus providing a better reproduction of the curves depicting recoverable aluminium from ingots and total and metallic aluminium in the two bottom ash fine fractions; furthermore, the sampling capacity was enlarged and more material was taken during each single sampling operation.

⁶ For instance, the weight of aluminium introduced with Triplex Alu/PE/Alu poly laminated foil (thickness: 12/60/12 µm with solvent glue 2.5 g m⁻² per each side) was determined as follows. First of all, the weight percentage content of aluminium in the foil was calculated by dividing the product (g m⁻²) between Al specific weight (2.7 kg dm⁻³), its total thickness (12+12=24 µm) and Al content in the alloy by the sum of the same products (between specific weight and the corresponding thickness, g m⁻²) for each component (2.7*24 for Al + 0.93*60 for PE + 2.5*2 for solvent glue). The weight percentage content of aluminium (52%) was then multiplied by the weight of the packaging introduced to the furnace (149 kg) to obtain the actual amount of fed aluminium (77 kg). The same procedure was repeated for all the types of poly laminated packaging foils and the overall amount of fed aluminium (616 kg) was calculated by summing all the individual results.

Despite the highest recovery of aluminium from the incineration residues has been obtained during this test, even for aluminium and poly laminated foils the closure of the mass balance is not achieved for the same reasons previously discussed.

The most relevant part of recovered aluminium (about 70%) is contained in the bottom ash fine fractions, especially the one resulting from the second screening (51%). This result was expected considering the extremely thin structure of the tested packaging.

Aluminium recovered in the ingots accounts for 27% of the total, considering both the coarse sub-fractions (0.8 - 5 mm and > 5 mm) sent to the crucible. Data referring to ingots are very interesting because they emphasize the contribution of the 0.8 - 5 mm sub-fraction to the overall amount of metallic aluminium recoverable from bottom ashes. Indeed, about 80% of this amount comes from the ingots resulting from the melting process of the 0.8 - 5 mm sub-fraction, meaning that the yield of aluminium recovery would increase by 390% by adding to the traditional ECS separation system an advanced ECS specifically calibrated on grains smaller than 5 mm.

Concerning the metallic content of aluminium recovered in the residues, overall it is much lower than the one registered in the first campaign, as expected considering the thinner structure of the packaging and, consequently, the potentially higher oxidation level of aluminium. In particular, the metallic/total Al ratio is 34.4% for fly ashes, 5.6% for the bottom ash fine fraction before grinding and 24.8% for the bottom ash fine fraction after grinding.

3.5. Conclusions

3.5.1. Partitioning of aluminium in the incineration residues

Tables 3.5.1 A-B summarize the partitioning of total (A) and metallic (B) aluminium recovered in the incineration residues for each type of tested packaging (except for spray cans whose results are not considered reliable from a scientific point of view, as explained in Paragraph 3.3.3). Aluminium in the ingots resulting from the melting process is all metallic by definition.

Table 3.5.1 A - Partitioning of total aluminium recovered in the incineration residues for each type of tested packaging.

Residue	Partitioning of total Al (%)		
	<i>Beverage cans</i>	<i>Trays</i>	<i>Foils</i>
<i>Fly ashes</i>	6.8	2.9	1.5
<i>Bottom ash fraction < 0.8 mm before grinding</i>	3.3	8.2	20.5
<i>Bottom ash fraction < 0.8 mm after grinding</i>	9.4	38.0	51.1
<i>Ingots</i>	80.5	50.9	26.9
Ingots from 0.8 - 5 mm sub-fraction	-	-	21.4
Ingots from > 5 mm sub-fraction	-	-	5.5
SUM	100	100	100

Table 3.5.1 B - Partitioning of metallic aluminium recovered in the incineration residues for each type of tested packaging.

Residue	Partitioning of metallic Al (%)		
	<i>Beverage cans</i>	<i>Trays</i>	<i>Foils</i>
<i>Fly ashes</i>	3.9	1.9	1.2
<i>Bottom ash fraction < 0.8 mm before grinding</i>	0.1	9.4	2.8
<i>Bottom ash fraction < 0.8 mm after grinding</i>	7.3	28.3	30.8
<i>Ingots</i>	88.7	60.4	65.2
Ingots from 0.8 - 5 mm sub-fraction	-	-	51.9
Ingots from > 5 mm sub-fraction	-	-	13.3
SUM	100	100	100

The amount of aluminium that is found in fly ashes, then not recoverable with current technologies, is below 7% for all the types of packaging. Regardless of the peculiarities of each packaging or alloy, this amount is in any case negligible. In contrast, data corresponding

to the bottom ash fine fractions (below 0.8 mm), both the “real” fine fraction resulting from the first screening and the one obtained from the second screening (after grinding), are characterized by high variability. In both fractions, aluminium metal fragments are extremely small and their recovery is virtually impossible through the current ECS technology: their aluminium content must be considered as an effective loss of material.

The partitioning of total aluminium in the fraction below 0.8 mm resulting from the first screening varies between 3.3% for beverage cans and 20.5% for foils. This variability may be related to the characteristics of the packaging and the alloy, as well as to operating conditions during the sampling. More specifically, the highest contents of aluminium have been found for trays (8.2%) and foils (20.5%) and this result might be explained mainly by their specific packaging structure. Compared to beverage cans, the thickness and the technical strength of trays and foils are lower, therefore aluminium lumps formed in the furnace are much smaller: this may facilitate their migration in the finer fraction of bottom ashes.

The partitioning of total aluminium in the fraction below 0.8 mm resulting from the second screening (after grinding) varies between 9.4% for beverage cans and 51.1% for foils. The value related to beverage cans is very low if compared to the others (38.0% for trays and 51.1% for foils). For this type of packaging, total aluminium partitioning in the two bottom ash fine fractions sums up to 12.7%: it follows that the loss of recoverable metal is low, as confirmed by the high amount of metallic aluminium recovered in the ingots. Similarly to what happens for the fine fraction from the first screening, the high values for trays and foils are once again explicable by their packaging structure and the size of aluminium lumps.

Concerning the ingots from the melting process, there are many differences between the three types of packaging: the partitioning of total aluminium shows that the ratio between the weight of aluminium recovered from ingots and the weight of the overall amount of aluminium found in the incineration residues is about 80% for beverage cans, 51% for trays and 27%⁷ for foils. As previously stated, data related to ingots are representative of the actual amount of aluminium that can be recovered through an advanced bottom ash treatment combined with the melting process in a saline furnace. In particular, data referring to aluminium foils are very interesting because they emphasize the contribution of the 0.8 - 5 mm fraction to the overall amount of metallic aluminium recoverable in the ingots. Indeed, about 80% of this amount comes from the ingots resulting from the melting of the 0.8 - 5 mm

⁷ Considering the ingots resulting from both the 0.8 - 5 mm and > 5 mm sub-fractions, about 21% and 6%, respectively.

sub-fraction, meaning that the recovery yield of aluminium from foils would increase by 390% by adding to the traditional ECS separation system an advanced ECS specifically calibrated on grains smaller than 5 mm.

The relationship between aluminium packaging thickness and the recoverable amount of aluminium from the incineration residues is shown in Figure 3.5.1.

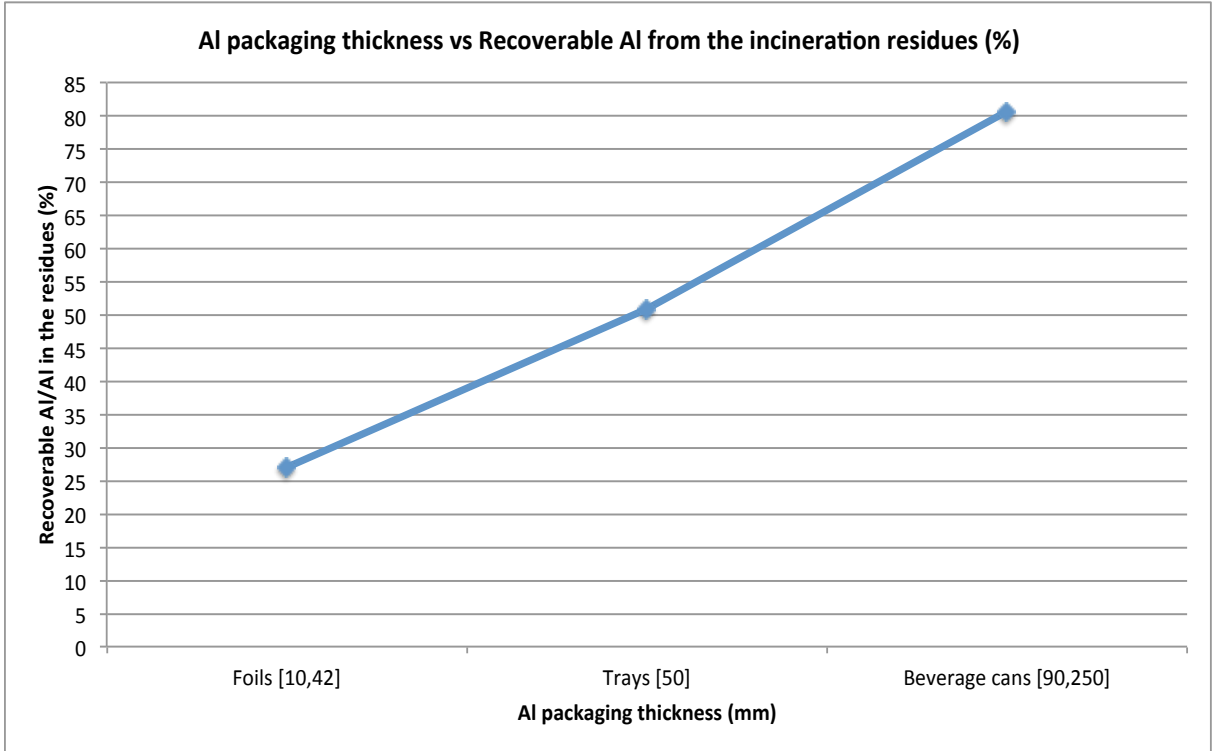


Figure 3.5.1 - Relationship between aluminium packaging thickness and the recoverable amount of aluminium from the incineration residues.

The trend depicted in Figure 3.5.2 reveals that the recovery of aluminium from the incineration residues increases proportionally to aluminium thickness in the tested packaging. Foils (Al thickness 10-42 µm) and trays (50 µm) are characterized by lower aluminium recovery yields if compared to beverage cans (90-250 µm), due to the formation of smaller lumps that are lost within the fine fractions.

3.5.2. Aluminium oxidation and potential for energy recovery

Table 3.5.2 shows the oxidation levels of aluminium recovered in the incineration residues for each type of tested packaging.

Table 3.5.2 - Oxidation levels of aluminium recovered in the incineration residues for each type of tested packaging.

Residue	Aluminium oxidation (%)		
	<i>Beverage cans</i>	<i>Trays</i>	<i>Foils</i>
<i>Fly ashes</i>	47	45	66
<i>Bottom ash fraction < 0.8 mm before grinding</i>	96	4	94
<i>Bottom ash fraction < 0.8 mm after grinding</i>	30	37	75
<i>Ingots*</i>	0	0	0
AVERAGE	9.2	17.4	58.8

*Aluminium contained in the ingots is all metallic by definition.

Values reported in Table 3.5.2 are representative of the real oxidation level of aluminium added through the doping of the waste, as they do not include the background concentration deriving from aluminium already present in the residual non-doped waste fed into the furnace. However, it is important to underline that all the values are certainly affected by the missing closure of the final mass balance.

Average oxidation levels show the importance of packaging thickness: overall, the thicker the packaging the less it is oxidized during the combustion process (see Figure 3.5.2). This is a consequence of the less surface area exposed to the oxidizing gases. Concerning this aspect, the packaging technical strength plays an important role too, avoiding or reducing the fragmentation of the material and the consequent increase in the exposed surface area.

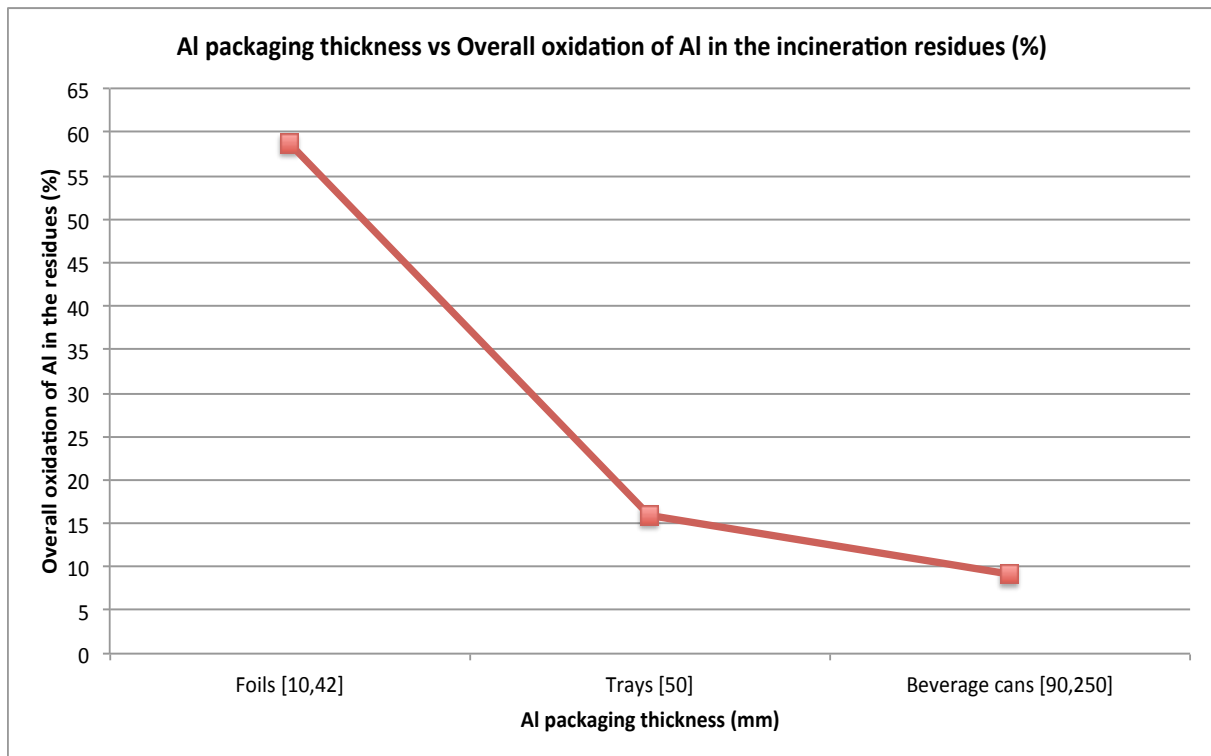


Figure 3.5.2 - Relationship between aluminium packaging thickness and the overall oxidation of aluminium in the incineration residues.

Considering each residue (rows of table 3.5.2), aluminium oxidation levels in fly ashes do not show high variability between the different types of tested packaging. The values corresponding to beverage cans and trays are similar (47% and 45%), while for foils it is slightly higher and equal to 66%.

In contrast, bottom ash fine fractions are characterized by oxidation levels significantly different between one another. Concerning the fraction below 0.8 mm from the first screening, aluminium is almost entirely present in the oxidized form for beverage cans and foils (whose oxidation levels are 96% and 94%), whereas it is almost all in its metallic form for trays (4%). In the fine fraction obtained from the second screening, the highest oxidation level belongs to foils (75%), while for trays and beverage cans it is much lower (37% and 30%).

As a general information and term of comparison, Table 3.5.3 reports the metallic/total aluminium ratio measured in the residues of the non-doped MSW incineration for Test 1, Test 2 and Test 4. In general, about half of the recovered aluminium is found in its metallic form: the lowest values belong to the bottom ash fine fractions (about 30%), whereas fly ashes are characterized by a much higher metallic content (about 90%).

Table 3.5.3 - Metallic aluminium content in the residues of the non-doped MSW incineration.

Residue	Metallic/Total Al (%)			
	Test 1	Test 2	Test 4	AVERAGE
<i>Fly ashes</i>	91.5	81.5	87	87
<i>Bottom ash fraction < 0.8 mm before grinding</i>	23	22	43	29
<i>Bottom ash fraction < 0.8 mm after grinding</i>	19	22	34	27
<i>Ingots*</i>	100	100	100	100
AVERAGE	41	40	54	45

*Aluminium contained in the ingots is all metallic by definition.

The potential for energy recovery from the oxidation processes on aluminium scraps in the furnace is strictly related to their corresponding oxidation levels. Indeed, at combustion temperatures above 850°C, the complete oxidation of 1 kg Al into Al₂O₃ releases an amount of energy equal to 31 MJ, which corresponds to the same amount released by 1 kg of coal or 0.8 kg of fuel (EAA, 1997).

The energy potentially recoverable from aluminium packaging oxidation was calculated for the three different tests on aluminium beverage cans, trays and foils, as reported in Tables 3.5.4 A-C. The specific energy release for each type of waste (second column) has been multiplied by the corresponding quantity introduced into the furnace (third column), resulting in the total amount of energy released by each type of waste during the combustion process (fourth column). The fifth column shows the percentage contribution of each type of waste to the overall energy release during the combustion process. It must be specified that all the aluminium in an oxidized form has been assumed to be Al₂O₃, thus resulting in a specific energy release equal to 31 MJ/kg. This is not necessarily true because aluminium in the 3+ oxidation state might be present in other mineral phases (such as ettringite, zeolites or other alumino-calcium hydrate compounds), resulting in different specific energy releases. Therefore, the results of the calculation must be considered as rough estimates.

Table 3.5.4 A - Potential for energy recovery from the oxidation of aluminium scraps during Test 1 on aluminium beverage cans.

Type of waste	Specific energy release	Quantity	Energy release	Energy contribution
	MJ/kg	kg	MJ	% of total energy release
Aluminium beverage cans (Al oxidized to Al₂O₃)	31	21*	647	0.5
Valmadrera residual waste	15 (LHV)	7,555	113,325	91.4
Seruso waste	22 (LHV)	455	10,010	8.1
TOTAL			123,982	100

Table 3.5.4 B - Potential for energy recovery from the oxidation of aluminium scraps during Test 2 on aluminium trays.

Type of waste	Specific energy release	Quantity	Energy release	Energy contribution
	MJ/kg	kg	MJ	% of total energy release
Aluminium trays (Al oxidized to Al₂O₃)	31	40*	1,252	0.9
Valmadrera residual waste	15 (LHV)	8,801	131,716	88.0
Seruso waste	22 (LHV)	745	16,652	11.1
TOTAL			149,620	100

Table 3.5.4 C - Potential for energy recovery from the oxidation of aluminium scraps during Test 4 on aluminium and poly laminated foils.

Type of waste	Specific energy release	Quantity	Energy release	Energy contribution
	MJ/kg	kg	MJ	% of total energy release
Aluminium+Polylam. foils (Al oxidized to Al₂O₃)	31	365*	11,318	2.4
Valmadrera residual waste	15 (LHV)	29105	435,585	92.2
Seruso waste	22 (LHV)	1131	25,280	5.4
TOTAL			472,184	100

* The values were obtained by multiplying the overall amount of aluminium introduced into the furnace with each type of packaging by the corresponding average oxidation level of the recovered aluminium for each test (Table 3.5.1).

As expected, in the case of aluminium beverage cans and trays the energy contribution deriving from the oxidation of Al into Al₂O₃ to the overall energy release during the combustion process is very low (0.5% and 0.9%), due to the low average oxidation levels of aluminium recovered in the incineration residues. In contrast, the contribution is much more relevant (2.4%) for aluminium and poly laminated foils, because of the higher oxidation level to which their extremely thin structures are subjected: this leads to an increase in the potential for energy recovery from this specific type of packaging.

3.5.2. Other metals in the ingots from the melting process

Table 3.5.5 shows the average contents of other non-ferrous metals and iron in the ingots obtained from the melting process in the crucible for each type of tested packaging. It must be said that the easily recognizable lumps of other metals (e.g. copper and brass) were separated from aluminium lumps before the melting process, therefore the real concentration of other metals in the ingots would be higher if no separation between the non-ferrous metals had occurred.

As it can be observed, the values are characterized by high variability and they do not follow a defined trend related to the type of packaging. Indeed, they strongly depend upon the composition of the residual waste incinerated at a specific time.

As a general indication, the highest contents of metals other than aluminium have been found for Cu, Zn and Si respectively. For what concerns aluminium and poly laminated foils, a peculiarity can be noticed: almost all the metal contents in the ingots obtained from the melting of the 0.8 - 5 mm sub-fraction are significantly higher than the corresponding values for the sub-fraction above 5 mm. The reason lies in the better identification and sorting of aluminium lumps in the sub-fraction above 5 mm (because of their larger size) resulting in the depletion of the other metals in the ingots obtained from that fraction and, on the other side, in the generally higher concentrations of heavy metals measured in the bottom ash fraction below 2 mm (Hu et al., 2007).

Table 3.5.5 - Average contents of other non-ferrous metals and iron in the ingots from the melting process for each type of tested packaging. Metal contents below 0.01% are not reported.

	Cu (%)	Zn (%)	Si (%)	Pb (%)	Mn (%)	Mg (%)	Fe (%)
Beverage cans							
<i>AVERAGE</i>	3.62	2.82	1.07	0.49	0.36	0.03	1.24
<i>STD. DEV.</i>	3.10	1.90	0.51	0.35	0.20	0.01	0.68
Trays							
<i>AVERAGE</i>	4.01	2.87	1.10	0.33	0.59	0.03	1.25
<i>STD. DEV.</i>	3.89	1.52	0.53	0.19	0.18	0.01	0.49
Foils (0.8 - 5 mm)							
<i>AVERAGE</i>	7.60	3.46	3.18	0.45	0.32	0.02	2.84
<i>STD. DEV.</i>	3.96	2.35	2.84	0.23	0.09	0.01	1.54
Foils (> 5 mm)							
<i>AVERAGE</i>	2.45	1.61	1.25	0.09	0.32	0.04	1.07
<i>STD. DEV.</i>	1.86	1.09	0.78	0.06	0.14	0.04	0.39

4. FUTURE PERSPECTIVES AND IMPROVEMENTS

This study is part of a broader project that is aiming to examine the behaviour of other aluminium packaging items during MSW incineration. The same tests will be repeated on different WTE plants and the results compared with all the previously gathered experiences. A new study on aluminium and poly laminated foils performed on a WTE plant located in Piacenza (Emilia Romagna, North of Italy) has already started. It is intended for the evaluation of waste combustion parameters influence on the recovery of aluminium from MSWI bottom ash. Some of these, such as the combustion temperature, the waste residence time, the concentration of acid gases in the flue gas or the typology of bottom ash extraction (dry or wet), considerably affect the oxidation process of metal scraps. The choice of this type of aluminium packaging to be further tested is linked both to its great availability in the residual waste routed to incineration (as it is not source-separated or collected), and to the interesting results emerged from the present study, showing that a large amount is not completely oxidized as expected and hence can be recovered from bottom ashes through an advanced ECS system configuration.

The issues raised during the tests reported in the present thesis suggest some changes to the applied methodology, useful from the perspective of future experimental campaigns.

Concerning the sampling plan, it seems necessary to extend the time period in order to reconstruct the complete trend of aluminium concentration curves (i.e. baseline related to the non-doped waste, increasing phase due to the waste doping and decreasing phase towards the baseline). This solution may remove one of the main factors causing the deficit in the final aluminium mass balance. However, it has proven to be very difficult to make reliable predictions on waste residence times because of the intrinsic variability of the combustion process. In this regard, it might be convenient to use a different tracer, comparable with the size of the tested packaging. The first three tests have shown that the cages were discharged long time before the appearance of the samples representative of the doped waste. This was probably due to the fact that they rolled down the furnace grate much faster than the waste mass because of their size and weight. Moreover, as the error in the analysis strongly depends on sample amounts, it would be better to increase the quantity of sampled bottom ashes during each sampling operation and to introduce the quartering procedure in order to increase their representativeness.

Another aspect that will need to be considered is the monitoring of aluminium concentration both in the bottom ash quenching water and in the flue gas emitted at the stack. In the estimate of the final aluminium mass balance, the contribution of aluminium contained in those media has been voluntarily neglected. However, in view of future experimental campaigns, it would be better to provide a dedicated monitoring system because it actually might have an influence on its closure. Even better would be the choice of a WTE plant featuring dry extraction of bottom ashes, which would also allow to quantify the differences in term of aluminium oxidation between a wet and a dry quenching system.

Concerning the laboratory analysis, the problems encountered in the measurement of metallic aluminium suggest the need to identify better solutions to the soda attack method or, alternatively, better equipment with higher precision. This choice is absolutely mandatory for the analysis on fly ash samples, in which the low sensitivity of the measuring instrument often caused metallic aluminium concentration to be higher than total aluminium concentration for the same sample. It will be also necessary to repeat the analyses more than two times for each sample, in order to estimate a reliable measuring accuracy and provide a statistical analysis leading to a possible range of results, despite it will be very time-consuming considering the large number of samples to be analyzed. Finally, a Scanning Electron Microscope (SEM) and/or X-Ray Diffraction (XRD) analysis should be implemented in order to distinguish among the different forms of oxidized aluminium and have a more robust estimate of the potential for energy recovery from the oxidation of aluminium scraps.

ACKNOWLEDGEMENTS

Desidero innanzitutto ringraziare l'Ing. Mario Grosso per l'opportunità e la fiducia concessami nell'avermi reso partecipe di questo importante progetto. Un grazie di cuore a Laura per il costante aiuto durante la preparazione, lo svolgimento e la stesura della tesi e a Simone, compagno di mille avventure in fonderia e negli impianti di incenerimento.

Un sincero e doveroso ringraziamento va alle persone senza la cui preziosa collaborazione e generosa disponibilità sarebbe stato impossibile portare a termine il lavoro: su tutti, Alessandro Gallina (a dispetto del cognome un vero gallo), Amhed Qist (detto Amedeo) e Alessandra Manini della fonderia Vedani Carlo Metalli.

Un ringraziamento speciale va ad Anna, che mi ha sempre aiutato, supportato (e sopportato) anche nei momenti più difficili, e a Carlo, un fratello con il quale ho condiviso i momenti più belli di questi anni. La Zappa-Caverna resterà per sempre nel mio cuore.

Grazie a mio fratello e a tutti i miei carissimi amici, i "milanesi" (fra i tanti, il mitico Berto e la famiglia Pisacane) e quelli di casa (in particolare Elio, Nico, Teo, Ale e Albi).

Infine, il ringraziamento più importante va ai miei genitori, per tutto. A voi dedico questo traguardo, perché soltanto grazie a voi ho potuto conseguirlo.

BIBLIOGRAPHY

Astrup, T., Riber, C., Pedersen, A.J., 2011. *Incinerator performance: effects of changes in waste input and furnace operation on air emissions and residues.* Waste Management & Research 29 (10), Supplement 57-68.

Bonelli, M., 2011. *Studio del comportamento di imballaggi di alluminio nel processo di incenerimento.* Master degree thesis, Politecnico di Milano. Supervisors: Grosso M., Biganzoli L.

Baun, D.L., Kamuk, B., Avanzi, P., 2007. *Treatment of bottom ash from Waste to Energy plants: overview and experiences.* Proceedings Sardinia 2007, Eleventh International Waste Management and Landfill Symposium, S. Margherita di Pula, Italy, 1-5- October 2007.

European Committee for Standardization, 2004. *CEN EN 13431:2004, Packaging – Requirements for packaging recoverable in the form of energy recovery, including specification of minimum inferior calorific value.* European Committee for Standardization.

CEWEP, EAA, 2011. *Metals Recycling from Waste-to-Energy bottom ashes contributes to a more “resource efficient” Europe.* Press Release, 14 December 2011.

CiAI, 2010. *Separazione e recupero dei metalli e valorizzazione delle scorie di combustione dei rifiuti urbani.* Study conducted by the Department of Environmental Engineering (DIAR) of Politecnico di Milano in collaboration with FederAmbiente.

Das, S.K., 2006. *Designing aluminium alloys for a recycle-friendly world.* Material Science Forum, vols. 519–521, Trans Tech Publications, Switzerland, pp. 1239–1244.

EAA, 2004. *Environmental Profile Report – reference year 2002.*

Giugliano, M., Cernuschi, S., Grosso, M., Aloigi, E., Miglio, R., 2001. *The flux and mass balance of PCDD/Fs in a MSW incineration full-scale plant.* Chemosphere 43, pp. 743-750.

Grosso, M., Biganzoli, L., Rigamonti, L., 2011. *A quantitative estimated of potential recovery from incineration bottom ashes.* Resources, Conservation and Recycling 55, pp. 1178-1184.

Hu, Y., Bakker, M.C.M, de Heij, P.G., 2011. *Recovery and distribution of incinerated aluminium packaging waste.* Waste Management 31, pp. 2422–2430.

Hu, Y., Rem, P., Di Maio, F., Muchova, L., 2007. *Metal distribution in Los Angeles MSWI bottom ash.* Proceedings Sardinia 2007, Eleventh International Waste Management and Landfill Symposium, S. Margherita di Pula, Italy, 1-5- October 2007.

Ishii, K., Ozaki, R., Kaneko, K., Fukushima, H., Masuda, M., 2007. *Continuous monitoring of aluminum corrosion process in deaerated water.* Corrosion Science 49, pp. 2581-2601.

ISPRA, 2009. *Rapporto rifiuti 2008.* www.ispraambiente.it

ISPRA, 2011. *Rapporto rifiuti 2010.* www.ispraambiente.it

Lopez-Delgado, A., Pena, C., Lopez, V., Lopez, F.A., 2003. *Quality of ferrous scraps from MSW incinerators: a case study of Spain.* Resources conservation and Recycling 40, pp. 39-51.

Manders, J.L.C., 2008. *The renewable Energy contribution of Waste to Energy across Europe.* CEWEP, www.cewep.com/storage/med/media/energy/283RenewEnergyEuropeJM7.pdf

Muchova, L., Rem, P., 2007. *Wet or dry separation.* Waste Management World, December 2007.

Muller, U., Rubner, K., 2006. *The microstructure of concrete made with municipal waste incinerator bottom ash as an aggregate component.* Cement and Concrete Research 36, pp. 1434-1443.

Pecqueur, G., Crignon, C., Quénée, B., 2001. *Behaviour of cement-treated MSWI bottom ash.* Waste management 21, pp. 229-233.

Pruvost, F., 2009. *The potential for the valorisation of used aluminium packaging in Waste-to-Energy plants in Europe - A study for EAA and IAI. Interim report. Main findings of the documentary search.* January 5, 2009.

Pruvost, F., 2011. *Potential for increased aluminium recovery from bottom ashes in Europe.* CEWEP-EAA Seminar, Copenhagen September 5-6 2011.

Rigamonti, L., Grosso, M., 2009. *Riciclo dei Rifiuti. Analisi del ciclo di vita dei materiali da imballaggio.* Dario Flaccovio, Chapter 3, Paragraph 3.3.

Sabbas, T., Poletini, R., Astrup, T., Hjelm, O., Mostbauer, P., Cappai, G., et al., 2003. *Management of municipal solid waste incineration residues.* Waste Management 23, pp. 61-88.

Schneider C., Wolf S., 1999. *Processing of salt slag from the secondary aluminium production.* Chair for Processing and Recycling of Solid Waste Material, RWTH Aachen.

Soler, L., Macanas, J., Munoz, M., Casado, J., 2007. *Aluminium and aluminium alloys as sources of hydrogen for cell applications.* Journal of Power sources 169, pp. 144-149.

Soler, L., Cendela, A.M., Macanas, J., Munoz M., Casado J., 2009. *In situ generation of hydrogen from water by aluminium corrosion in solutions of sodium aluminate.* Journal of Power Sources 192, pp. 21-26.

Stockburger, D., Stannard, J.H., Rao, B.M.L., Kobasz, W., Tuck, C.D., 1991. *Hydrogen storage materials, battery and electrochemistry.* Eds: Corrigan A., Srinivasan S. Electrochemical society USA, pp. 431-444

Stucchi, S., 2003. *Il bilancio degli elementi tossici nel processo di termovalorizzazione dei rifiuti solidi urbani. Esperienza su due impianti reali.* Master degree thesis, Politecnico di Milano. Supervisors: Cernuschi S., Grosso M.

Tenorio, J.A.S., Espinosa, D.C.R., 2000. *High-temperature oxidation of Al-Mg alloys.* Oxidation of metals 53, pp. 361-373.

Vargel, C., 2004. *Corrosion of aluminium.* Elsevier edition.

Young, D.J., 2008. *High temperature oxidation and corrosion of metals.* Elsevier edition.

